MPB TECHNOLOGIES INC.
1725 North Service Road | Trans-Canada Highway
Dorval, Québec H9P 1J1
(514) 683-1490 Telex 05-823509

MPB

TP6606E

DEVELOPMENT OF AN ANTENNA FOR A REMOTE SEA-ICE THICKNESS SENSOR

Prepared for:

TRANSPORTATION DEVELOPMENT CENTRE

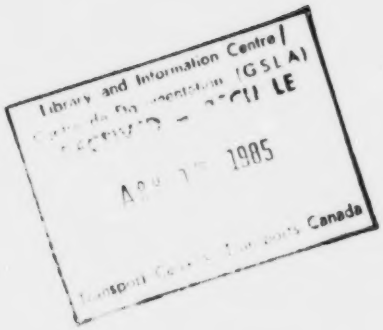
Library and Information Centre /
1985
Canada

March, 1984

MPB TECHNOLOGIES INC.
1725 North Service Road | Trans-Canada Highway
Dorval, Québec H9P 1J1
(514) 683-1490 Telex 05-823509

MPB

DEVELOPMENT OF AN ANTENNA FOR A REMOTE SEA-ICE THICKNESS SENSOR

By:

S.Y.K. Tam, A. Shoamanesh,
B.W. Gibbs, G. Riedel

MPB Technologies Inc.
1725 North Service Road
Trans Canada Highway
Dorval, Quebec
H9P 1J1.

March, 1984

Approved by:

Dr. M.P. Bachynski
President

The contents of this report reflect the views of the contractor and not necessarily the official views or policies of the Transportation Development Centre.

PROJECT TEAM:

The project team for MPB Technologies Inc. was composed of:

Dr. S.Y.K. Tam
Dr. A. Shoamanesh
Mr. B.W. Gibbs
Mr. G. Riedel

and others

REPORT DOCUMENTATION FORM

1 Transport Canada Report No.	2. TDC Project No.	3 Recipient's Catalogue No.
TP 6606E	4232	

4 Title and Subtitle	5 Report Date
Development of an Antenna for a Remote Sea-Ice Thickness Sensor	March 1984
	6 Performing Organization Report No. MPB-179-1
7 Author(s)	8 Transport Canada File No.
S.Y.K. Tam, A. Shoamanesh, B.W. Gibbs, G. Riedel	D 1460-126-2
9 Performing Organization Name and Address MPB Technologies Inc. 1725 North Service Road, Trans Canada Highway Dorval, Quebec H9P 1J1	10 DSS File No. 09SD.T8200-0-0510
	11 DSS or Transport Canada Contract No. OSD80-00051
12. Sponsoring Agency Name and Address Transportation Development Centre (TDC) Complexe Guy Favreau Suite 601 Montreal, Quebec H2Z 1X4	13. Type of Report and Period Covered
	14 Sponsoring Agency Code
15 Supplementary Notes	16 TDC Project Officer M. Audette

17 Abstract

Using subscale antennas ten times smaller than actual size, it was possible to study the electrical characteristics of several candidate antenna configurations in the laboratory for a remote sea-ice thickness sensor avoiding the use of inconveniently large test facilities. The study included measurements of voltage standing wave ratios (VSWR) transient responses, antenna bandwidths, power radiation patterns and antenna-aircraft interactions for five types of candidate broadband antennas in several reflector geometries.

After the subscale antenna study, several full-size antennas were fabricated and tested in the field at real VHF frequencies from 30 MHz to 200 MHz. Consistent with the subscale antenna study, a design having a tapered loaded dipole in a rectangular reflector was found to have the best overall characteristics. A new prototype with a tapered resistively loaded dipole in an open grid-structure, rectangular reflector was fabricated and flight-tested on a Canadian Coast Guard helicopter. The prototype was found to have suitable overall electrical characteristics, sound mechanical strength with good structural integrity and small air resistance. Despite a "fix-mounting" arrangement, it can be installed or removed from the helicopter in a few minutes. This prototype successfully passed the airworthiness test by the Coast Guard and is recommended for a sea-ice thickness sensor.

18 Key Words	19 Distribution Statement
Antenna, Sea-Ice, Remote Sensor, Radar, Ice Thickness, VHF	Limited number of copies available from Transportation Develoopment Centre (TDC)

20 Security Classification (of this report)	21 Security Classification (of this page)	22 No. of Pages	23. Price
Unclassified	Unclassified		Nil

TDC CDT 79-005

FORMULE DE DOCUMENTATION POUR RAPPORT

1 N° du rapport Transports Canada	2 N° de l'étude — CDT	3 N° de catalogue du destinataire
TP 6606E	4232	

4 Titre et sous-titre	5 Date du rapport
Development of an Antenna for a Remote Sea-Ice Thickness Sensor	Mars 1984
	6 N° du rapport de l'organisme executant: MPB-179-1
7 Auteur(s)	8 N° de dossier Transports Canada
S.Y.K. Tam, A. Shoamanesh, B.W. Gibbs, G. Riedel	D 1460-126-2
9 Nom et adresse de l'organisme executant	10 N° de dossier — ASC
MPB Technologies Inc. 1725 North Service Road, Trans Canada Highway Dorval, Quebec H9P 1J1	09SD.T8200-0-0510
	11 N° de contrat — ASC ou Transports Canada: OSD80-00051
12 Nom et adresse de l'organisme parrain	13 Genre de rapport et période visée
Centre de développement des transports (CDT) Complexe Guy Favreau Suite 601 Montréal, Québec H2Z 1X4	14 Code de organisme parrain
15 Remarques additionnelles	16 Agent de projet — CDT: M. Audette

17 Resumé Ce rapport rend compte des essais en laboratoire que l'on a fait subir à cinq types d'antennes à bande large, destinés à la télémesure de l'épaisseur des glaces, dans le but de déterminer les caractéristiques électriques de leur fonctionnement. Pour éviter les inconvénients d'essais en vraie grandeur, ces essais ont porté sur des modèles réduits à l'échelle 1/10. Les paramètres mesurés comprenaient les rapports d'onde stationnaire en tension, les bandes passantes, les diagrammes de rayonnement en puissance et les interactions antenne-aéronef pour diverses configurations de réflecteur dans chaque cas.

Une fois les essais sur modèles réduits terminés, plusieurs antennes grandeur nature ont été fabriquées et testées sur le terrain dans la gamme THF, soit entre 30 et 200 MHz. Ces essais ont confirmé les résultats des essais précédents, c'est-à-dire que l'antenne présentant les meilleures caractéristiques globales était celle à doublet à chaque série à répartition en cloche, couplée à un réflecteur de forme rectangulaire. Il a donc été décidé de fabriquer un nouveau prototype combinant un doublet à charge résistive série à répartition en cloche et un réflecteur rectangulaire en forme de grillage. Les essais en vol de ce prototype monté sur un hélicoptère de la garde cotière canadienne (GCC) ont révélé des caractéristiques électriques globalement satisfaisantes, une bonne résistance mécanique des éléments constitutifs et une solidité suffisante de l'ensemble, ainsi qu'une faible traînée aérodynamique induite. Sans avoir des fixations dites rapides, cette antenne se pose et se dépose en quelques minutes seulement. Les essais de navigabilité conduits par la GCC ayant été probants, il est recommandé d'adopter cette antenne plutôt que les autres.

18 Mots-clés	19 Diffusion
Antennes, glace de mer, télédétecteur, radar, épaisseur des glaces, THF.	Le CDT dispose d'un nombre limité d'exemplaires.

20 Classification de sécurité (de ce rapport)	21 Classification de sécurité (de cette page)	22 Nombre de pages	23 Prix
non classifié	non classifiée		-

CDT TDC 79-005

FOREWORD

The Development of a Remote Sea-Ice Thickness Sensor at MPB Technologies Inc. is sponsored by Transport Canada Research and Development Centre. This report comprises two parts. Part one describes the testing and simulation experiments on candidate helicopter-borne antennas using subscale models. Designs, constructions and testing of the VHF antenna of actual size are presented in part two.

PART 1

ANTENNA REQUIREMENTS, DESIGNS,
DEVELOPMENT AND MEASUREMENTS

PART 1

TABLE OF CONTENTS

		PAGE NO.
1.0	INTRODUCTION	1
1.1	Background	1
1.2	Requirements and Limitations on Antennas	3
2.0	LABORATORY ANTENNA MODELLING	6
2.1	Scaling Analysis	6
2.2	Experimental Arrangement	7
2.3	Measurements Using Candidate Antennas	12
2.3.1	Choice of Test Antennas	12
2.3.2	Superturnstile (Bow Tie) Antenna	13
2.3.3	Triangular dipole	16
2.3.4	Spiral Antenna	19
2.3.5	Modified Spiral (Fig. 13)	25
2.3.6	Tapered resistively loaded cylindrical dipole	25
2.3.7	Summary	32
3.0	STUDY OF CAVITY BACK ANTENNAS	34
3.1	General Requirements	34
3.2	VSWR Measurements	34
3.3	Discussion on VSWR results	49
4.0	ANTENNA RADIATION PATTERN MEASUREMENTS	50
4.1	Siting Considerations	50
4.2	Experimental Arrangement & Results	50
4.3	Antenna Directivity	69
4.4	Transmission Characteristics	71
5.0	STUDY OF ANTENNA - AIRCRAFT INTERACTIONS	74
6.0	SUMMARY AND RECOMMENDATIONS	91
7.0	REFERENCES	93

LIST OF FIGURES

		PAGE NO.
FIGURE 1	Experimental arrangement for subscale antenna experiments	8
FIGURE 2	1 nsec. input pulse for subscale antenna measurement	10
FIGURE 3	Arrangement of subscale antennas for measuring reflections from conductive wall	11
FIGURE 4	Arrangement with subscale antennas facing free space	11
FIGURE 5	Sketch showing various configurations of superturnstile (Bow Tie) Antenna	14
FIGURE 6(a)	Superturnstile antenna used in measurements	15
(b)	Oscillograms showing signal output of superturnstile receive antenna	15
FIGURE 7(a)	Geometry of triangular dipole	17
(b)	Measured gain characteristics of triangular dipole	17
FIGURE 8(a)	Sketch showing geometry of triangular (butterfly) antenna	18
(b)	Picture of triangular antenna used in experiment.	18
FIGURE 9	Oscillograms showing responses of triangular transmit, receive antennas in rectangular boxes	20
FIGURE 10	Picture of triangular antennas with curved surface	21
FIGURE 11	Oscillogram showing receiver antenna output when 1 ns pulse is input to transmit antenna	21
FIGURE 12	Two arms equiangular spiral antenna.	22
FIGURE 13	Subscale spiral antennas used in measurements	23
FIGURE 14	Oscillogram showing transient response of spiral antenna whose geometry is given...	26
FIGURE 15(a) & (b)	Oscillograms showing mutual coupling and reflections from metal wall 1 m away from antennas	26
FIGURE 16	Relative power versus angle θ for a tapered resistive loaded cylindrical dipole....	28

LIST OF FIGURES, cont'd....

		PAGE NO.
FIGURE 17	Input impedance of a tapered resistive loaded antenna vs frequency with antenna wire...	29
FIGURE 18	Tapered resistively loaded antenna with value of resistance in ohms on each subsection	31
FIGURE 19	Tapered resistively loaded antenna with broadband transformer balun ...	31
FIGURE 20	Mutual coupling between two resistively loaded antenna when they are facing the free space.	33
FIGURE 21	Comparison between two resistively loaded dipole with that of two triangular antennas.	33
FIGURE 22	Block diagram of experimental arrangement for antenna VSWR measurement	35
FIGURE 23	Geometry of cylindrical reflector	37
FIGURE 24(a)	Comparison between signals reflected by TRLD antenna in cylindrical box and a short circuit...	37
FIGURE 24(b)	Short circuit	38
24(c)	Antenna	38
FIGURE 24(d)	Short circuit	39
24(e)	Antenna	39
FIGURE 25	VSWR of a tapered resistively loaded dipole in a cylindrical cavity versus frequency	40
FIGURE 26(a)	Short Circuit	42
26(b)	Antenna	42
FIGURE 26(c)	Short Circuit	43
26(d)	Antenna	
FIGURE 26(e)	Short Circuit	44
26(f)	Antenna	44
FIGURE 27	VSWR of tapered resistively loaded dipole in square box, versus frequency	45
FIGURE 28(a)	Comparison between amplitude of reflected signal from the TRLD antenna in a rectangular box...	46

LIST OF FIGURES, cont'd...

		PAGE NO.
FIGURE 28(b)	500 to 900 MHz	47
28(c)	900 to 1350 MHz	47
FIGURE 29	VSWR of tapered resistively loaded cylindrical dipole in a rectangular box	48
FIGURE 30	Tapered resistively loaded antenna in cylindrical rectangular reflector in anechoic chamber....	53
FIGURE 31(a)	E-Plane Radiation Pattern of a TRLD in a cylindrical cavity.	54
31(b)	" " "	54
FIGURE 31(c)	E-Plane Radiation Pattern of a TRLD in a cylindrical cavity.	55
31(d)	" " "	55
FIGURE 31(e)	E-Plane Radiation Pattern of a TRLD in a cylindrical cavity	56
31(f)	" " "	56
FIGURE 32(a)	H-Plane radiation pattern for TRLD in a cylindrical cavity	57
32(b)	" " "	57
FIGURE 32(c)	H-Plane radiation pattern for TRLD in a cylindrical cavity	58
32(d)	" " "	58
FIGURE 32(e)	H-Plane radiation pattern for TRLD in a cylindrical cavity	59
32(f)	" " "	59
FIGURE 33(a)	E-Plane radiation pattern of a TRLD in a rectangular cavity	60
33(b)	" " "	60
FIGURE 33(c)	E-Plane radiation pattern of a TRLD in a rectangular cavity	61
33(d)	" " "	61
FIGURE 33(e)	E-Plane radiation pattern of a TRLD in a rectangular cavity	62
33(f)	" " "	62
FIGURE 33(g)	E-Plane radiation pattern of a TRLD in a rectangular cavity	63
33(h)	" " "	63

LIST OF FIGURES, cont'd...

		PAGE NO.
FIGURE 34(a)	H-Plane radiation pattern of a TRLD in a rectangular cavity	64
34(b)	" " "	64
FIGURE 34(c)	H-Plane radiation pattern of a TRLD in a rectangular cavity	65
34(d)	" " "	65
FIGURE 34(e)	H-Plane radiation pattern of a TRLD in a rectangular cavity	66
34(f)	" " "	66
FIGURE 34(g)	H-Plane radiation pattern of a TRLD in a rectangular cavity	67
34(h)	" " "	67
FIGURE 34(i)	H-Plane radiation pattern of a TRLD in a rectangular cavity	68
34(j)	" " "	68
FIGURE 35(a)	Antenna with square reflector	77
35(b)	Antenna with cylindrical reflector	77
FIGURE 36(a)	E-Plane radiation pattern for TRLD in a cylindrical cavity with subscale helicopter	78
36(b)	" " "	78
FIGURE 36(c)	E-Plane radiation pattern for TRLD in a cylindrical cavity with subscale helicopter	79
36(d)	" " "	79
FIGURE 36(e)	E-Plane radiation pattern for TRLD in a cylindrical cavity with subscale helicopter	80
36(f)	" " "	80
FIGURE 37(a)	E-Plane radiation patterns for TRLD in a square cavity with & without metal back plate	81
37(b)	" " "	81
FIGURE 37(c)	E-Plane radiation patterns for TRLD in a square cavity with & without metal back plate	82
37(d)	" " "	82
FIGURE 37(e)	E-Plane radiation patterns for TRLD in a square cavity with & without metal back plate	83
37(f)	" " "	83

LIST OF FIGURES, cont'd....

		PAGE NO.
FIGURE 37(g)	E-Plane radiation patterns for TRLD in a square cavity with & without metal back plate	84
FIGURE 37(i)	E-Plane radiation patterns for TRLD in a square cavity with & without metal back plate	85
37(j)	" " "	85
FIGURE 38(a)	H-Plane radiation patterns for TRLD in a square cavity with & without metal back plate	86
38(b)	" " "	86
FIGURE 38(c)	H-Plane radiation patterns for TRLD in a square cavity with & without metal back plate	87
38(d)	" " "	87
FIGURE 38(e)	H-Plane radiation patterns for TRLD in a square cavity with & without metal back plate	88
38(f)	" " "	88
FIGURE 38(g)	H-Plane radiation patterns for TRLD in a square cavity with & without metal back plate	89
38(h)	" " "	89
FIGURE 38(i)	H-Plane radiation patterns for TRLD in a square cavity with & without metal back plate	90

1.0 INTRODUCTION

1.1 Background

The development of an airborne antenna for a remote sea-ice thickness sensor is part of an ongoing development at MPB Technologies Inc. under the sponsorship of Transportation Development Centre of the Department of Transport. Its objective is to develop a helicopter-borne antenna which can be fix-mounted under a standard, small helicopter such as the Bell 206 helicopter being used by the Canadian Coast Guard.

The development of an airborne remote sea-ice thickness sensor is important since there is a growing need in navigation in the arctic for the exploration of resources. Optical and microwave sensors may provide images of sea-ice surfaces from which gross features of the ice covered regions can be determined. For example, multi-year and first year sea-ice can have signiificantly different surface features which can be discriminated from the radar images. However, the correlation between the surface characteristics and the ice thickness is usually poor and ambiguous. Unambiguous determination of sea-ice thickness, therefore, requires the use of radar echo sounding.

Despite the advanced stage of development of modern microwave radars, their applications to sea-ice thickness measurements are limited. The major difficulty is the severe attenuation of microwave signals by sea-ice which prevents their penetration to a useful depth in the sea-ice layer. VHF signals can be used to measure sea-ice thickness by radar echo sounding since they can penetrate sea-ice from tens of centimeters to many metres, depending on the sea-ice characteristics. However, one major difficulty in using a remote VHF radar is

the development of a VHF airborne antenna with convenient dimensions and suitable electromagnetic characteristics.

The VHF antenna development at MPB Technologies Inc. consists essentially of two parts. Instead of embarking at the start on real size VHF antennas which would require large test ranges. antenna towers and test facilities with awkwardly large dimensions, subscale antennas and subscale models are used to study various antenna characteristics which are scaleable. By increasing the test frequency ten times higher than the real frequency, it was possible to use subscale antennas and test facilities ten times smaller. The subscale antenna tests provided valuable information on the response of various conventional, candidate broadband antennas to narrow pulse. broadband signals or a steady state sinusoidal signal over a wide range of frequencies. They also provided results of VSWR, transmission characteristics, radiation patterns and the antenna-aircraft interactions on various antenna types and configurations. Such results are directly applicable to a full scale (real size) VHF antenna to be used in the actual sensor.

The present report describes the experimental study, the design and tests of the various subscale models of candidate antennas. The design, development and tests of real size VHF antenna will be described in a separate report.

1.2 Requirements and Limitations on Antennas

Among the various components in the sea-ice thickness sensor, the Antenna presents one of the more difficult technical problems. As discussed in previous reports (Tam et al [1], Keelty and Tam [2]), a useful, operationally feasible antenna has to meet the following requirements:

(a) Broadband frequency response - for transmitting large bandwidth signals;

(b) Good transient response - for the least distortion on narrow pulses;

(c) Suitable directivity - for spatial resolution and good efficiency;

(d) Relatively small size - for fix-mounting on a small helicopter;

(e) Ease of deployment - for operational convenience;

(f) Airworthy construction - for safety.

Requirements (a) and (b) are essentially related to the electrical properties of the antenna. They are difficult problems at all frequencies, microwaves and VHF. Requirements (c), (d), (e) and (f) are related to antenna shapes and sizes and are major problems for an operational airborne VHF antenna. At VHF, physical law requires that an efficient and reasonably directive antenna be large and relatively inconvenient to deploy. The development of a sea-ice sensor antenna that meets the above conditions, therefore, requires good understanding of the electromagnetic principle, antenna properties, operational environments and, above all, a vast amount of ingenuity.

The broadband frequency response implies that the antenna should transmit efficiently over the VHF range typically between 30 MHz and 200 MHz, and that the electrical properties remain relatively constant over the same frequency range. This requirement suggests that the antenna has to have a bandwidth larger than its centre frequency. Except for log-periodic antennas or antennas of the travelling-wave type, the broadband requirement is generally extremely difficult to meet.

An antenna that has a broadband characteristic when it is tested with a steady-state sinusoidal electromagnetic wave, may not be suitable for transmitting pulse signals. In order to retain the pulse shape of sea-ice radar signal, which are superpositions of electromagnetic signals over a wide VHF bandwidth, the radar antenna should have a suitable transient response. Otherwise, the pulse shape of the transmitted signal cannot be recovered.

As an example, a log-periodic antenna may have a wide bandwidth covering the bandwidth of the radar pulse, the waveform can be distorted because the various frequency components are transmitted or received at different locations of the antenna with different time delays. The received pulse shape can be significantly different from the one transmitted. Lack of practical data on the transient response of broadband VHF antenna, therefore, requires extensive experimental measurements during the antenna development.

Besides the previously discussed limitations, the long wavelength at VHF introduces severe problems on the antenna size. To achieve reasonable antenna efficiency and directivity, the dimensions

of the antenna with its reflector should be comparable to the wavelength of the transmitted signals. At 30 MHz, a half-wavelength resonant dipole should have a dipole length of about 5 metres. With a reflector, the antenna dimensions are comparable to that of a small helicopter, e.g. a Bell 206 Helicopter. It is easy to understand why ingenuity and compromise are needed for fix-mounting such an antenna on a helicopter without significantly affecting the aerodynamic conditions.

In the following sections, we discuss the tests of various candidate antenna designs. In Section 2, we present the study of antennas using subscale models. Justifications of the scaling procedure are given in Section 2.1, the experimental arrangement in Section 2.2, and measurements using various candidate antennas in Section 2.3. Effects of a reflector on the antenna are discussed in Section 3. Radiation pattern measurements and antenna-aircraft interactions are discussed in Sections 4 and 5.

Summary and Recommendations are presented in Section 6.

2.0 LABORATORY ANTENNA MODELLING

2.1 Scaling Analysis [3]

Subscale models have been used for a number of years in studying various properties of electromagnetic systems. The purpose of this section is to show the relationship between the models and the real systems.

The validity of a study using subscale models is based on the fact that the Maxwell's equations, which describes the electromagnetic fields and the constitutive relation which dictates the properties of the media, are essentially linear over the range of conditions relevant to the scaling procedure. The modelling study, therefore, excludes non-linear media such as ferromagnetic media or ionized media in the presence of a magnetic field. It is applicable to homogeneous and inhomogeneous media since the Maxwell's equations are valid for both.

If the scaling factor is p, then a linear dimension L_m in the model is related to the corresponding dimension L on the actual antenna by

$$L_m = L/p$$

The frequency f_m used in the subscale model must be related to the real VHF frequency f used by the actual (full scale) antenna by

$$f_m = pf$$

A further requirement of an accurate model for pattern and impedance measurements is that the conductivity of the antenna metal be scaled according to the relation

$$\sigma_m = p\sigma$$

where σ and σ_m are conductivities governed by constitutive relations, σ_m is the conductivity of metal in the subscale model, and σ is the conductivity of metal in the actual antenna. However, if σ is sufficiently large, the metal can be considered to be a «perfect conductor» ($\sigma \to \infty$) and no scaling is required for the conductivity.

In practice, subscale systems can provide quantitative results for the actual system being modelled if the scaling factor p is below 10. In our subscale modelling, we use a scaling factor of 10 so that the wavelength and the dimensions of the subscale model are 10 times smaller than those of the real size systems.

2.2 Experimental Arrangement

The experimental arrangement for the antenna measurements is as shown in Fig. 1a. The test antennas are used for transmitting and receiving simulated radar signals at frequencies from 150 MHz to 1.8 GHz, ten times the actual VHF to be used in actual sea-ice thickness measurements. A reflector is used for each antenna configuration tested so as to reduce interaction between the antenna dipole element, the antenna feed line and the supporting structure. Microwave absorber is used wherever necessary to reduce spurious reflections.

For transmission measurements, the transmit-receive antennas are separated by a suitably chosen distance and the transmitted and received signals are monitored on an oscilloscope. When the effect of antenna mutual coupling is studied, the transmit-receive antennas are positioned

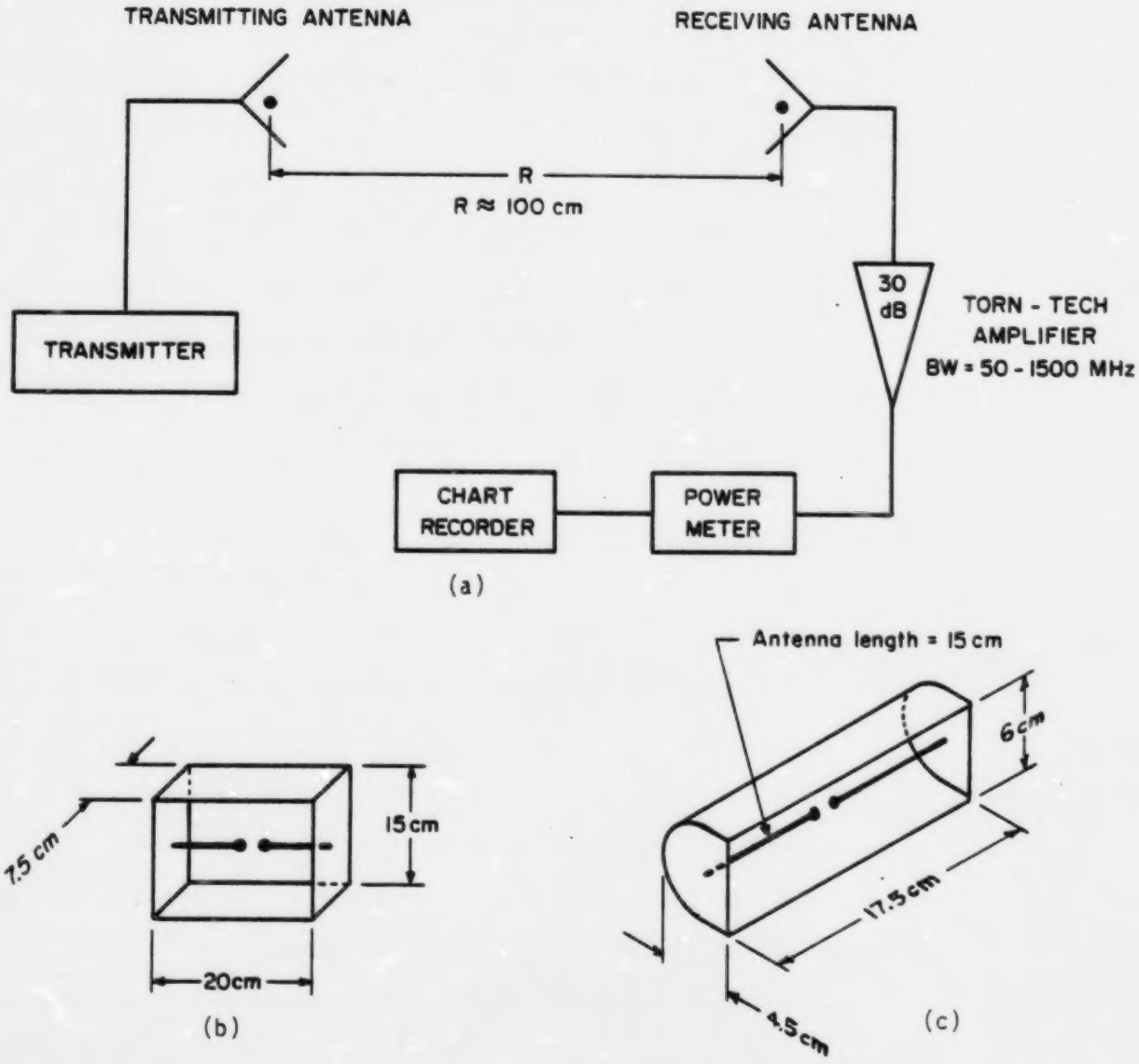

FIGURE 1 - Experimental arrangement for subscale antenna experiments:
(a) Experimental arrangement;
(b) Antenna with rectangular reflector;
(c) Antenna with cylindrical reflector.

side by side while both of them are facing a wall of microwave absorber about 5 m away.

During the measurements the antenna dipole is placed in a rectangular box with dimensions 20 cm (width) by 15 cm (height) by 7.5 cm (depth). The dipole element is positioned 4 cm from the back of the reflector (see Fig. 1b). The input to the antenna is a 1 nanosecond pulse (Fig. 2). Both the input pulse to the transmitting antenna and the output pulse from the receive antenna are observed on a high frequency oscilloscope (Tektronix 485 and/or 7835 with a sampling unit). Distortions, ringing and lengthening of pulse width on the received pulse shapes, are used as criteria for evaluating a particular antenna configuration.

Fig. 3 shows the experimental arrangement for reflection tests. The antennas are placed about 1 to 2 m away from a metal wall. A 1 nanosecond pulse (equivalent to a 10 nsec pulse in real situations) is transmitted by an antenna and the reflection from the metal wall is received by an identical receive antenna and observed on an oscilloscope. Typically, the received signals consist of a signal due to the mutual coupling between the antennas and another signal due to the reflection from the wall. The wall reflection arrives at a time delay corresponding to the transit time in free space. To observe the mutual coupling above, the antennas are rearranged so that both the transmit and receive antennas face the free space (see Fig. 4)

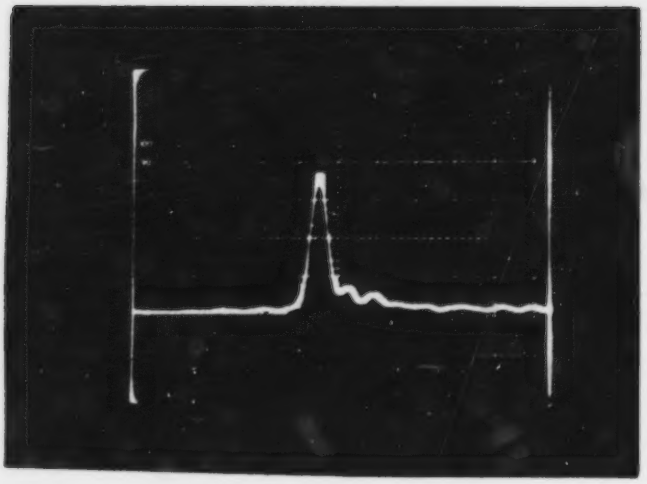

FIGURE 2 - 1 nsec. input pulse for subscale antenna measurement, 5 V/div (Vertical) and 2 nsec./div (Horizontal)

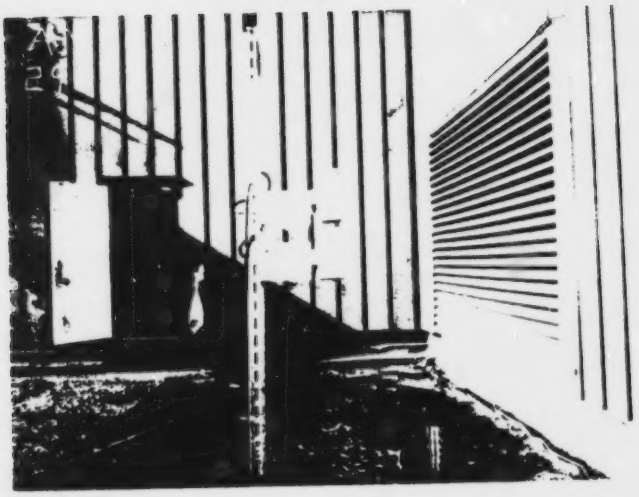

FIGURE 3 - Arrangement of subscale antennas for measuring reflections from conductive wall.

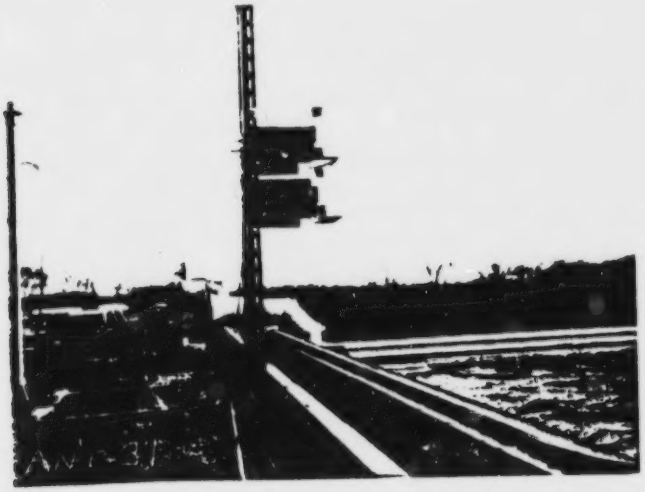

FIGURE 4 - Arrangement with subscale antennas facing free space to observe mutual coupling between antennas with no reflections from conductive wall.

2.3 Measurements Using Candidate Antennas

2.3.1 Choice of Test Antennas

Earlier broadband antennas employed rhombic, biconical or helical configurations as well as arrays of basic elements to achieve moderate improvement in the antenna bandwidth. Since the early 1960's, the linear log-periodic antenna has become more and more popular. The great advantage of the linear log-periodic is its wide bandwidth, fairly good directivity and relatively simple configuration. In fact it has been used in an earlier sea-ice thickness sensor experiment (see [1] and [2]) where the antenna was suspended under a helicopter. Unfortunately advice from helicopter pilots suggested that none of the antenna configurations mentioned above would be suitable for fixed installation on a helicopter either for reasons of airworthiness or antenna helicopter interactions.

In choosing a candidate antenna for the sea-ice thickness sensor, it was decided to first select a suitable antenna driving element such as a simple broadband dipole. The dipole would then be installed in a cavity which would act as a reflector to provide directivity and as a shield to prevent electromagnetic interferences from the helicopter body. Candidate antenna dipole elements chosen for the tests were the superturnstile (bow tie), the butterfly, the equiangular and the tapered resistively loaded antenna (TRLA). The dimensions of the antennas were chosen with the limitations dictated by the helicopter dimensions.

In the following sections, measured results of subscale antennas will be presented. These measurements include the superturnstile (Section 2.3.1), the triangular dipole (Section 2.3.2), the spiral antenna (Section 2.3.3), the modified spiral (Section 2.3.4), and the resistively loaded dipoles (Section 2.3.5).

2.3.2 Superturnstile (Bow Tie) Antenna

The superturnstile antenna evolves from a standard dipole which is essentially a narrow band device [3]. It has been found that the bandwidth of the dipole is greatly increased with little sacrifice in the radiation efficiency when each of the two dipole arms is shaped in the form of a cone (see Fig. 5a). The bandwidth can be further increased if the autumn feed point is connected to a quarter-wave stub (see Figure 5b).

For easier construction and improved performance, the superturnstile antenna may take the following modified versions. The dipole arm may be modified from a solid cone into a solid metal sheet (Fig. 5c). The combination of this configuration with a quarter-wave stub mentioned before has been reported to yield a bandwidth of 35 percent and a VSWR of 1.1 or less. In another version, the outside edge of the sheets are notched (Fig. 5d) in order to obtain a more uniform current distribution.

Typical measurements for the subscale superturnstile antenna are as shown in Figure 6. With a 1 nsec pulse input to the transmitting antenna, the output from an identical receive antenna shows oscillations lasting for tens of nanoseconds.

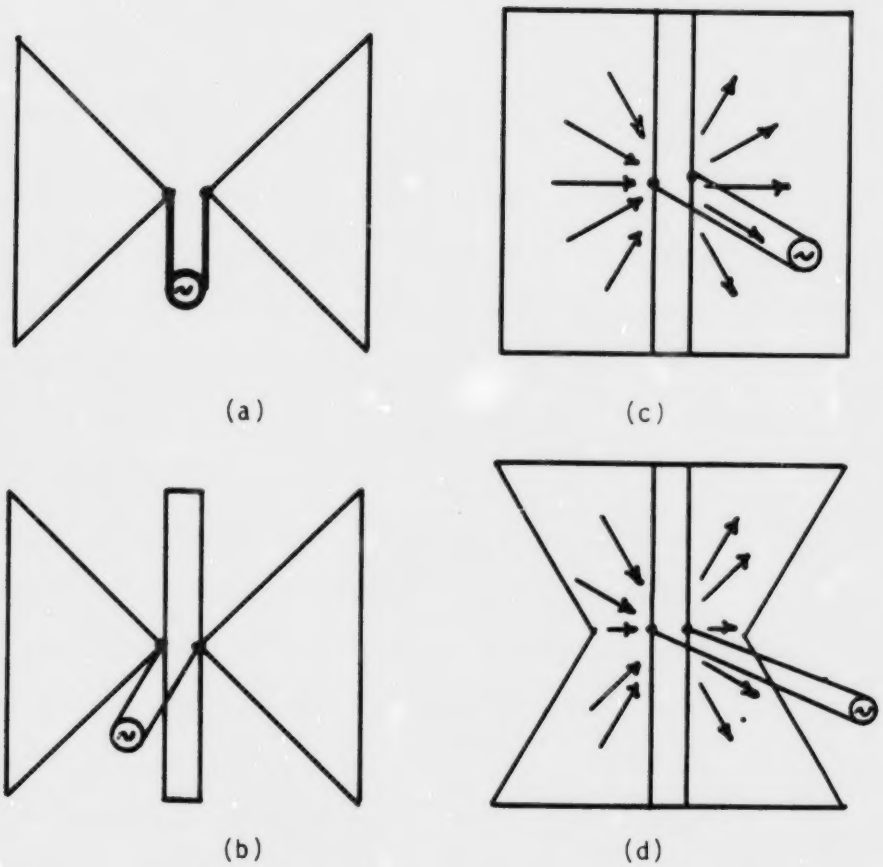

FIGURE 5 - Sketch showing various configurations of superturnstile (Bow Tie) Antenna.

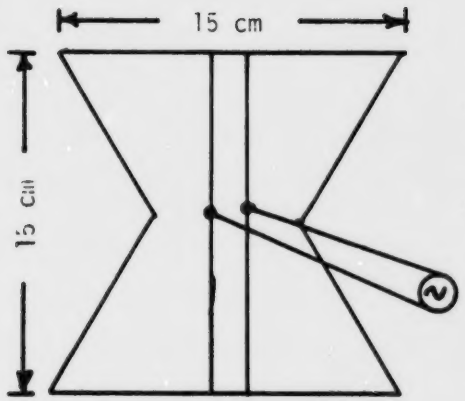

FIGURE 6(a) - Superturnstile antenna used in measurements.

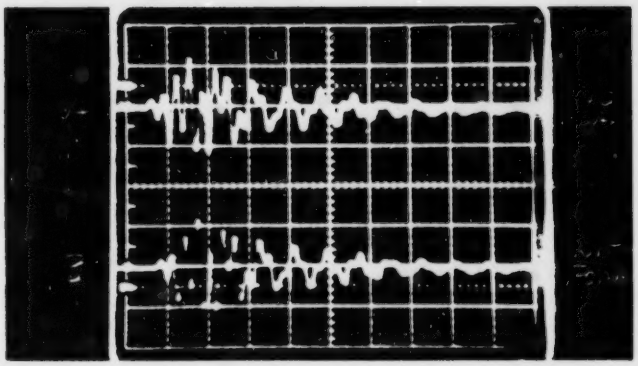

FIGURE 6(b) - Oscillograms showing signal output of superturnstile receive antenna after a 1 ns pulse is input to an identical transmit antenna. Scales 5 mV/div(Vertical) and 5 ns/div(Horizontal). Both transmit, receive antennas are housed in rectangular boxes respectively and are situated side by side. Top and bottom traces are separate measurements with and without styrofoam filler in the boxes. Typical responses showing initial mutual coupling with long last ringing which mask reflections from the wall. The ringing is a result of narrow band response.

This suggests that the antenna configuration severely distorts the transmitted signal and is not suitable for the sea ice thickness radar

2.3.3 Triangular dipole

The triangular dipole is generally regarded as a broadband antenna and has the advantage of a simple structure (see Fig. 7).

The radiation pattern of the triangular dipole is similar to that of a conical dipole except that the vertical pattern (in the yz plane) is no longer circular because of the asymmetry of its construction. The larger the values of α, the more the pattern in xy plane deviates from those in the yz plane and also the more dominant are the side lobes [3] [4]. Based on the pattern and the impedance characteristics, a compromise value of α of about 60° to 80° may be used.

Figure 7 shows the measured gain characteristics of a triangular dipole. It is seen that the antenna has a broadband characteristic with a fairly constant gain from 550 to 900 MHz.

Figure 8 shows the experimental model used for transient test. As shown in the figure, in one case the antenna was coated in the base section with resistive paint. It was believed that properly loading the antenna at the end would decrease the current amplitude at the end of antenna and, therefore, would decrease the reflected current. This in turn should decrease the standing wave current resulting in an increase in antenna bandwidth.

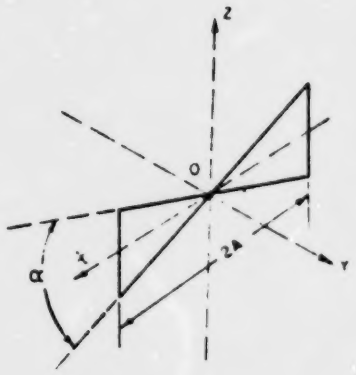

FIGURE 7(a) - Geometry of triangular dipole

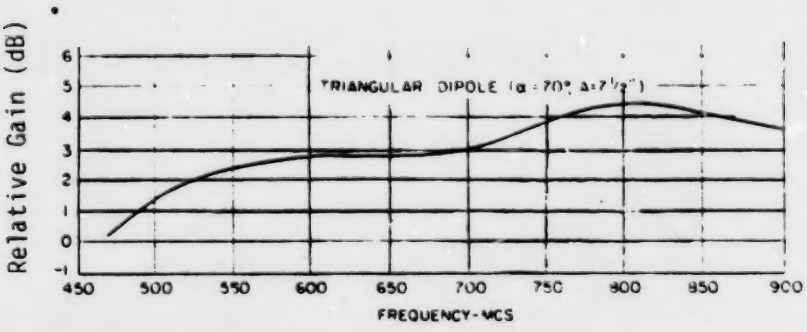

FIGURE 7(b) - Measured gain characteristics of triangular dipole (α = 70°, A = 19 cm, [3], [4]) Values of gain in dB relative to a half wave dipole.

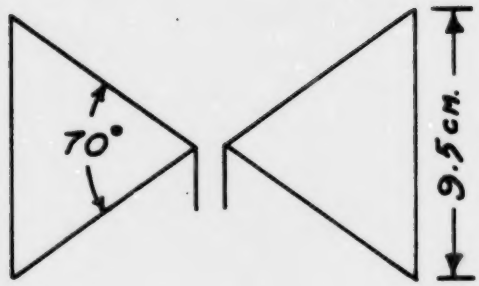

(a)

FIGURE 8(a) - Sketch showing geometry of triangular (butterfly) antenna.

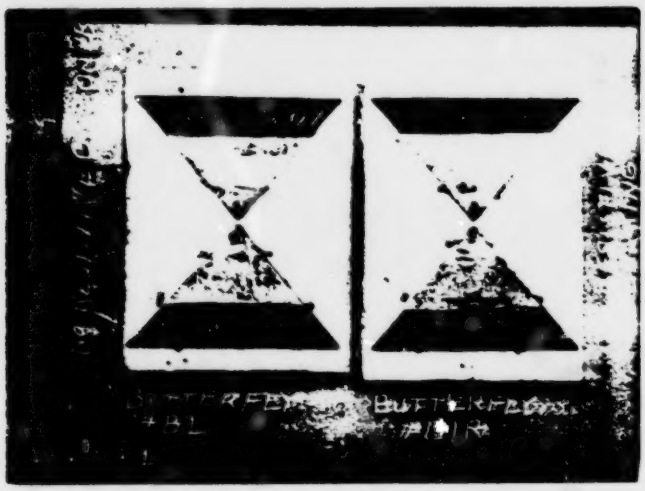

FIGURE 8(b) - Picture of triangular antenna used in experiment. Left antenna (butterfly #B1) has no resistive coating. Right antenna (butterfly #B2) has resistive coating at triangular bases as shown in photo, to study its effects on antenna response.

The signal from mutual coupling and the received signal reflected from the wall are shown in Figure 9. It is interesting to note that the ringing for both coupling and reflected signals decays rapidly after 5 nsec.

In order to investigate how the curvature of triangular antennas would affect transient response, the antennas were curved as shown in Figure 10. The mutual coupling between this type of radiator is shown in Figure 11. The ringing which lasts for about 5 nsec, indicates that such an antenna is not suitable for our applications.

2.3.4 Spiral Antenna

The properties of an antenna, impedance and radiation pattern, are determined by its shape and by its dimensions relative to the wavelength. If a structure could be defined entirely by angles (without any characteristic length dimension) then it should have characteristics that are independent of frequency [5]. One class of antenna satisfying this condition is the equiangular spiral antenna.

The geometry of the equiangular spiral antenna is shown in Figure 12. The antenna radiates a broad lobe normal to the plane of the antenna over a practical range of parameters. This radiation is bidirectional with equal beams radiated from the front and the back of the structure. The beam is circularly polarized on its axis, over the usable bandwidth. For frequencies such that the antenna arms are very short compared with the wave length, the radiated field is linearly polarized [6].

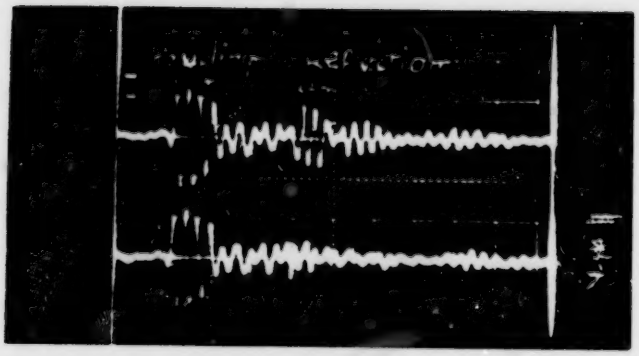

FIGURE 9 - Oscillograms showing responses of triangular transmit.receive antennas in rectangular boxes. 1 ns pulse is input to transmit antenna and received signal from output of identical antenna side by side is observed on scope. Top trace shows initial antenna mutual coupling and later reflection from a metal wall. Bottom trace is obtained with antennas facing free space. Vertical and horizontal scales are 5mV/div and 5ns/div respectively.

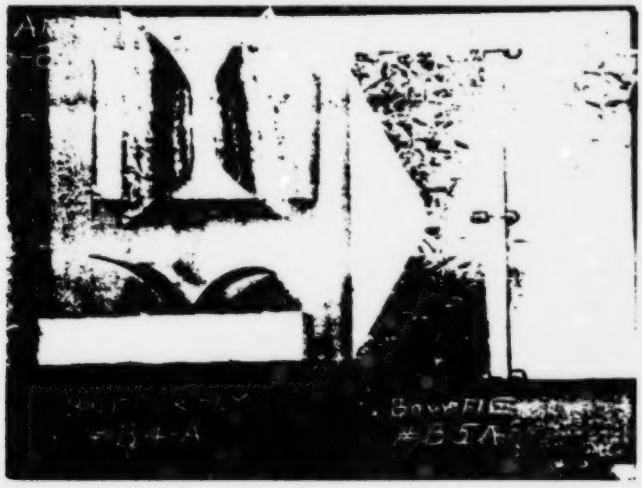

FIGURE 10 - Picture of triangular antennas with curved surface (left). Antenna on the right is a superturnstile antenna.

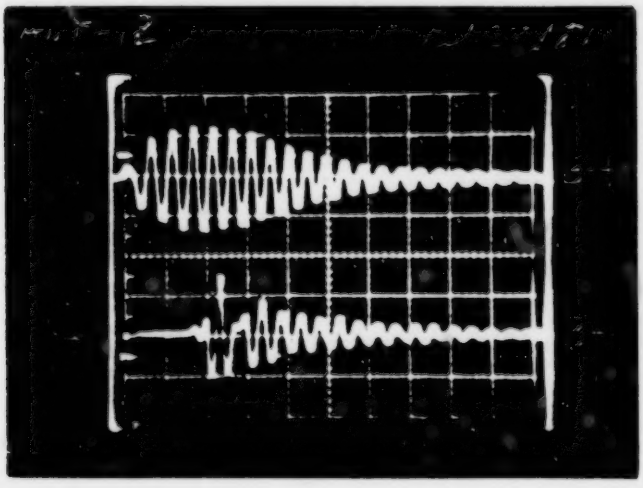

FIGURE 11 - Oscillogram showing receiver antenna output when 1 ns pulse is input to transmit antenna. Long lasting oscillations (ringing) suggest narrow band response of triangular antennas with curved surfaces.

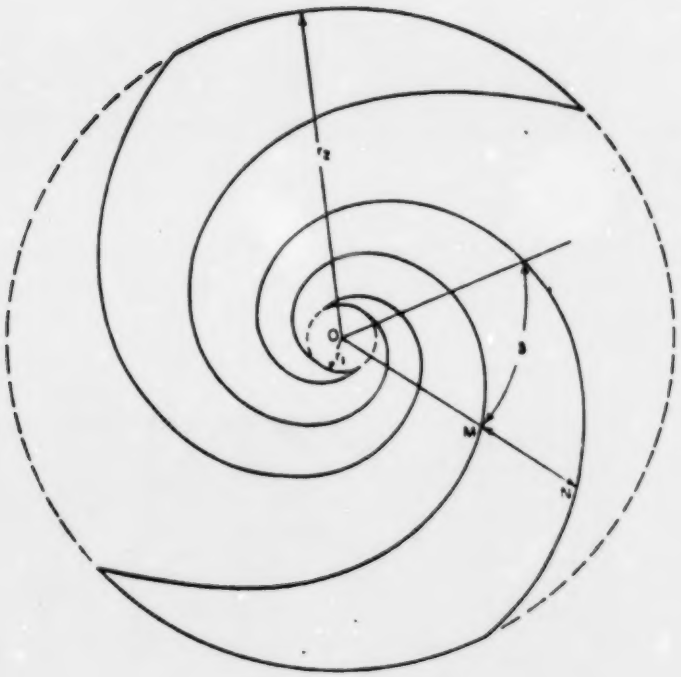

FIGURE 12 - Two arms equiangular spiral antenna. Polar coordinates (r,4) have positive polar angle in clockwise direction

A B C

FIGURE 13 - Subscale spiral antennas used in measurements. Equations defining antennas A are $r_2 = \exp(1.283\psi) = r_1/0.75$, $r_3 = r_1 \exp(-a\tau)$, $r_4 = r_2 \exp(-a\tau)$. Corresponding equations for antenna C are $r_2 = \exp(1.283\psi) = r_1/0.6$, $r_3 = r_1 \exp(-a\tau)$, $r_4 = r_2 \exp(-a\tau)$. Antenna B is a modified spiral whose second antenna arm is rearranged as shown

The bandwidth of such an antenna has been shown to be limited only by the chosen arm length and the precision of construction at the feed point. An extension of the bandwidth is a practical matter since the arm need only be of the order of one wavelength at the lowest frequency of operation. The input impedance converges with increasing frequency and properly designed spiral generally has a VSWR less than 3 when connected to a 50 ohm line.

The equiangular spiral is an antenna whose conducting arms are confined between two spirals. These spirals are identical but one of them has been rotated by a finite angle δ with respect to the other (see Fig. 12)

In polar coordinates (r, ψ), the edges of one of the spiral arms are given by

$$r_1 = k \exp (a \psi)$$

$$r_2 = k \exp (a (\psi - \delta))$$

where k, a, ψ, δ are real constants. For the second arm, the corresponding edges are given by

$$r_3 = r_1 \exp (-a\pi)$$

$$r_4 = r_2 \exp (-a\pi)$$

The subscale spiral antennas for the measurements are as shown in Figure 13. Their specific configurations are chosen for more convenient installation on a helicopter. The experimental results for the subscale spirals are given in the oscillograms Figure 14.

Again, these oscillograms show the mutual coupling between the transmit-receive antennas and the reflected signals from a metal wall at a later time. In comparison with the super-turnstile and the triangular antennas discussed previously, the spiral antenna gives a better transient response as evident by the shorter decay in ringing.

2.3.5 Modified Spiral (Fig. 13)

For completeness the properties of a modified spiral was also studied. The observed mutual coupling and reflected signals are as shown in Fig. 15 a,b. Except for minor differences, the modified spiral has essentially the same properties as the spiral antenna described in the previous section.

2.3.6 Tapered resistively loaded cylindrical dipole

The transient response of a cylindrical dipole antenna is usually characterized by a number of reflections from the ends of dipole arms. A simple pulse transmitted through the antenna can excite oscillations long after the excitation pulse is removed. This phenomenon has been demonstrated in the experimental results on other types of antennae reported earlier. An interesting approach to improve the transient characteristics of a cylindrical dipole is to load the cylinders with a series resistance or a reactance so as to reduce or prevent the multiple reflections. One such «reflection free» antenna reported by Wu and King [7] has dipole arms whose internal resistance per unit length are tailored to enable

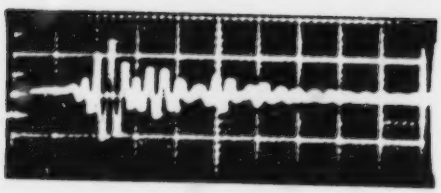

FIGURE 14 - Oscillogram showing transient response of spiral antenna whose geometry is given by $r_2 = r_1 / 0.75$. Signal in oscillogram is the receive antenna output when a 1 ns pulse is input to an identical antenna. Initial 5 ns are dominated by mutual coupling. Later signals are from reflections from metal wall. Vertical scale is linear at 20 mv/div. Horizontal scale is 5 ns/div.

(a) (b)

FIGURE 15 - Oscillograms showing mutual coupling and reflections from metal wall 1 m away from antennas.
Oscillograms (a) and (b) correspond to Antennas A and C respectively in Fig. 13.

Vertical scale is linear at 20 mv/div. Horizontal scale is 5 ns/div.

purely outward travelling waves. Wu and King have developed the theory for the case where the impedance per unit length of cylindrical antenna depends on the position on the dipole arm and the current is represented by an outward travelling wave with no reflected wave. The computations showed that such an antenna should have broadband characteristics if it could be built. Since this type of antenna has a constant input impedance over a relatively wide range of frequencies, it is likely to possess a transient response suitable for a sea ice thickness sensor.

Figure 16 shows the power pattern measurements of a resistively loaded antenna, having a cross-section of 0.2 cm and a half-length of 25 cm. Its broadband characteristics is demonstrated by the smoothness and uniformity of the pattern over the frequency range tested (0.3 to 26 GHz [8]).

Figure 17 gives the input impedance of the same antenna as a function of frequency. The variation of input admittance is relatively small up to 3 GHz. Therefore, a very broadband resistive antenna which exhibits no resonance effect can be practically realized.

As it was mentioned before, the distribution of resistance along the antenna would have a peculiar form in order to obtain a very broadband characteristics. The internal impedance per unit length should be a function of position, increasing toward the end of antenna. Such an arrangement is expected to reduce

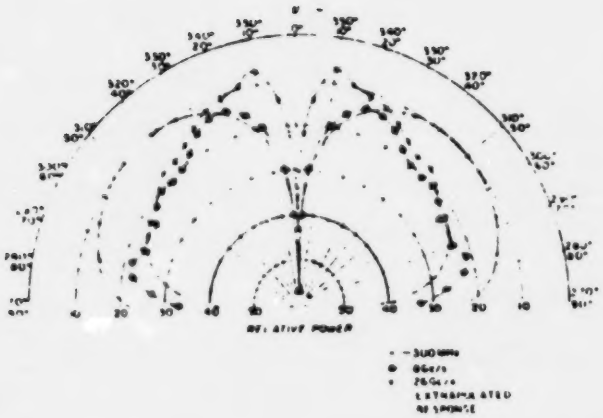

FIGURE 16 - Relative power versus angle θ for a tapered resistive loaded cylindrical dipole at frequencies of 0.3, 8 and 26 GHz. Antenna wire cross section is of radius 0.2 cm and half length is 25 cm. (See reference [8])

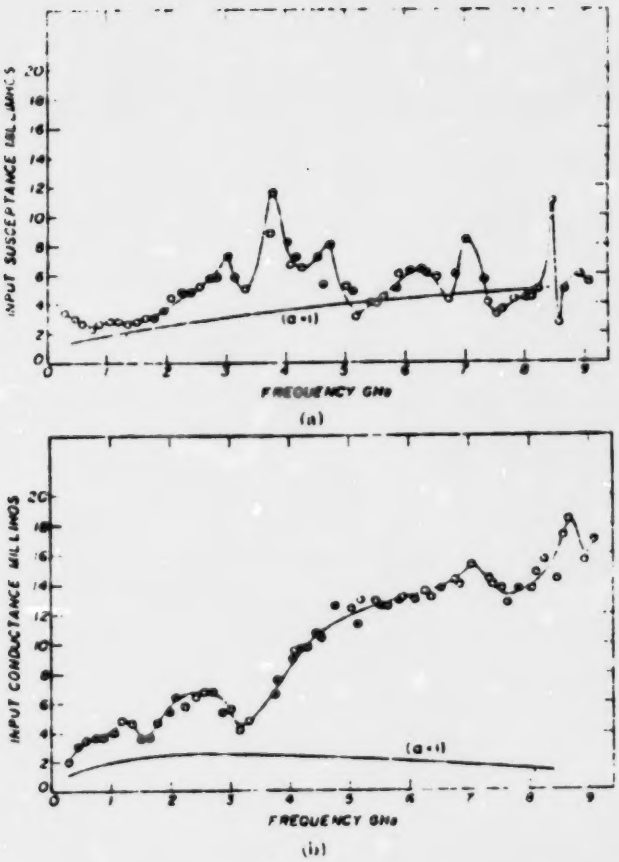

FIGURE 17 - Input impedance of a tapered resistive loaded antenna vs frequency with antenna wire cross section radius of 0.2 cm and half length of 25 cm. (a) input susceptance, (b) input conductance (See Reference [8])

the reflections of current from the end of the antenna arms allowing purely outward travelling waves.

Strictly speaking, the resistance per unit length (specific resistance) should be continuously increasing towards the end of each dipole arm. However, for ease of fabrication, each antenna arm is divided into a number of sections of suitable lengths. Within each section, the specific resistance is constant and is equal to the averaged value calculated for that particular section. The resulting distribution of impedance along the dipole arm is a series of steps that zigzags around the desired smooth curve [9].

For the present study, a tapered resistively loaded cylindrical dipole has been designed for a scaled centre frequency of 1 GHz (corresponding to the real VHF centre frequency of 100 MHz). The value of the specific resistance along the dipole arm has been computed according to the theory [9] with the help of a computer program. Each dipole arm is fabricated from a plexiglass rod having a diameter of .6 cm, a length of 7.5 cm. The resistive loading is obtained by dividing the dipole arm into five sections, each of which is coated with a carbon-based conductive coating (ECCOCOAT 258A by Emerson and Cumming) to a desired specific resistance. The dipole is symmetrically fed by a 50 ohm semi-rigid coaxial cable through a wide band balun (TP-103 by ANZAC). Details of the antenna construction is shown in Figures 18 and 19.

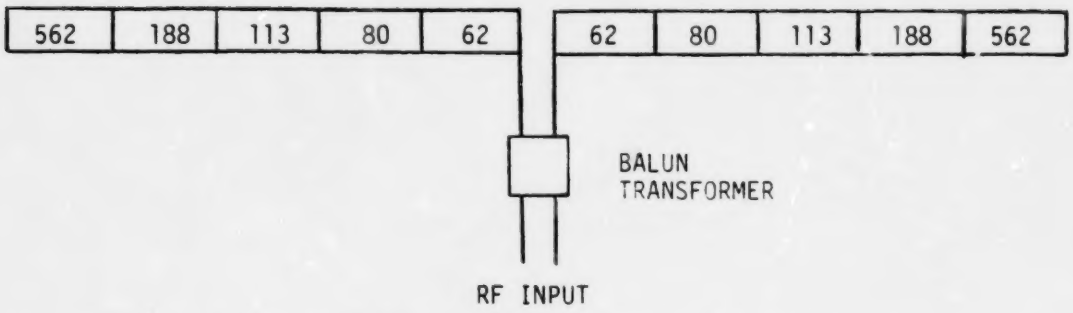

Fig. 18: Tapered resistively loaded antenna with value of resistance in ohms on each subsection

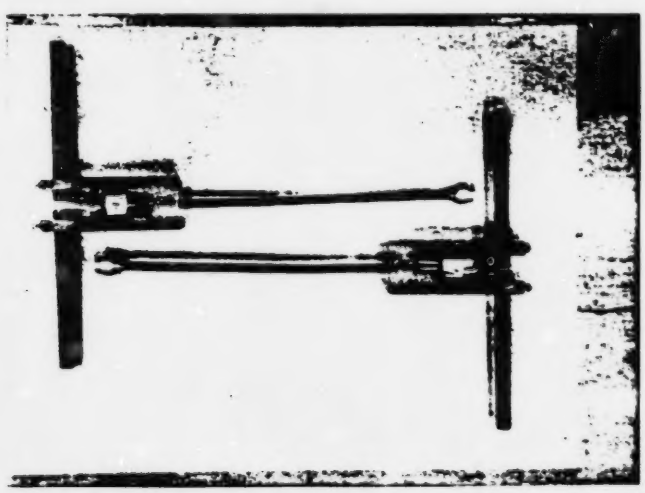

Fig. 19: Tapered resistively loaded antenna with broadband transformer balun fed by semirigid coaxial cable

The mutual coupling between two resistively loaded dipoles in a rectangular cavity (see Section 2.2) facing the free space, is shown in Figure 20. It is found to vary significantly depending on the location of the dipole from the front end and the bottom of the rectangular reflector box. The closer the dipole is to the reflector front end, the larger the mutual coupling.

The superior transient response of the TRLD is demonstrated by the received signal of a 1 nanosecond dc pulse. The received signal has no significant ringing and it resembles fairly well the transmitted pulse except for the negative going signals besides the main pulse -- a result of passing a dc signal through an ac circuit. A comparison between the TRLD and the superturnstile antennas are shown in Figure 21, where the former shows significantly less ringing.

2.3.7 Summary

Subscale antennas have been studied for various candidate antenna configurations. Although antennas such as superturnstile, triangular, etc. show fairly broadband characteristics, their respective bandwidths and transient response are not adequate for the sea-ice thickness radar requirements. Resistively loaded dipole, on the other hand, demonstrates a good transient response and should be useful for the sea-ice sensor applications. In the next section, the radiation and circuit properties of tapered resistively loaded dipole in different types of reflector cavity is investigated. In addition, the antenna interaction with helicopter body is studied.

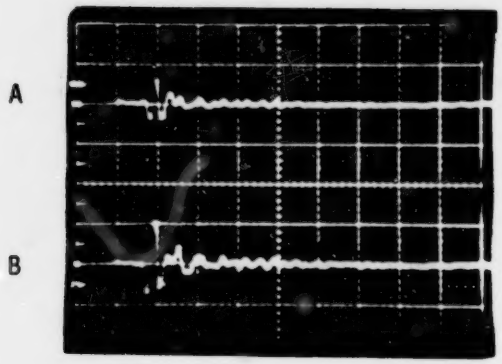

FIGURE 20 - Mutual coupling between two resistively loaded antenna when they are facing the free space. Input signal is 1 nsec. pulse and scope sweep is 5 nsec/div.
(A) antenna is spaced 5 cm from bottom of box
(B) antenna is spaced 5 cm from bottom of box

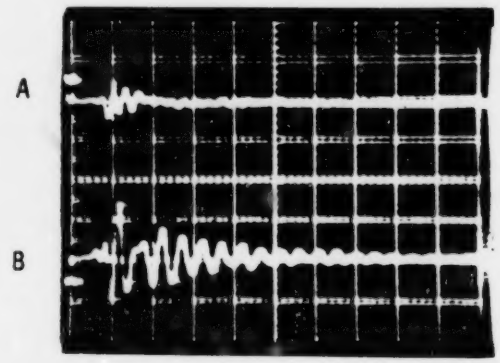

FIGURE 21 - Comparison between two resistively loaded dipole with that of two triangular antennas. Scope sweep is 5 nsec/div and input pulse is 1 nsec in width.
(A) mutual coupling for TRLD
(B) mutual coupling for triangular

3.0 STUDY OF CAVITY BACK ANTENNAS

3.1 General Requirements

The general requirements for a helicopter borne antenna for the sea-ice thickness sensor have been discussed in Section 1.2. During the early stage of the antenna development, it was not clear what antenna reflector configuration would be best aerodynamically for the helicopter. Discussions with helicopter pilots and aerodynamic experts from Transport Canada generated concerns about the airworthiness of any reflector of realistic dimensions and configurations.

Despite the initial uncertainty on the reflector configuration and airworthiness, it was decided that the configuration should be either cylindrical or rectangular. The cylindrical reflectors were to be installed beside the skids of the helicopter while the rectangular reflectors were for installation under the helicopter. As a result, these two configurations were chosen for the subscale antenna tests.

3.2 VSWR Measurements

The experimental arrangement for evaluating the antenna matching and the reflection of signals from the antenna input terminal is as sketched in Figure 22. It is chosen for its simplicity and the fact that it can be used for both the steady state and the pulsed RF signals respectively. The antenna is connected to the «input» port of the power divider (Model T-1000 by ANZAC). RF signals are fed to the «output» port A and transmitted to the antenna through the «input» port B. Reflected signals from the antenna are divided equally between the A and C ports and monitored by a detector and an oscilloscope. The minimum

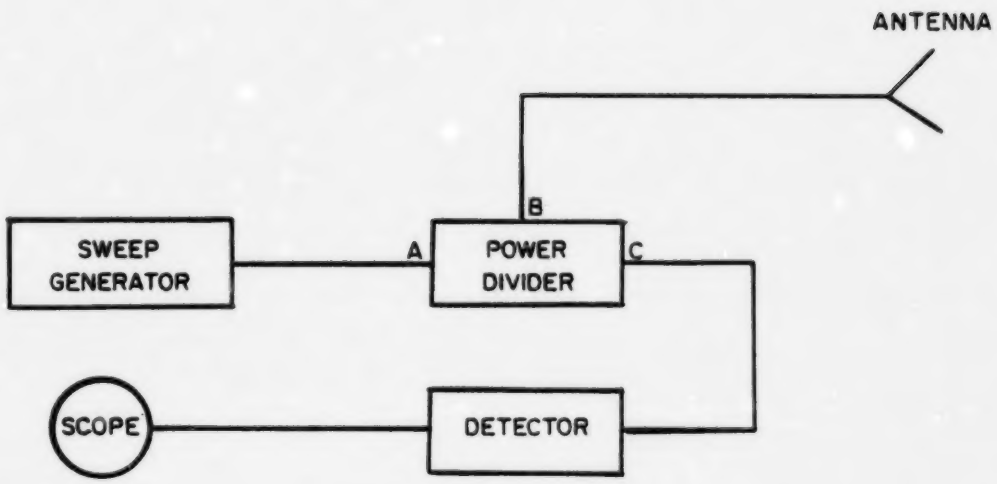

FIGURE 22 - Block diagram of experimental arrangement for antenna VSWR measurement.

isolation between port A and C is 25 dB.

The voltage standing wave ratio (VSWR) is measured first by replacing the antenna with a short circuit to produce maximum reflections at the antenna terminal. The frequency response of the measuring system is calibrated by sweeping the generator frequency from 100 MHz to about 1.5 GHz and observing the reflected signal at the detector output. The same procedure is then repeated with the antenna properly reconnected. The magnitude of the reflection coefficient R as a function of frequency is obtained from the ratio of the corresponding reflected signals from the two measurements. The VSWR is computed from the usual formula

$$VSWR = (1-R) / (1+R)$$

Results of the VSWR measurements for the tapered resistively loaded dipole (TRLD) in (A) a cylindrical reflector (B) a rectangular box with a square aperture, and (C), a rectangular box with a rectangular aperture, are as follows:

(A) Cylindrical Reflector

The reflected signal from TRLD in a cylindrical reflector 17.5 cm wide by 6 cm high by 4.5 cm deep are as shown in Figure 23. For steady state measurements, the swept frequency was between 100 MHz to 1350 MHz (see Figures 24 a to e).

The VSWR computed from these results are given in Figure 25.

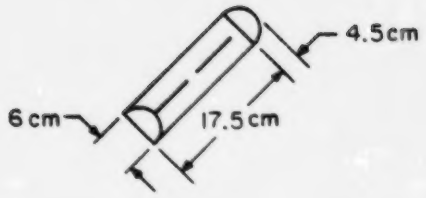

FIGURE 23 - Geometry of cylindrical reflector

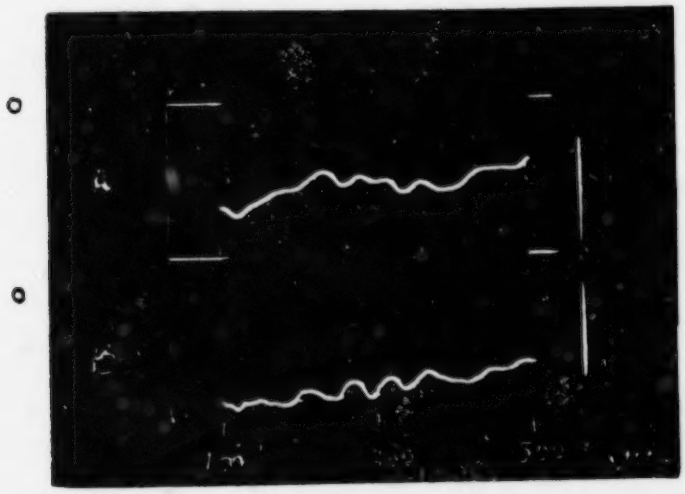

FIGURE 24(a)

FIGURE 24 - Comparison between signals reflected by TRLD antenna in cylindrical box and a short circuit respectively at various frequencies from 100 to 500 MHz. (Fig. 24a). 500 to 900 MHz (Fig. 24b c) and 900 to 1350 MHz (Fig. 24d, e). Signals are negative. Vertical scale is 10mV/div.

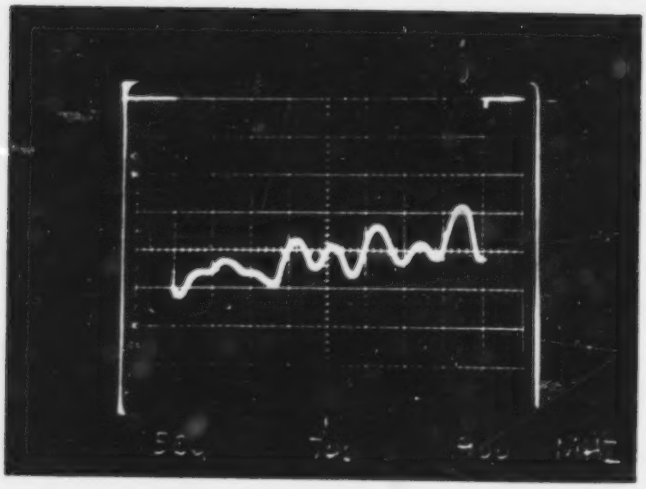

FIGURE 24(b) - Short circuit

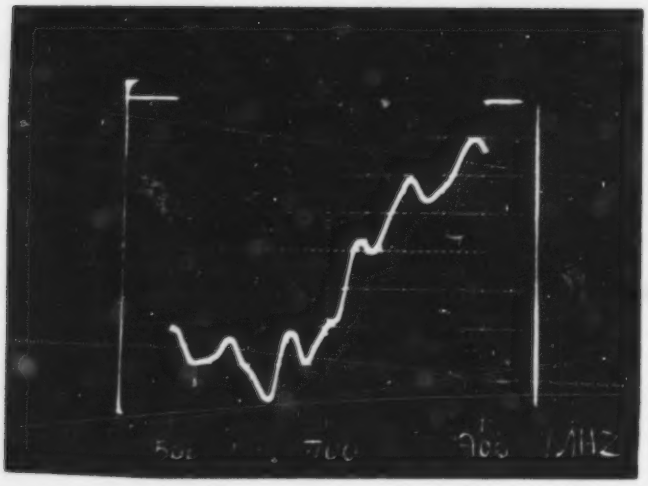

FIGURE 24(c) - Antenna

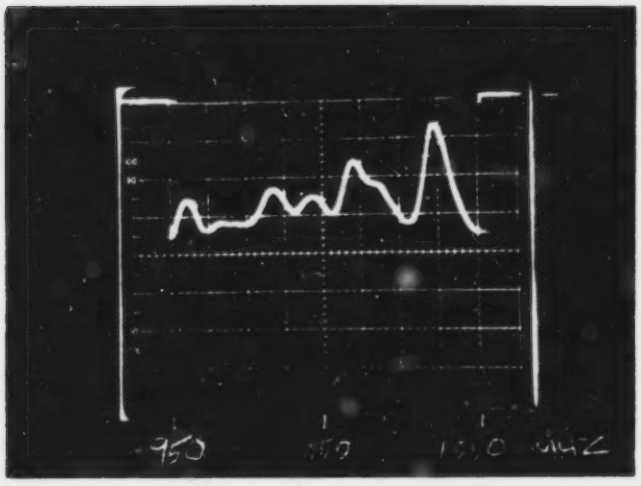

FIGURE 24(d) - Short circuit

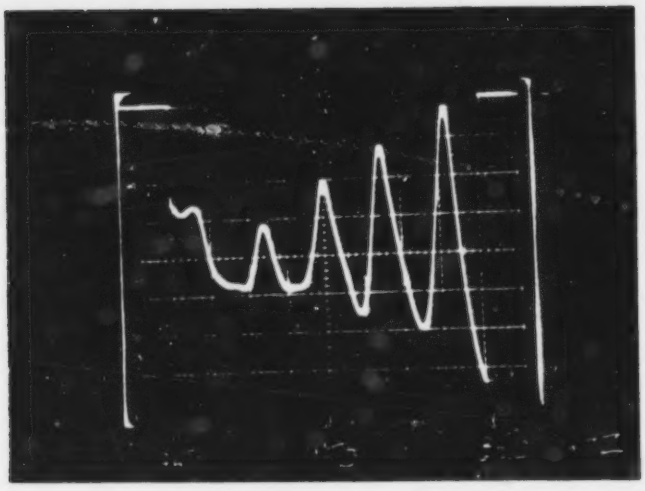

FIGURE 24(e) - Antenna

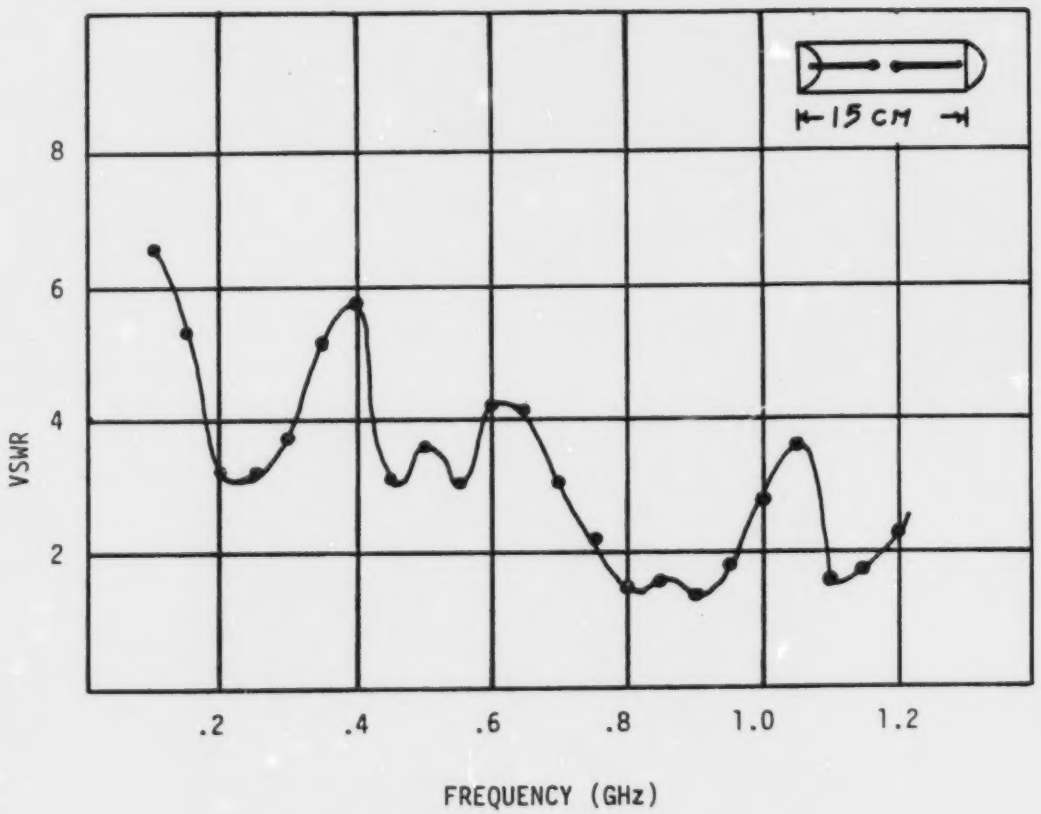

FIGURE 25 - VSWR of a tapered resistively loaded dipole in a cylindrical cavity versus frequency.

(B) Rectangular Box with a Square Aperture

A rectangular reflector with a square opening and a driving antenna located along a diagonal. This configuration has been studied because it has the most compact arrangement for a rectangular reflector. The dimensions of the box are 13 cm by 13 cm by 5 cm deep. The antenna is recessed 1 cm from the opening. Results for this antenna configuration are shown in Figures 26 a to f, and Figure 27. Figures 26 a to f give the reflected signal and Figure 27 gives the computed VSWR versus the frequency.

(C) Rectangular Box with a Rectangular Aperture

Results of the measurements for a rectangular box with a rectangular aperture, 20 cm (width) x 12 cm (height) x 7.5 cm (depth), are shown in Figures 28 a to f. The calculated VSWR is given in Figure 29.

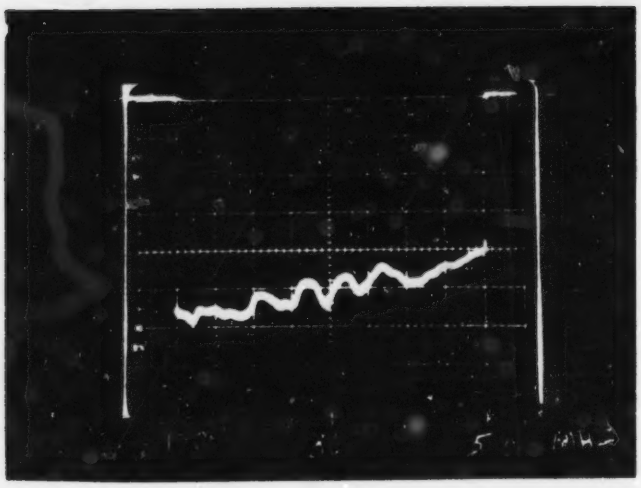

FIGURE 26(a) - Short Circuit

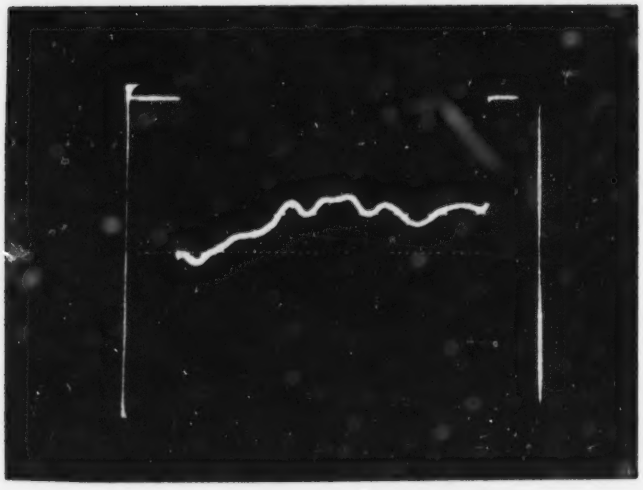

FIGURE 26(b) - Antenna

FIGURE 26 - Reflected signals from a short circuit and TRLD antenna in a square box respectively for various frequencies from 100 to 500 MHz (Fig. 26a, b), 500 to 900 MHz (Fig. 26c, d) 900 to 1350 MHz (Fig. 26e, f). Signals are negative. Vertical scale is 10 mV/div.

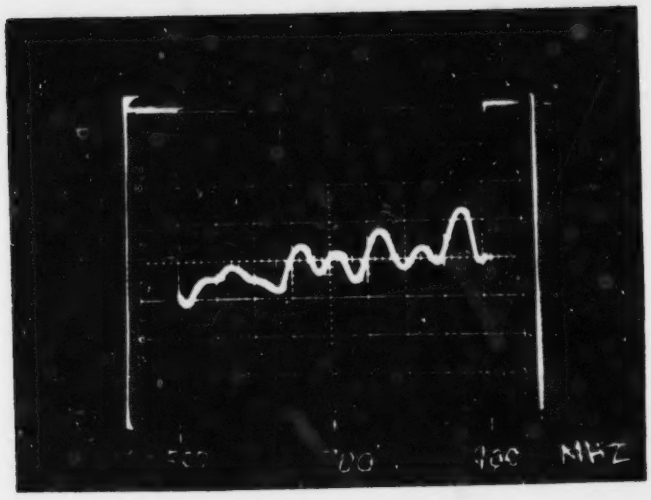

FIGURE 26(c) - Short Circuit

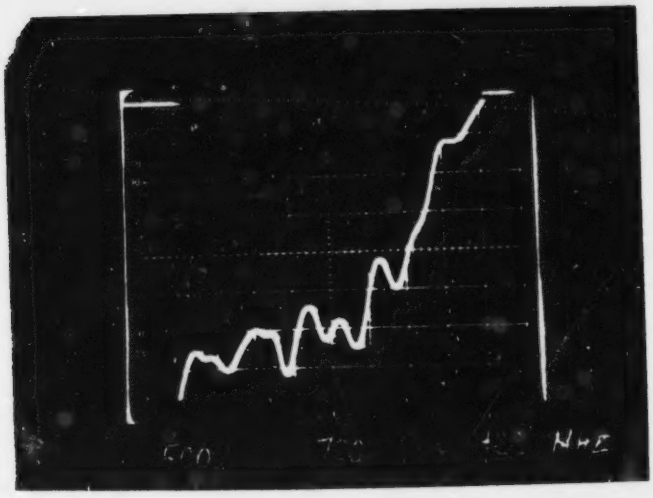

FIGURE 26(d) - Antenna

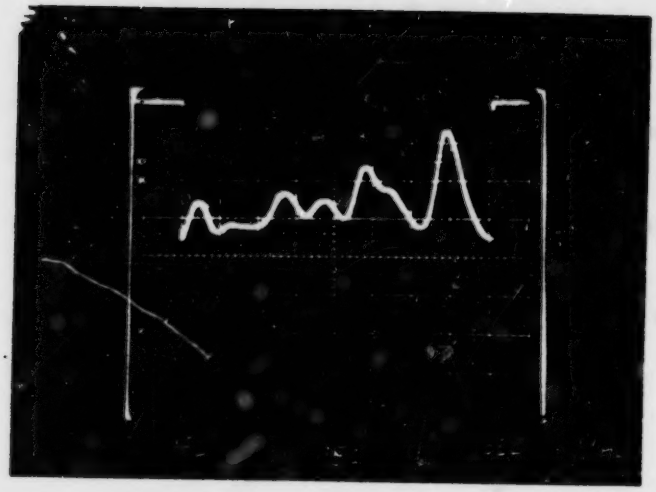

FIGURE 26(e) - Short Circuit

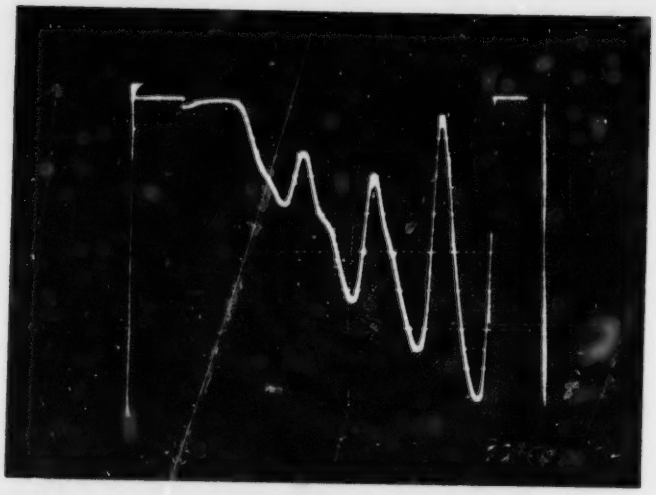

FIGURE 26(f) - Antenna

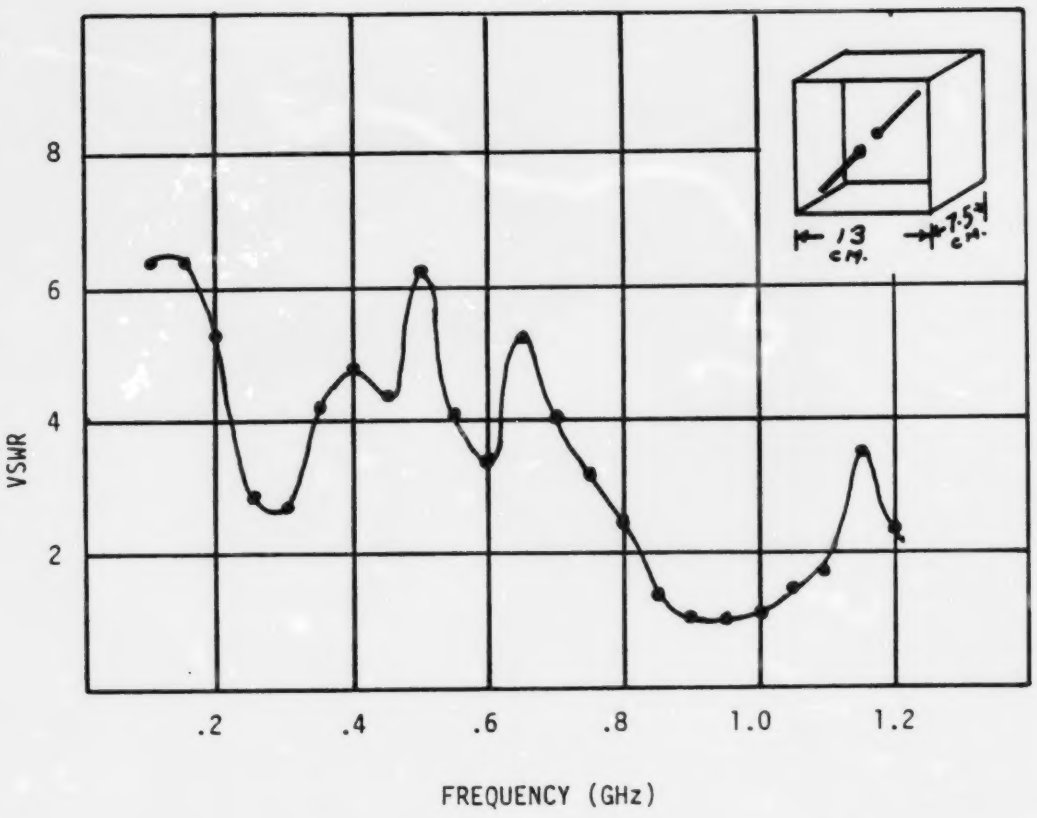

FIGURE 27 - VSWR of tapered resistively loaded dipole in square box, versus frequency

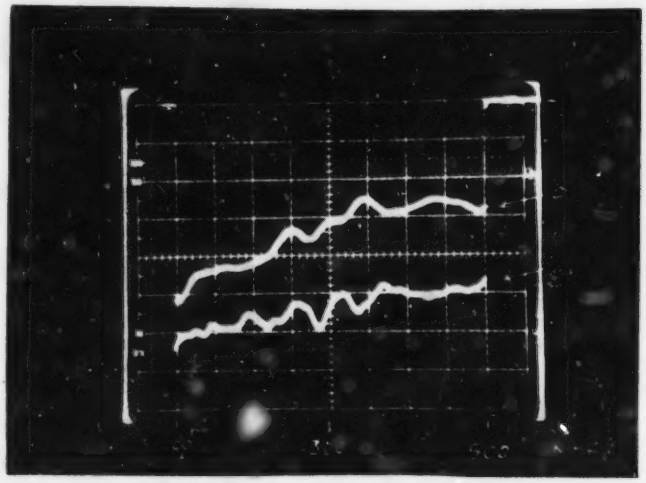

FIGURE 28(a) - 100 to 500 MHz

Fig. 28 - Comparison between the amplitude of reflected signal from the TRLD antenna in a rectangular box and that of a short circuit respectively from 100 to 500 MHz (Fig. 28a), 500 to 900 MHz (Fig. 28b), and 900 to 1350 MHz (Fig. 28c). Signals are nagative at 10mV/div. In each figure, (A) gives reflection from antenna and (B) from short circuit.

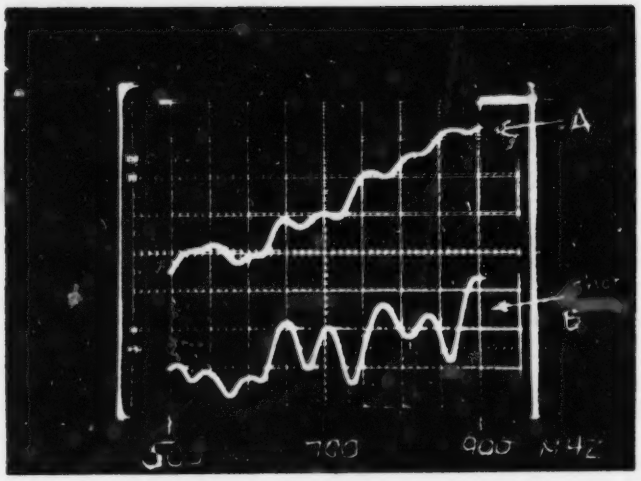

FIGURE 28b - 500 to 900 MHz

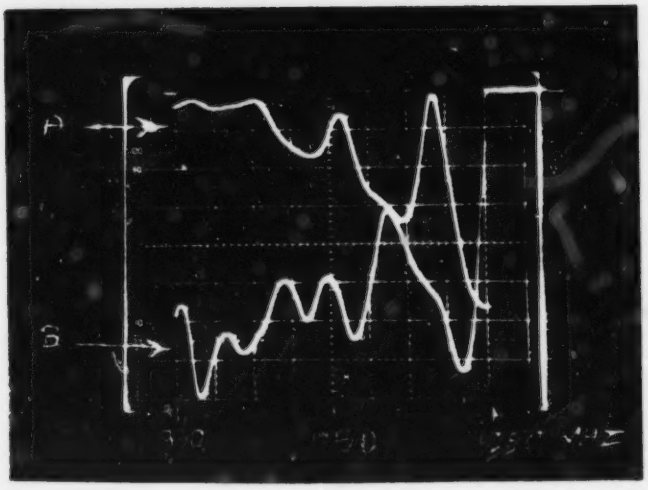

FIGURE 28c - 900 to 1350 MHz

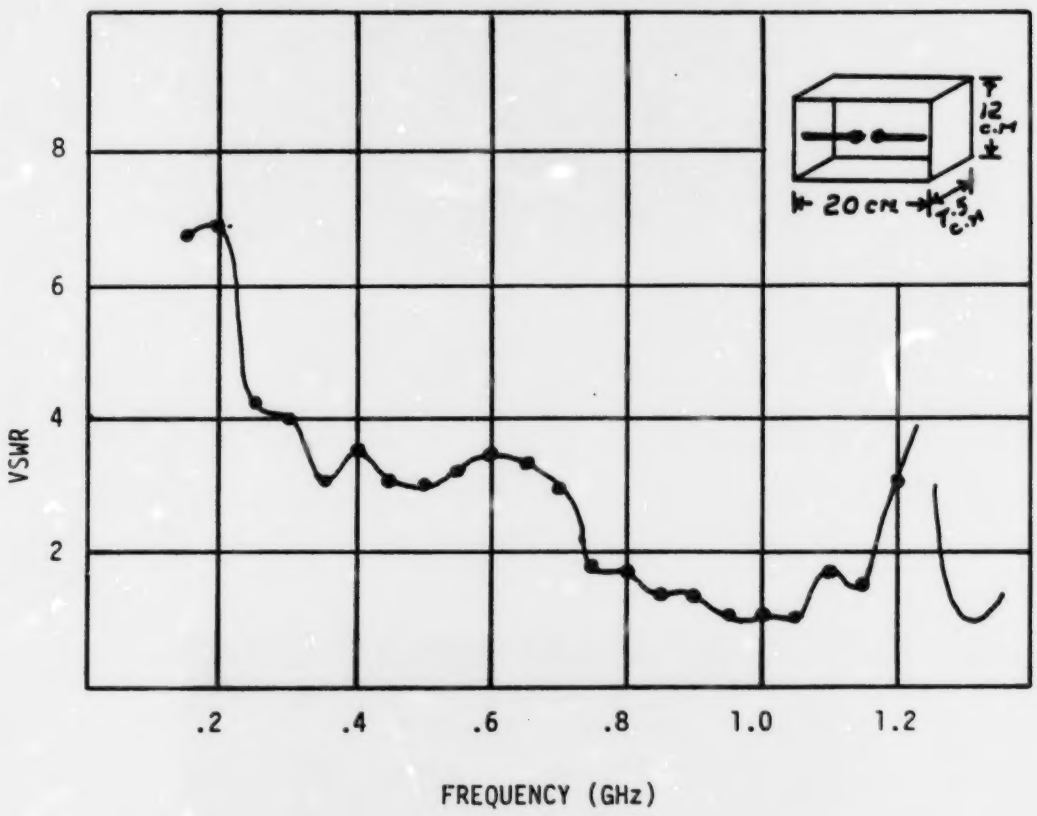

FIGURE 29 - VSWR of tapered resistively loaded cylindrical dipole in a rectangular box.

3.3 Discussion on VSWR results

Comparing VSWR of three different reflector cavity used in measurement shows that the TRLD antenna in rectangular aperture (Case (C)) has the best VSWR of the three. Its VSWR is less than 3.5 above 330 MHz, except around 1225 MHz where it starts to fluctuate. The VSWR of this type of antenna system is less than 2 from 830 - 1170 MHz. The antenna in cylindrical cavity is slightly higher but it has the advantage of being more compact than the other two. The VSWR for the antenna with a square aperture lies between VSWR of the other two. Its size is a compromise between those of the other two, as well. There are several limitations in the measuring system which tend to degrade the genuine antenna characteristics at frequencies beyond 1,000 MHz. First, the combination of the transformer balun at the antenna input terminal and the power divider has a workable frequency range between 10 MHz and 1,000 MHz. The measured frequency characteristics beyond 1,000 MHz for the various configurations are subjected to errors. However, when the scaled frequency is above 1,000 MHz, the actual frequency for the full-size antenna would be beyond 100 MHz, and would correspond to a wavelength smaller than 3 metres. Measurements corresponding to these frequencies become manageable and can be obtained using the full size antenna.

No attempt has been made to reduce the VSWR by introducing impedance matching devices at the antenna terminal. Firstly, it would be difficult to obtain a good impedance match over a large bandwidth. Secondly, the impedance matching techniques and devices for the subscale antenna would be significantly different either in construction or in principle from those actually used in a real size VHF antenna. Impedance matching will, therefore, be done after the latter is chosen and constructed.

4.0 ANTENNA RADIATION PATTERN MEASUREMENTS

4.1 Siting Considerations

In principal, the far field radiation pattern of a test antenna can be obtained by transmitting signals from the test antenna and receiving signals with a probing antenna at a distance R $2D^2/\lambda$ where D is the characteristic dimension of the antenna aperture and λ the signal wavelength (see [13]). For minimum disturbance by ground reflections, the probing antenna should have an adequate directivity and both the transmitting and the probing (or receiving) antennas should be as far above the ground as possible to avoid reflections due to the ground or other nearby objects. A detailed discussion of the antenna measurements has been given in [13].

For VHF antennae where the minimum frequency is 30 MHz, the minimum height for an elevation of three wavelengths is about 30 meters and the radiation pattern measurements require a test range with an antenna tower at considerable heights.

Measurements of the corresponding radiation pattern at the subscale frequency enables meaningful measurements to be taken in a reasonably small test range in the laboratory.

4.2 Experimental Arrangement & Results

The transmitting antenna was a tapered resistively loaded dipole in a reflector cavity. The receiving antenna had the same type of dipole as the transmitter, but placed in a cylindrical cavity. Both antennas were placed on a pair of masts of equal length so that their respective phase centers were on a horizontal line.

The distance R between the transmit and receive antennas was chosen so that it can always satisfy the relation $R \geq 2D^2/\lambda$ in the highest frequency of interest.

The block diagram of experimental arrangement is shown in Fig. 1. The transmitting antenna radiates power, part of which is intercepted by the receiving antenna. The received power after amplification by a broadband amplifier (50 - 15000 MHz, by TRONTECH) is fed to a power meter whose output is monitored by a chart recorder.

Figure 30 shows the receiving antenna on a mast in an anechoic chamber.

The E-plane radiation patterns of a TRLD in cylindrical box are given in Figure 31 for different frequencies. Two dipole locations in the cavity were used. Those curves which are labelled (1) are for the dipole location at the front end of reflector, (i.e., when the dipole is flush with the open end of the box). Those with label (2) are for dipole about 1/4 inches recessed from the front end. These measurements show that the sensitivity of the antenna is higher when it is farther away from the back of the cavity, but the side lobes of the radiation patterns are, in turn, higher.

The H-plane radiation patterns of the antenna in cylindrical cavity are given in Figure 32.

The radiation pattern for the TRLD in a cylindrical reflector has a reasonable H plane pattern and beamwidth. There is no unusually large sidelobes except at frequecies below .3 GHz or above 1.2 GHz. The E plane pattern has significant sidelobes and is

strongly dependent on the location of the TRLD inside the cavity. The measured patterns suggest that the cylindrical reflector may not be able to shield the antenna radiation from antenna aircraft interaction.

As expected, the radiation pattern for a rectangular reflector (Fig. 33, 34) has a reasonable typical half power beamwidth of about 100 degrees at low frequencies between .3 and 1 GHz. The beamwidth narrows above 1 GHz to about 60 degrees at 2 GHz. There is negligible sidelobes at most frequencies suggesting that the reflector cavity can help in reducing antenna aircraft interactions considerably. Thus, even if the reflector cannot increase the directivity significantly, its presence enables the antenna to operate quite independently with small interference from the helicopter body.

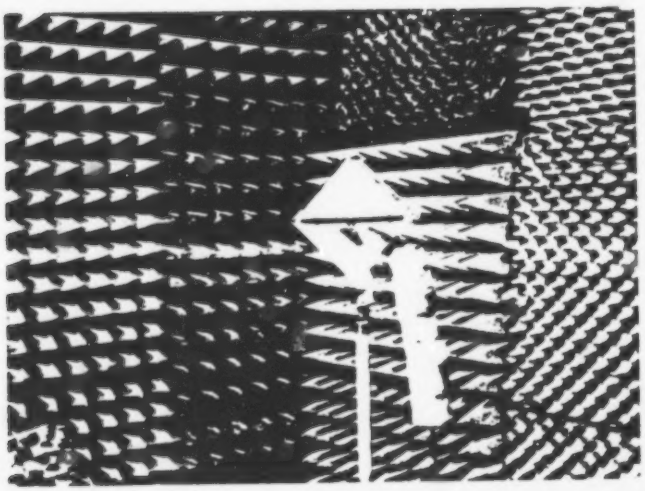

FIGURE 30 - Tapered resistively loaded antenna in cylindrical rectangular reflector in anechoic chamber for power radiation pattern measurements

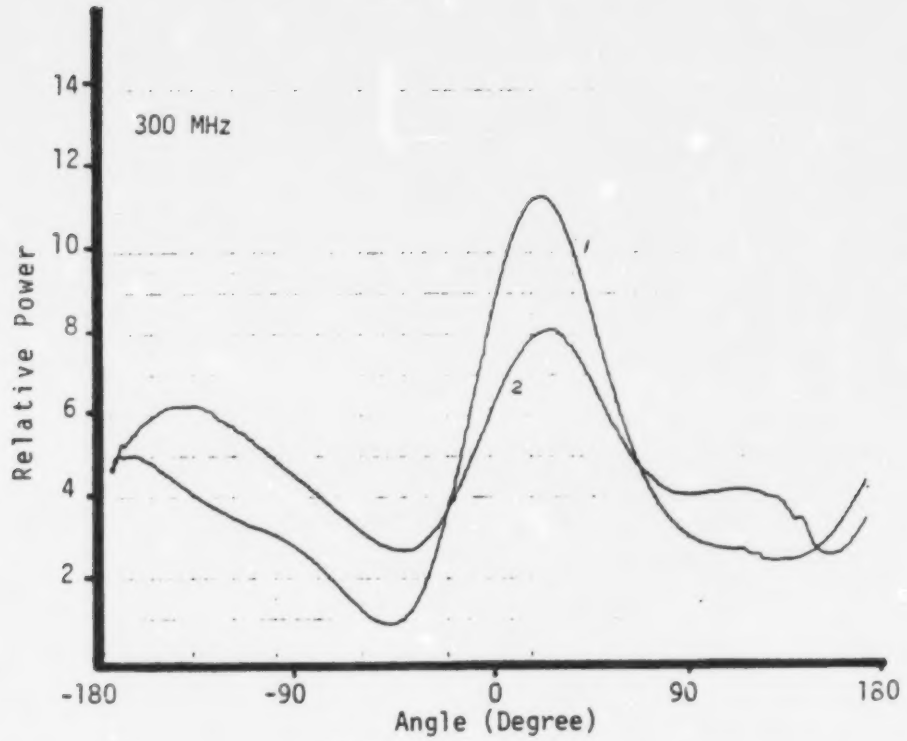

FIGURE 31(a)

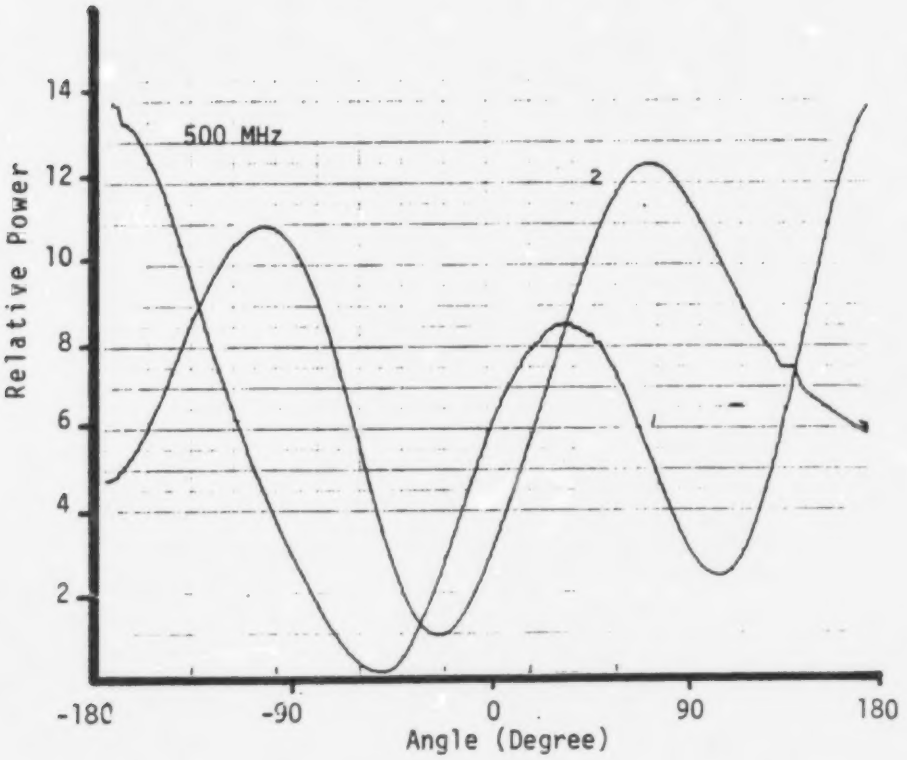

FIGURE 31(b)

FIGURE 31 - E-Plane Radiation Pattern of a TRLD in a cylindrical cavity.

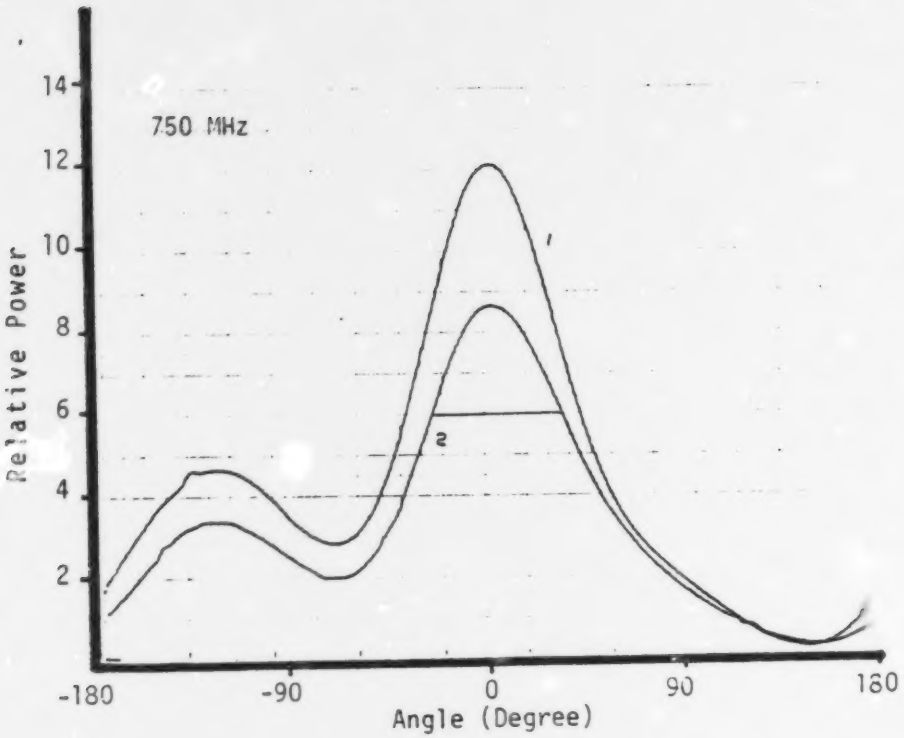

FIGURE 31(c)

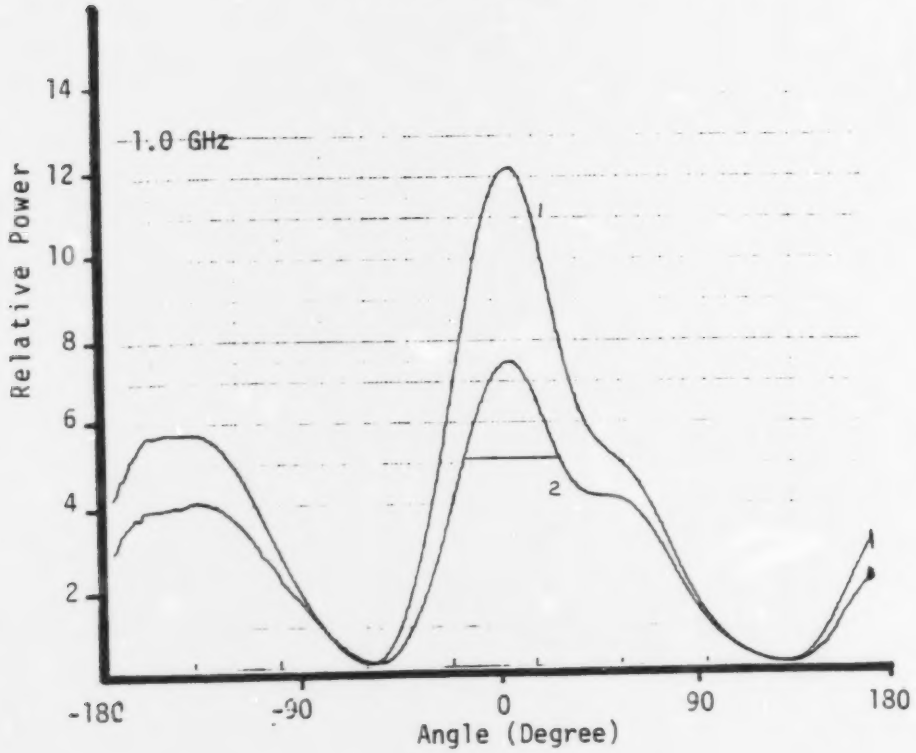

FIGURE 31(d)

FIGURE 31 - E-Plane Radiation Pattern of a TRLD in a cylindrical cavity

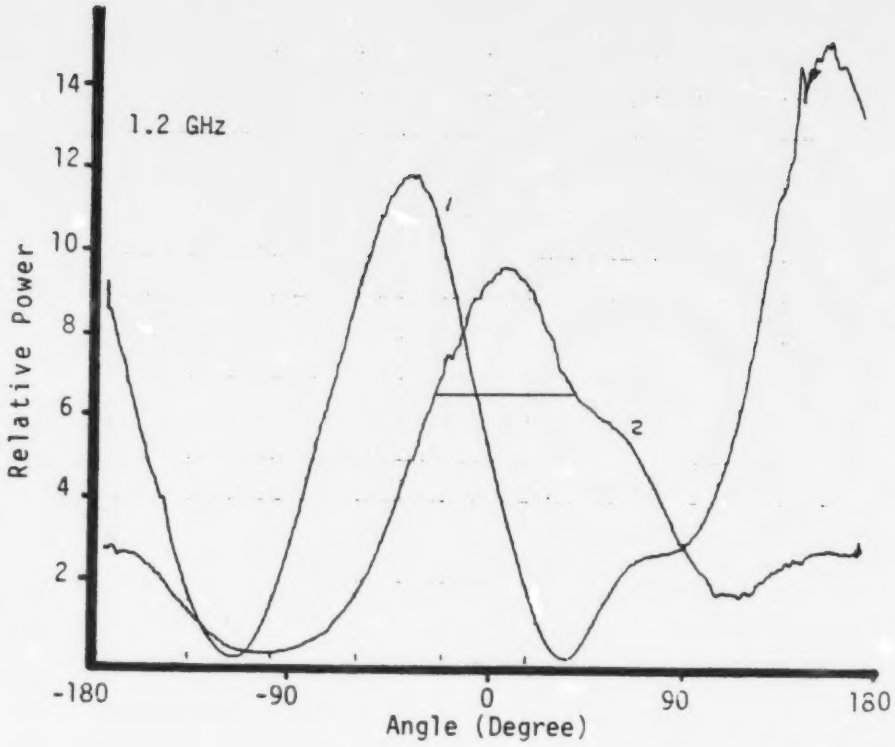

FIGURE 31(e)

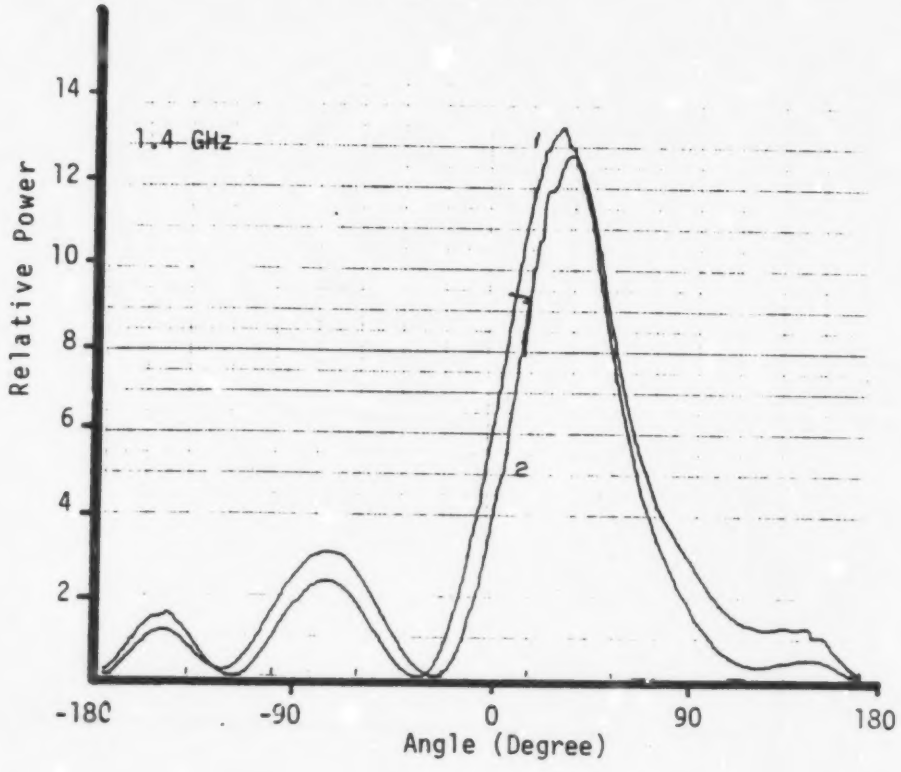

FIGURE 31(f)

FIGURE 31 - E-Plane Radiation Pattern of a TRLD in a cylindrical cavity

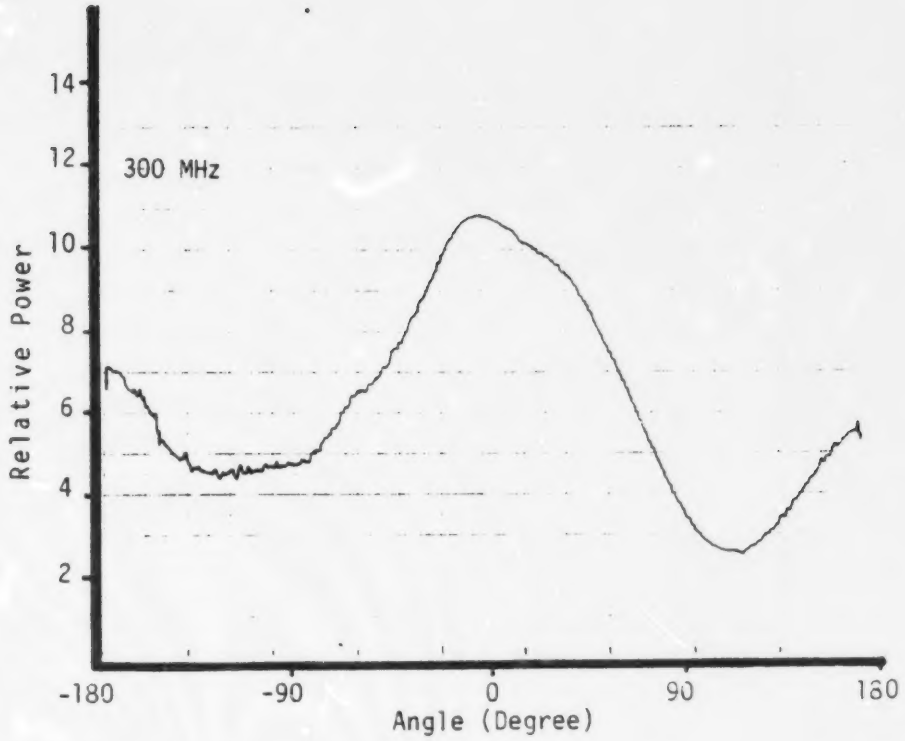

FIGURE 32(a)

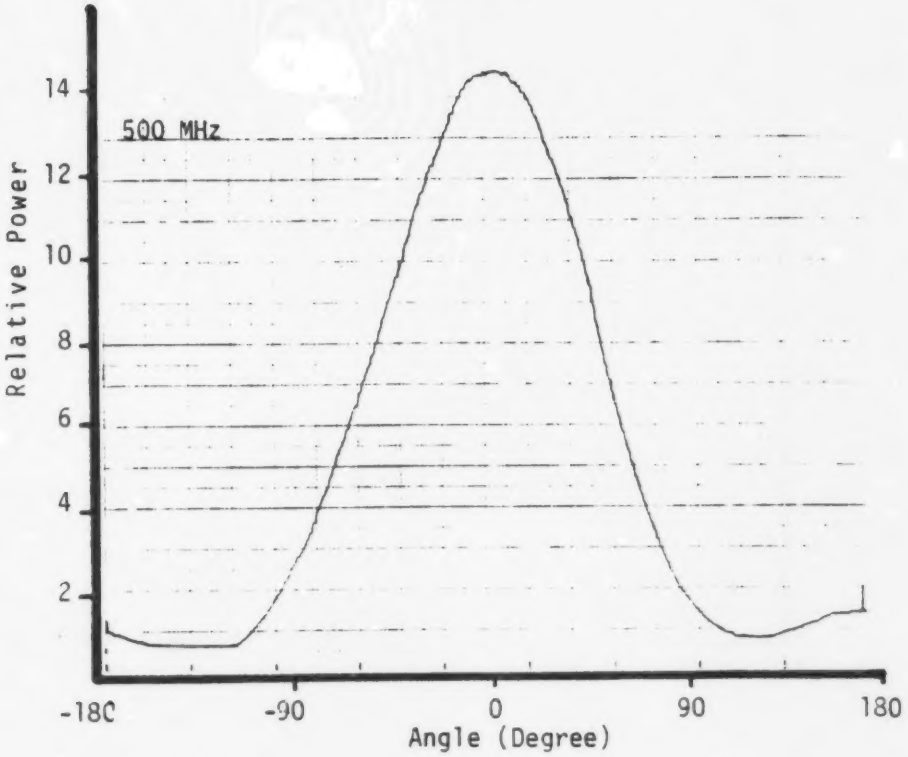

FIGURE 32(b)

FIGURE 32 - H-Plane radiation pattern for TRLD in a cylindrical cavity

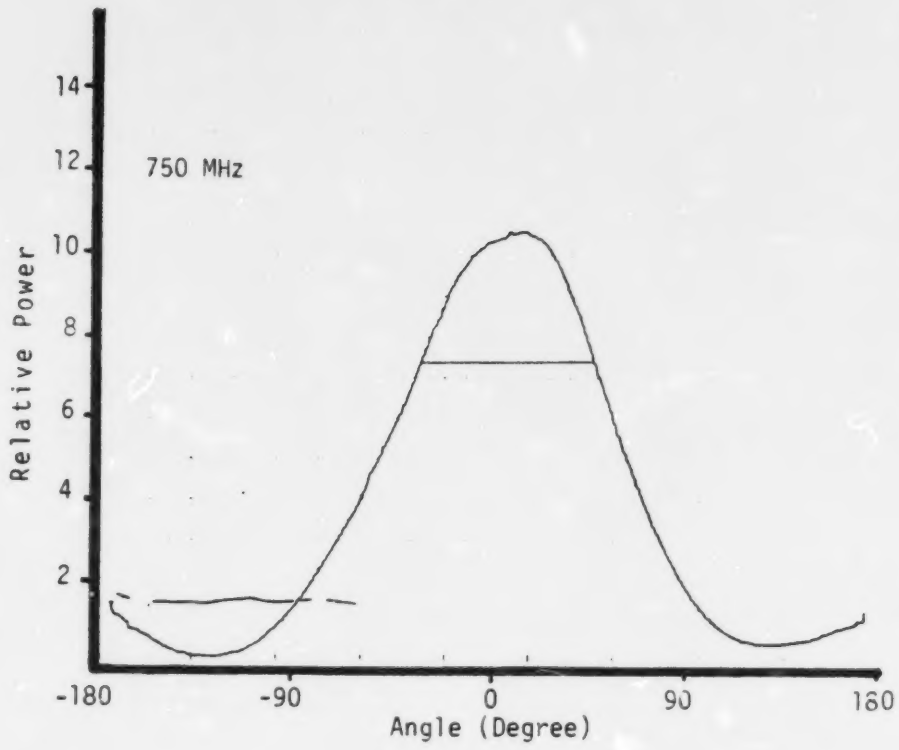

FIGURE 32(c)

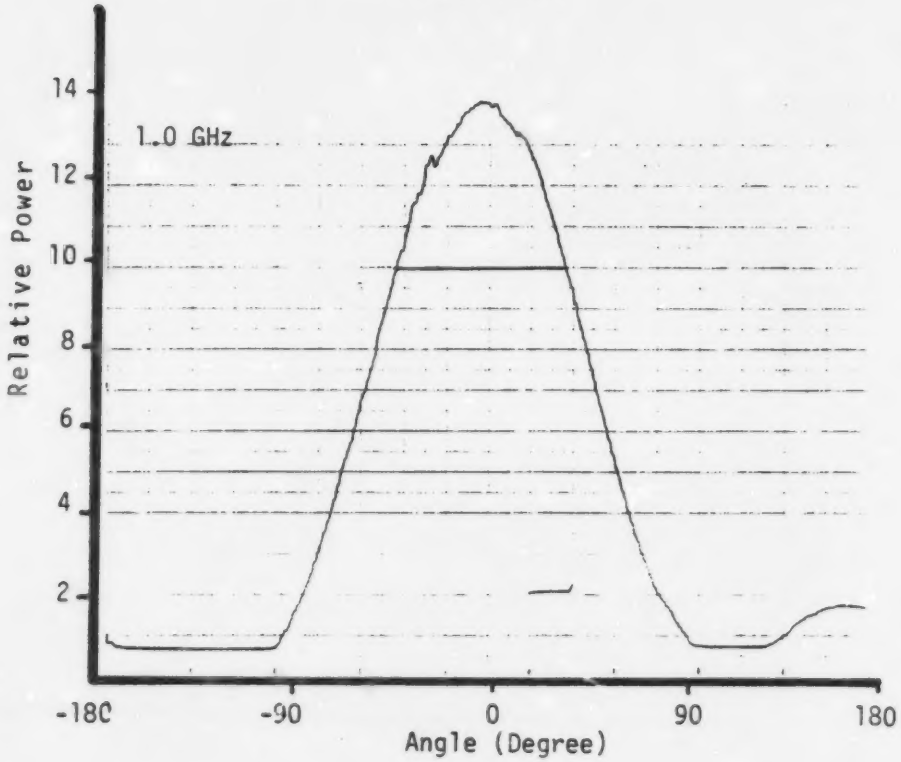

FIGURE 32(d)

FIGURE 32 - H-Plane radiation pattern for TRLD in a cylindrical cavity

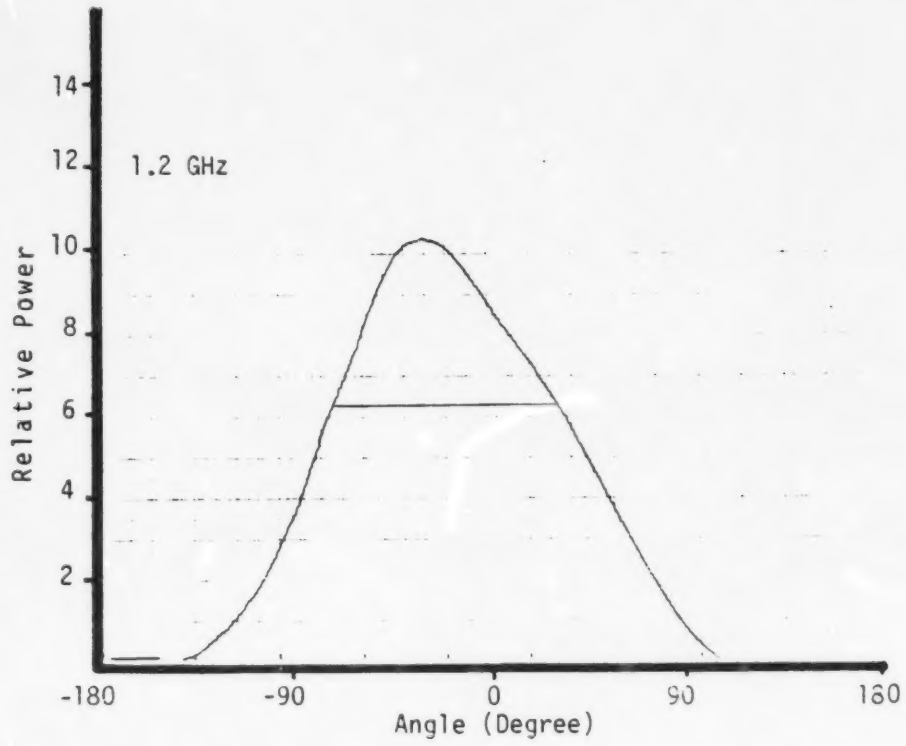

FIGURE 32(e)

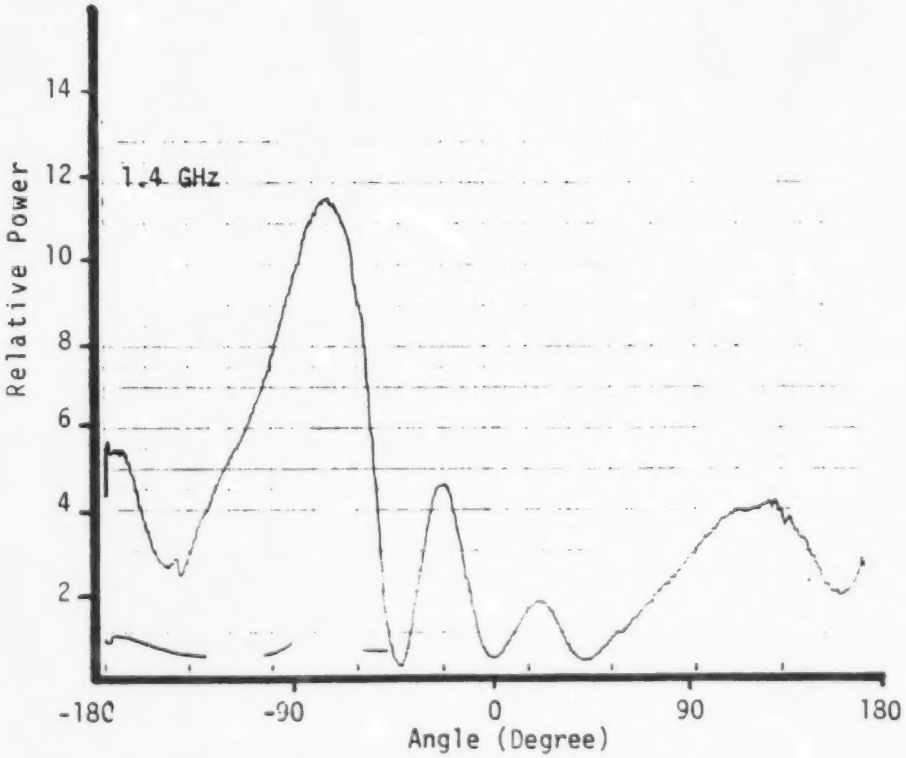

FIGURE 32(f)

FIGURE 32 - H-Plane radiation pattern for TRLD in a cylindrical cavity

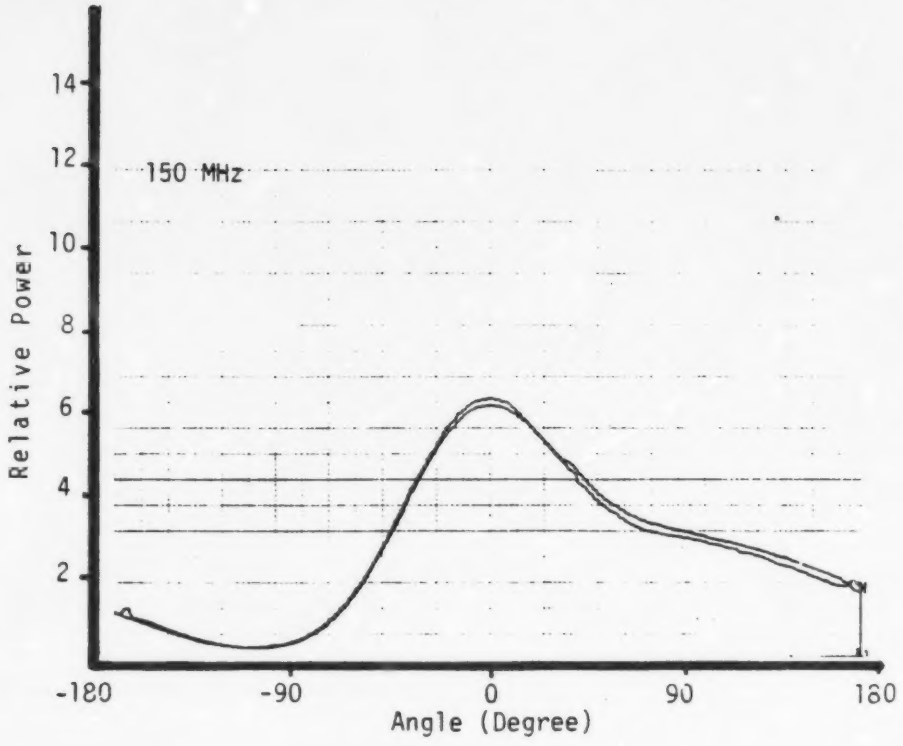

FIGURE 33(a)

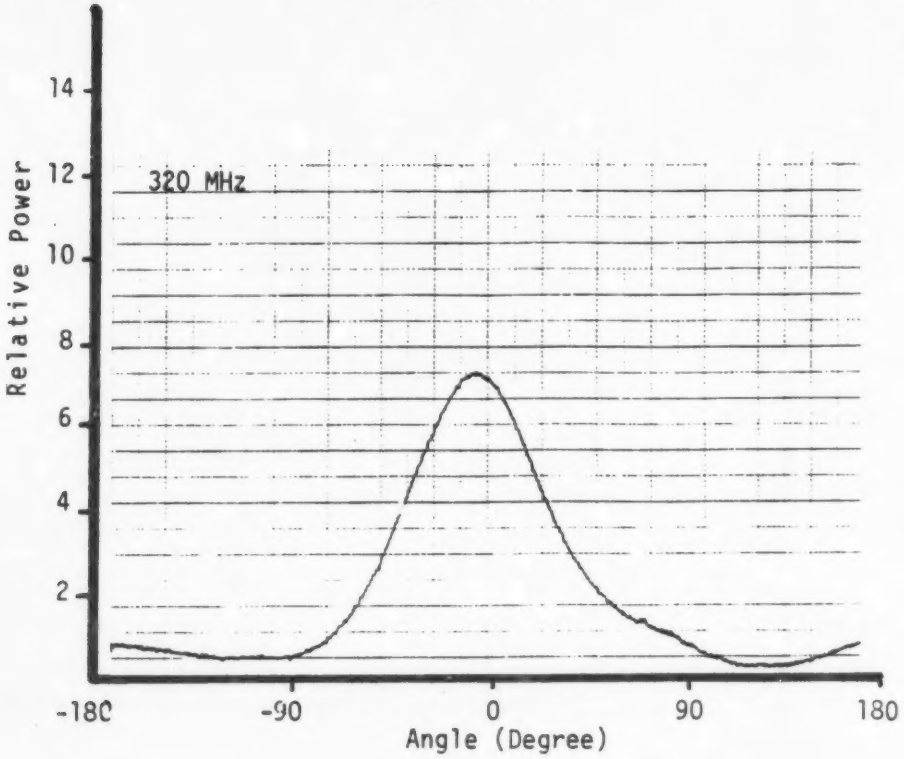

FIGURE 33(b)

FIGURE 33 - E-Plane radiation pattern of a TRLD in a rectangular cavity

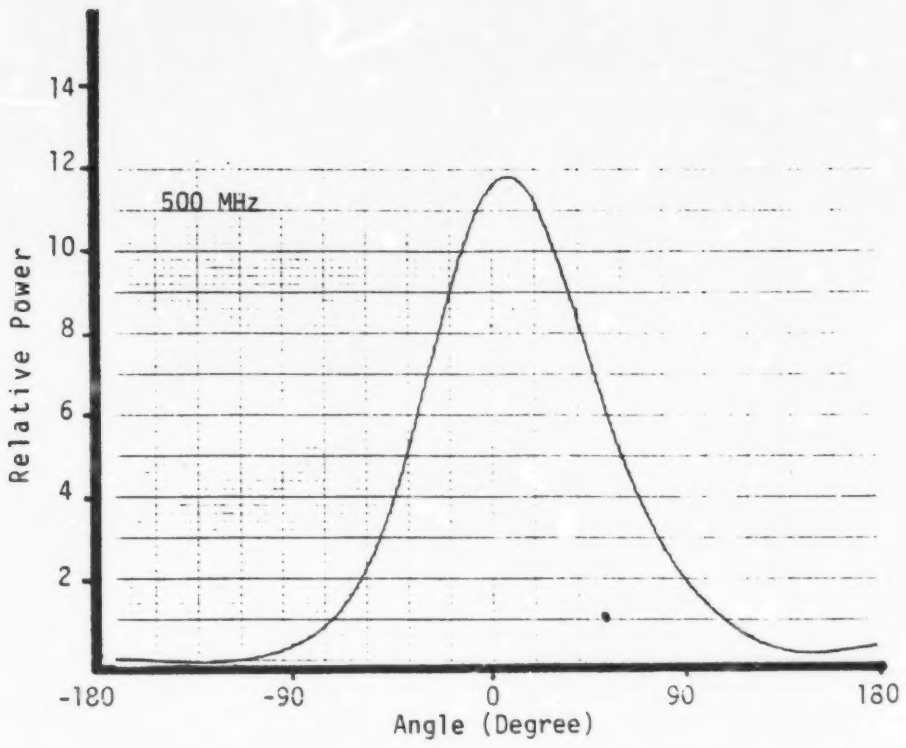

FIGURE 33(c)

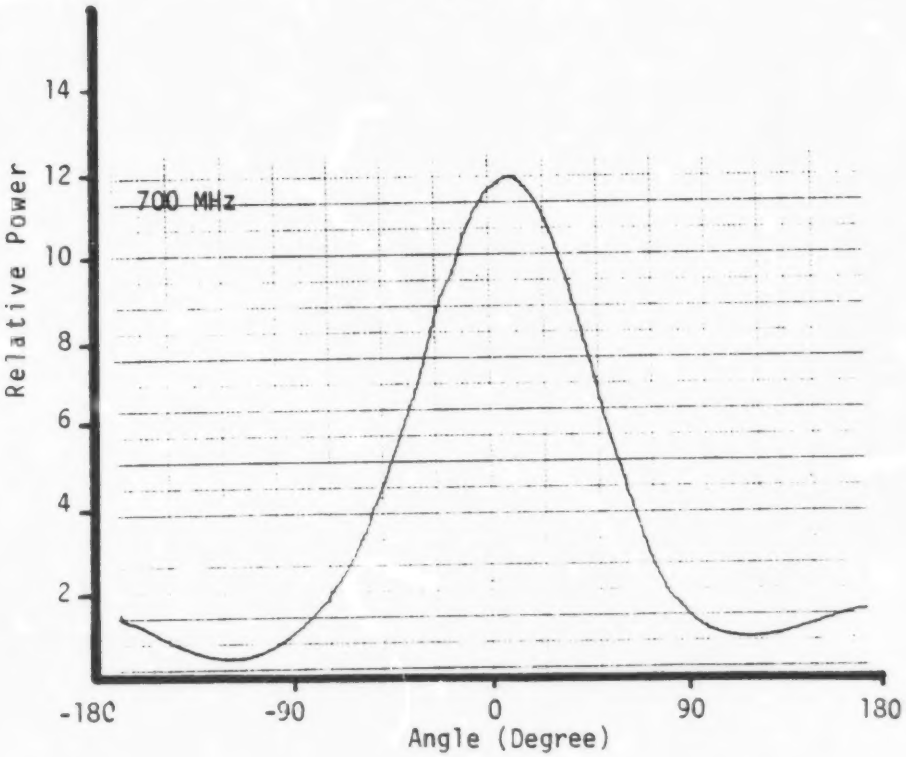

FIGURE 33(d)

FIGURE 33 - E-Plane radiation pattern of a TRLD in a rectangular cavity

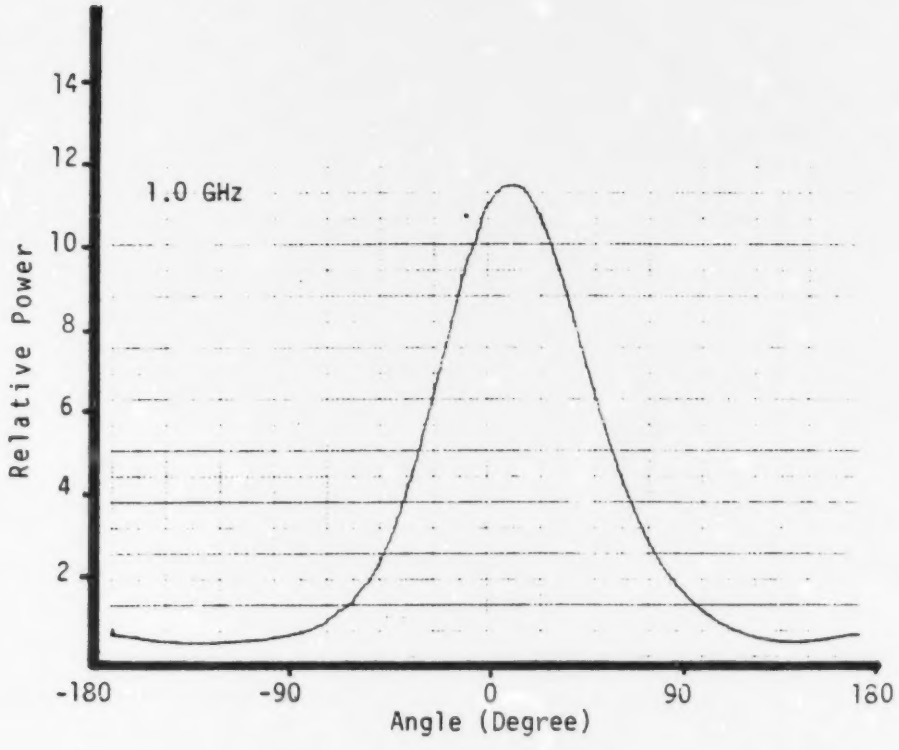

FIGURE 33(e)

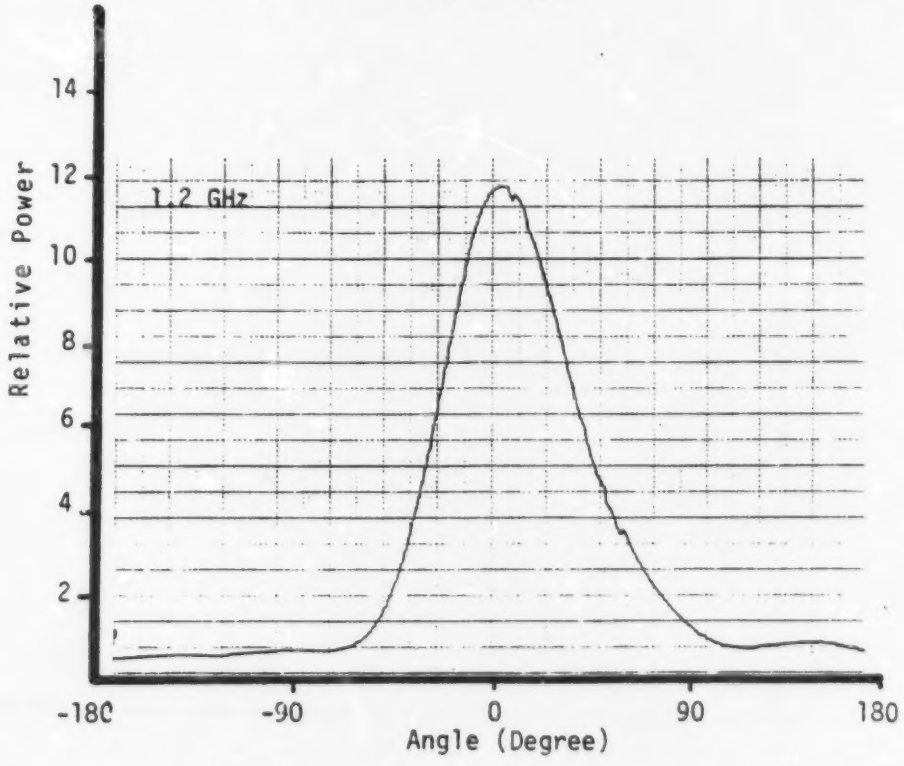

FIGURE 33(f)

FIGURE 33 - E-Plane radiation pattern of a TRLD in a rectangular cavity.

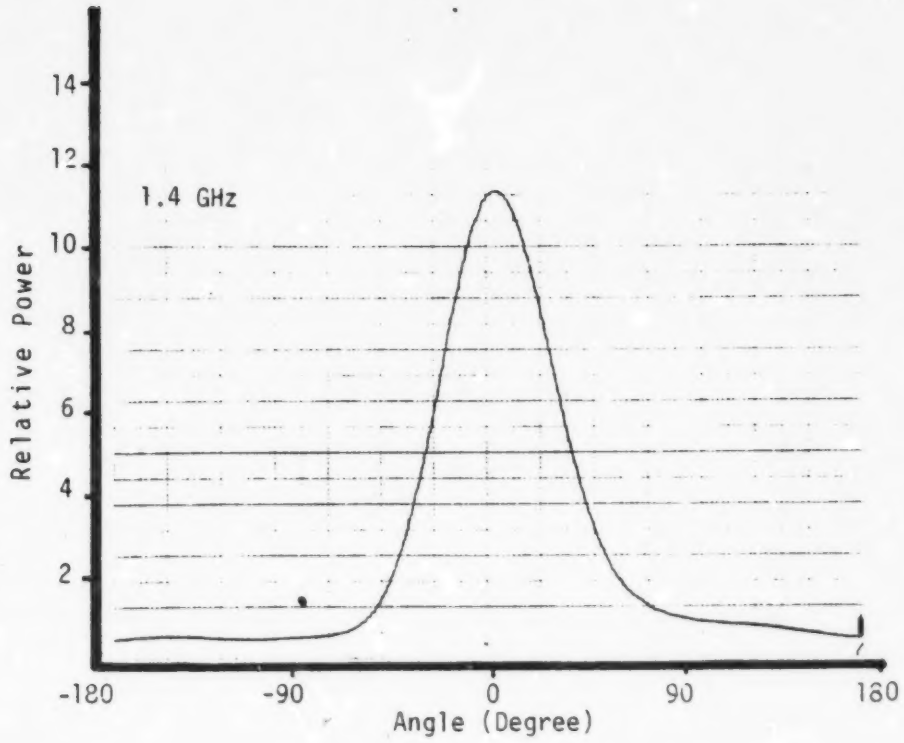

FIGURE 33(g)

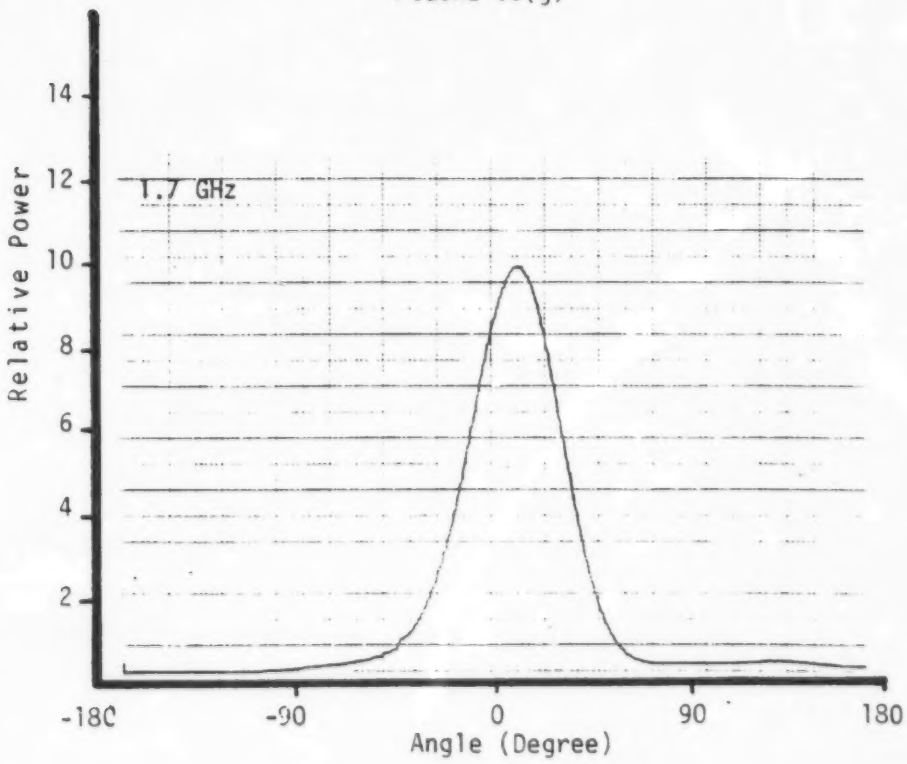

FIGURE 33(h)

FIGURE 33 - E-Plane radiation pattern of a TRLD in a rectangular cavity.

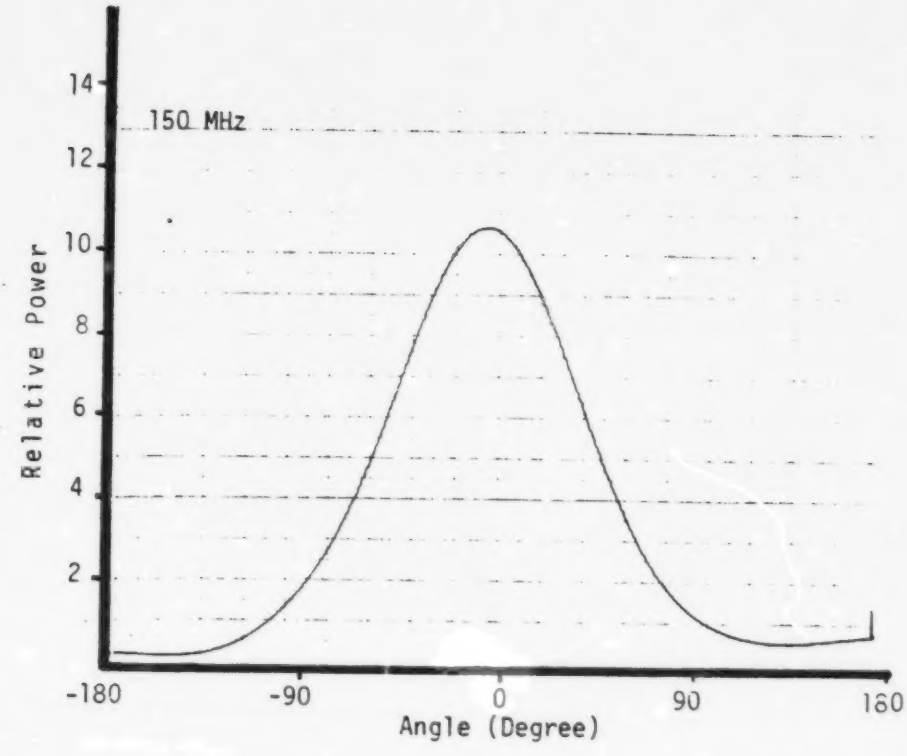

FIGURE 34(a)

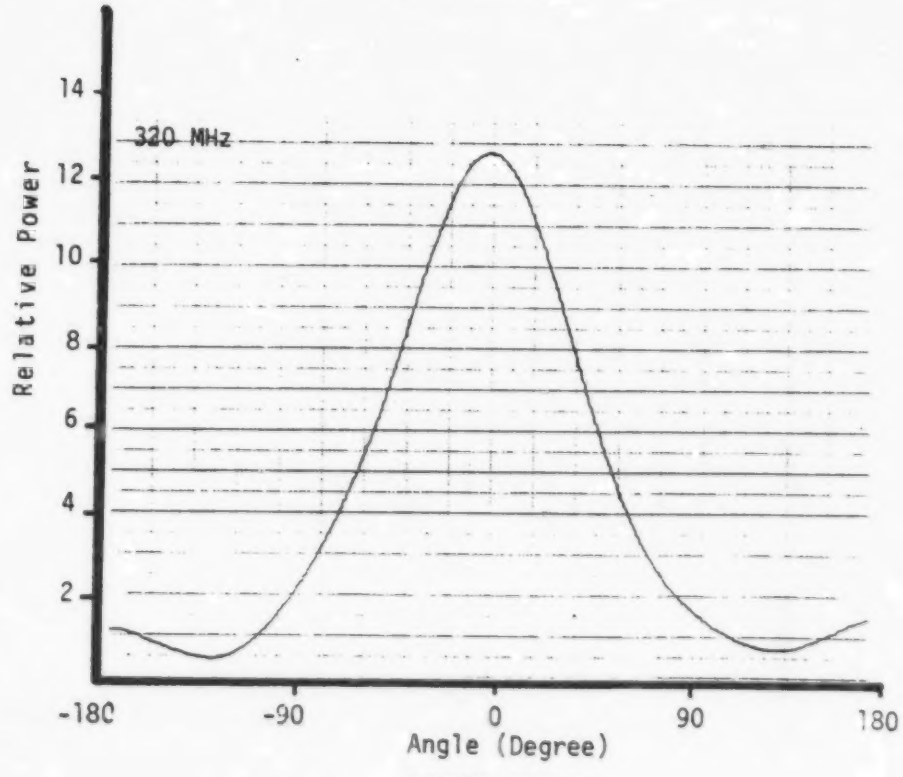

FIGURE 34(b)

FIGURE 34 - H-Plane radiation pattern of a TRLD in a rectangular cavity

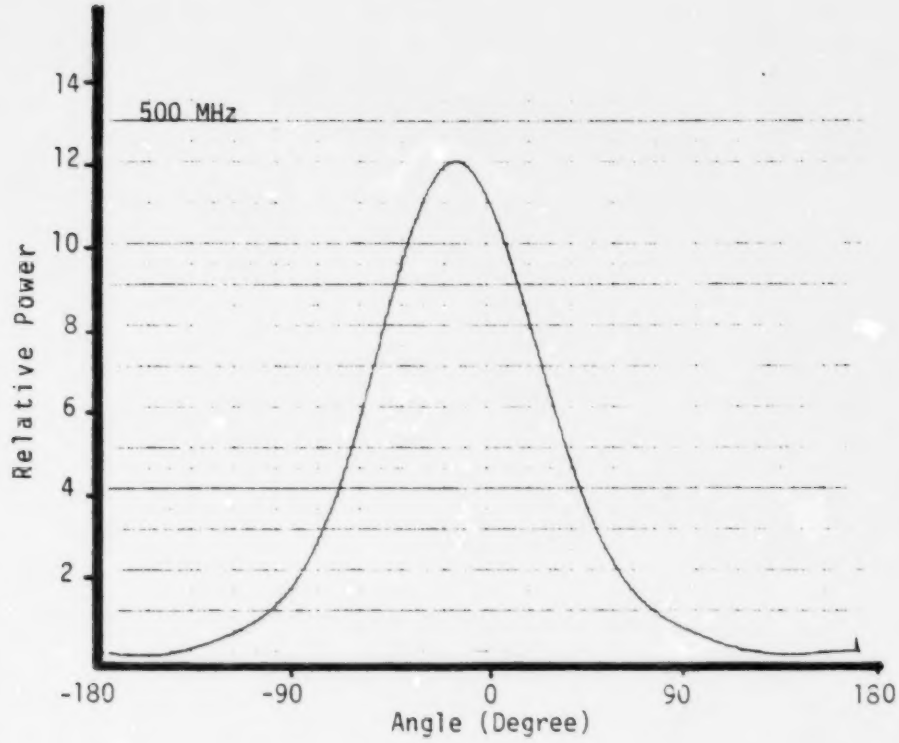

FIGURE 34(c)

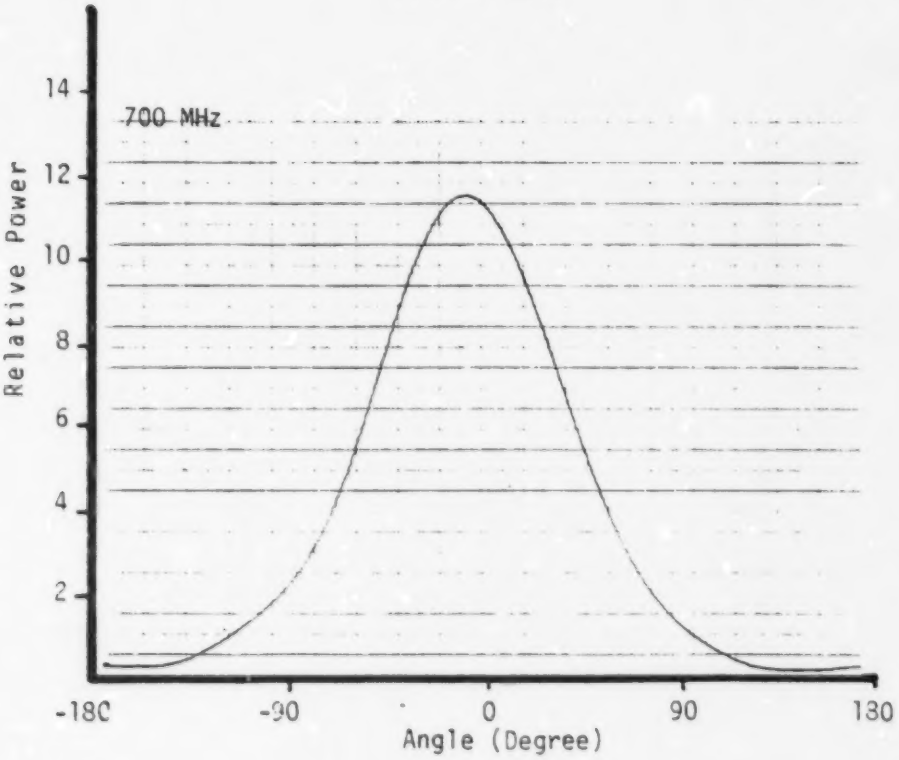

FIGURE 34(d)

FIGURE 34 - H-Plane radiation pattern of a TRLD in a rectangular cavity

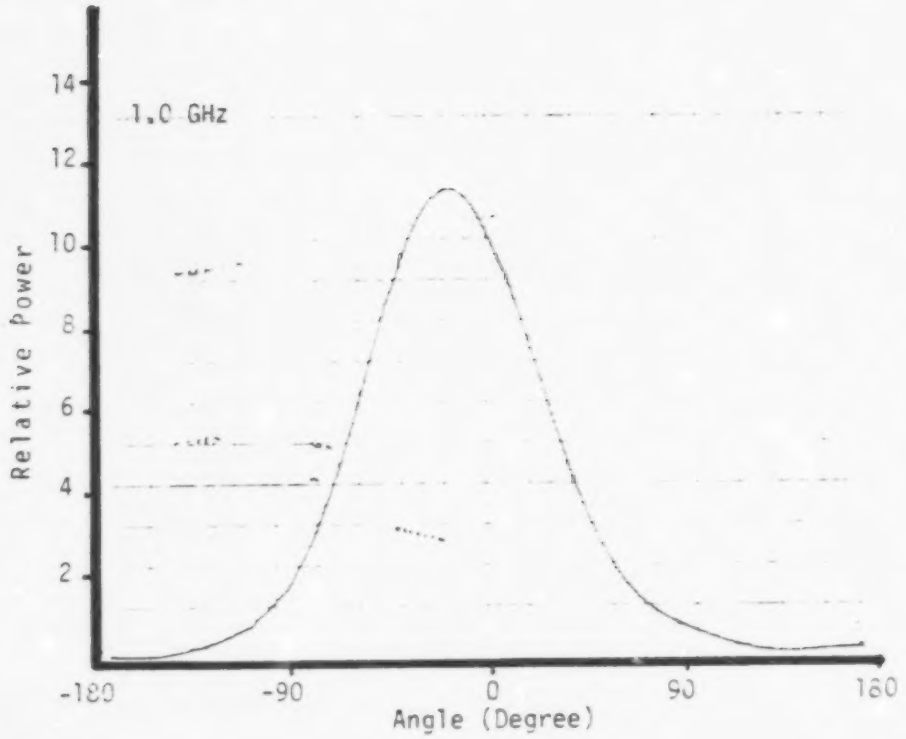

FIGURE 34(e)

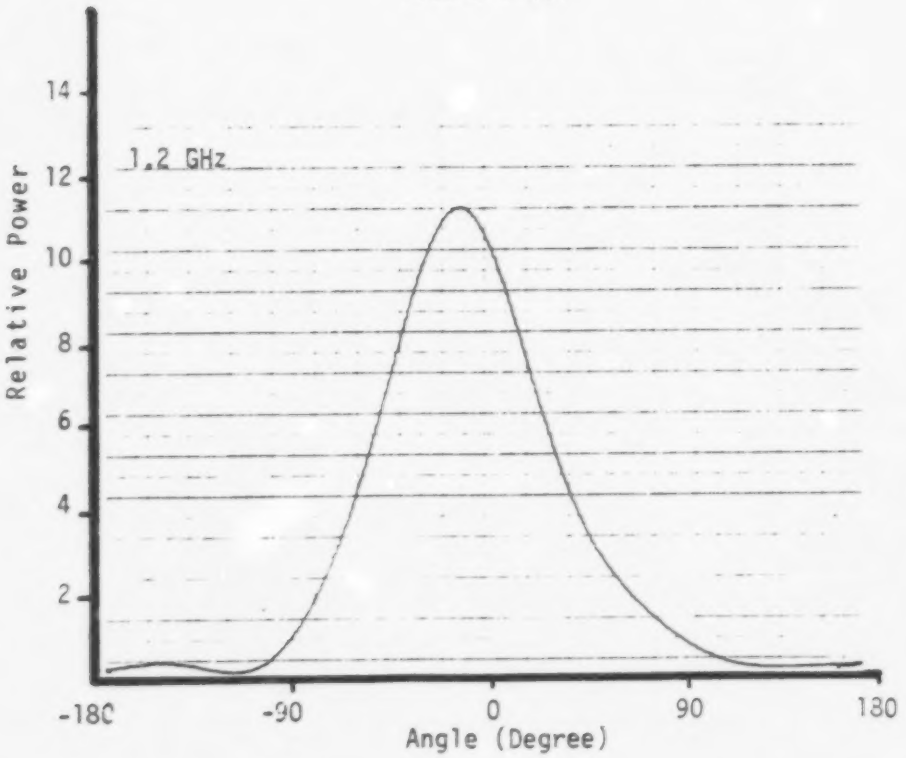

FIGURE 34(f)

FIGURE 34 - H-Plane radiation pattern of a TRLD in a rectangular cavity

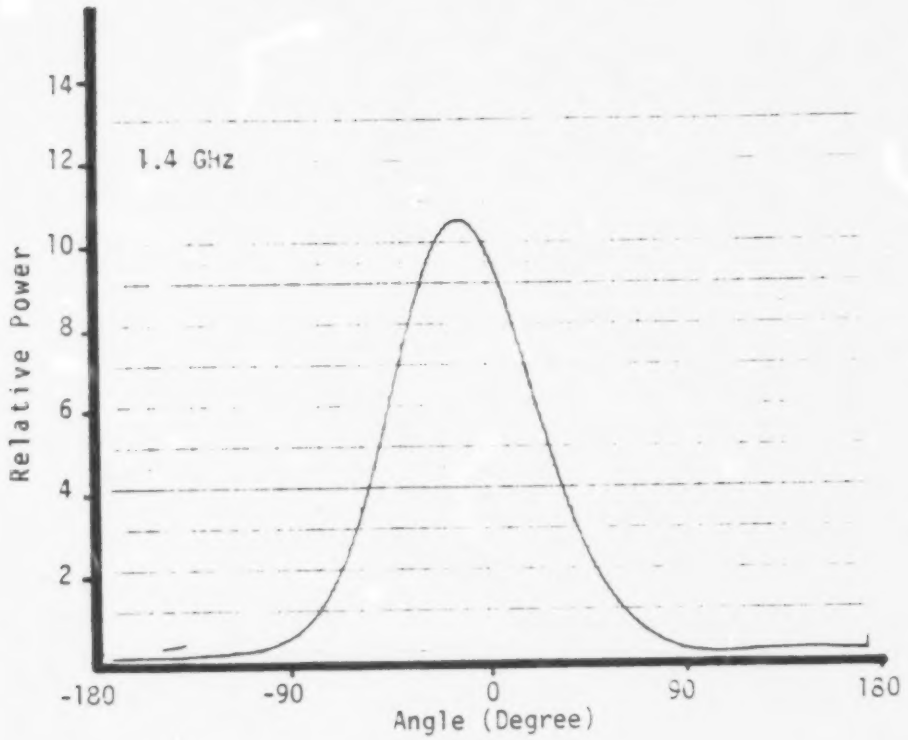

FIGURE 34(g)

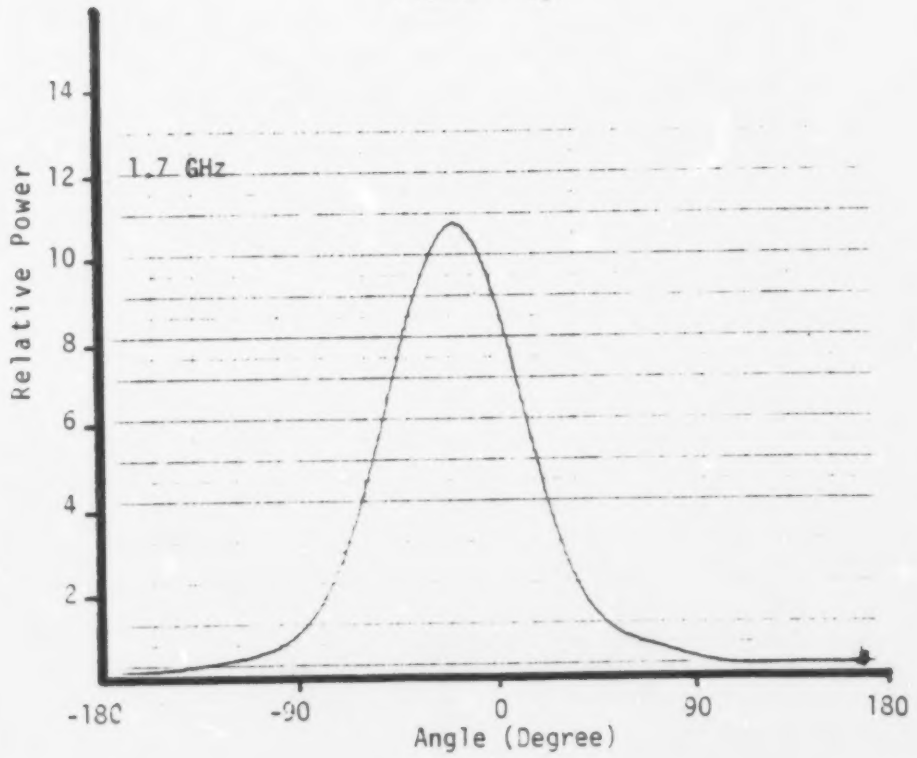

FIGURE 34(h)

FIGURE 34 - H-Plane radiation pattern of a TRLD in a rectangular cavity

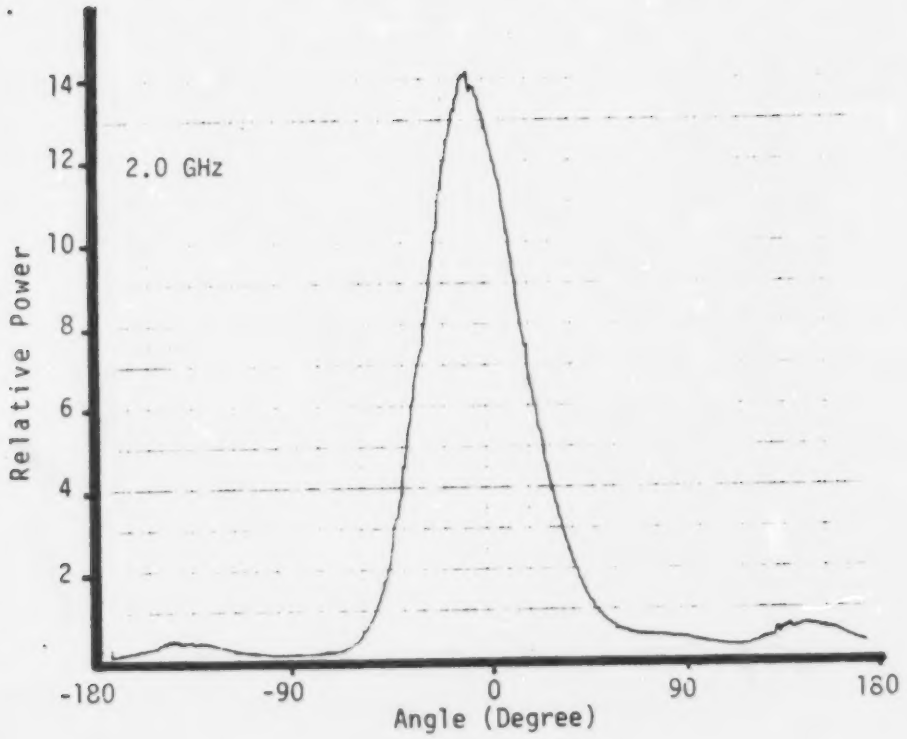

FIGURE 34(i)

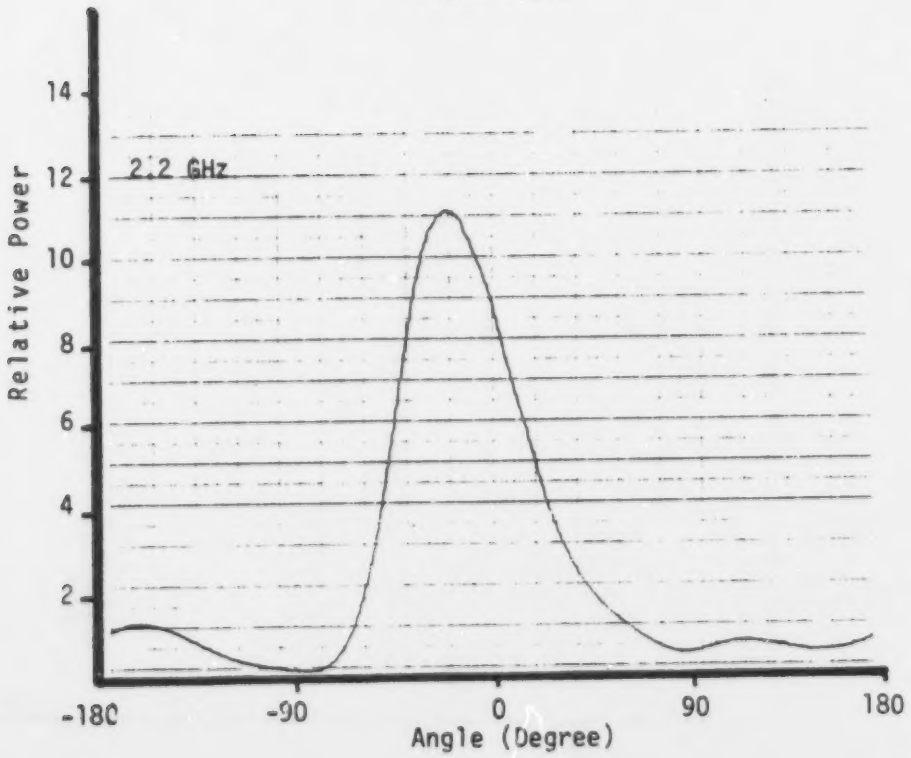

FIGURE 34(j)

FIGURE 34 - H-Plane radiation pattern of a TRLD in a rectangular cavity

4.3 Antenna Directivity

The ability of an antenna to concentrate energy in a particular direction or to be more sensitive to energy incident from a specific direction, is described in terms of antenna gain. Two different, but related, definitions of antenna gain have been developed:

(1) The «directive gain» or directivity. This considers the antenna as a lossless transducer that includes only the effects of the aperture distribution.

(2) The «power gain». This is usually denoted simply as the gain, and includes losses associated with the antenna, such as ohmic and RF heating.

The directivity D is defined as the ratio of the maximum radiation intensity or watts per steradian from the source under consideration, to the radiation intensity from an isotropic source radiation the same power (that is, average radiation intensity from the source under consideration). Thus

$$D = \frac{\text{max. radiation intensity}}{\text{average radiation intensity}}$$

A simple approximate method of calculating the directivity for a single lobed pattern, is based on an estimate of the beam area from the half power beam-widths of the patterns in two planes at right angles. Thus, suppose that θ (in radian) is the beam width between half power points in one plane and ϕ (in radian) is the width in a

plane at right angles

Then, (see [3])

$$D = \frac{4\pi}{\theta_1 \phi_1} \qquad (1)$$

expressing the above in degrees gives,

$$D = \frac{41253}{\theta^\circ_1 \phi^\circ_1} \qquad (2)$$

For a dipole antenna, doughnut-type pattern, equation (2) reduces to

$$D = \frac{114.6}{\theta^\circ_1} \qquad (3)$$

For special case of a bidirectional pattern with two identical lobes the directivity is half that obtained on the basis of a single lobe. If equation (2) is applied to a unidirectional beam type of pattern with minor lobes, the calculated directivity is too high. The higher the level of minor lobes, the larger the inaccuracy of equation 2.

From the above discussion, it is clear that the directivity of an antenna is based entirely on the shape of radian pattern.

Using equation (2), the directivity of a TRLD in a cylindrical cavity at varying frequency is given in the following table:

f (MHz)	Directivity (dB)
750	6.3
1000	7.5
1200	5.0

The corresponding results for a TRLD in a rectangular cavity are given below:

f (MHz)	Directivity (dB)
320	6.6
500	6.6
700	5.7
1000	6.3
1200	8.5

Although the previous tables suggest a better directivity for a cylindrical reflector at 750 MHz, its sidelobes at frequencies below 700 MHz became so dominant that the directivity formula (Equation (2)) no longer holds. However, the main lobe of an antenna with a rectangular reflector retains its shapes at all frequencies. In fact it is surprising that effects of diffraction has not severely distorted the main lobe below 300 MHz as they have done to the cylindrical reflector.

4.4 Transmission Characteristics

One of the most important parameters for the sea-ice sensor antenna is the efficiency of transmission and reception at various frequencies. For real VHF signals and real size antennas, quantitative measurements of these properties on the ground based test range suffer the same experimental limitations as the radiation pattern measurements discussed before. Quantitive measurements can be obtained relatively more easily with the help of subscale antennas.

The transmission efficiency at various frequencies of the tapered resistively loaded antenna in a rectangular reflector box described before was studied using the same experimental arrangement as shown in Figure 1. The transmitter was a signal generator which fed a steady state signal to the transmit antenna located 2m above ground. An identical receive antenna was located 2m away at the same height. With the transmit-receive antenna facing each other, the output of the receive antenna was amplified and fed to a power meter. The measured received power is given in Table 1. The two 2-way loss in the transmit-receive configuration was about 34 dB at 1.1 GHz, the optimum frequency at which the antenna was most efficient. The 2-way loss increases to 74 dB at .30 GHz, corresponding to a 40 dB difference in efficiency. Between .6 and 1.4 GHz, the maximum deviation in 2-way antenna efficiency is about 40 dB. The most efficient frequency range is between .6 and 1.4 GHz. Since the scaling factor is 10, the test frequencies in Table 1 correspond to real frequencies between 30 and 140 MHz. No higher frequency measurements were taken because the transformer balun at the antenna feedpoint has a deteriorating characteristic about 1.1 GHz.

Due to the limiting characteristics of the antenna transformer balun and the dimensions of the reflector, the frequency response of the antenna shows fluctuating characteristics around 1.2 GHz. This is not surprising since the reflector has dimensions close to resonant dimensions of signals at these frequencies. Unfortunately, the maximum size of an airworthy antenna is limited by the dimensions of the helicopter. There are very few choices of configurations and practically

no choice in the maximum allowable antenna dimensions. The same limitations would result in the deteriorated antenna efficiency around 30 MHz as observed in the subscale antenna measurements around .3 GHz.

TABLE 1 - Measured Efficiency of TRLD Antenna in Rectangular Reflector Transmitter Power = 27dBmW

Test Frequency (GHz)	Received Power (dBmW)	Frequency (GHz)	Received Power (dBmW)
.30	-47.0	.90	-10.0
.35	-46.0	.95	- 7.5
.40	-42.0	1.00	- 7.1
.45	-39.5	1.05	- 8.8
.50	-35.0	1.10	- 6.6
.60	-26.0	1.20	- 9.3
.70	-24.5	1.25	- 6.6
.75	-18.0	1.30	- 9.3
.80	-19.0	1.35	-13.24
.85	-12.5	1.40	-11.47

5.0 STUDY OF ANTENNA - AIRCRAFT INTERACTIONS

One of the greatest problems in the development of a helicopter-borne sea-ice thickness sensor is the constraint on the antenna size. Since the wavelength of the VHF signal is comparable to the antenna reflector and the helicopter dimensions, wave diffractions and near-field effects can be significant. As a result, the exact geometries of conductive materials in the near-fields of the antenna are important. Any variation of these geometries can, in principle, significantly change the antenna characteristics such as resonance, radiation patterns or the antenna impedance. A quantitative treatment of this problem not only requires the solution of an extremely complex boundary value problem which is practically impossible to solve (because of the complex geometries of the boundaries), but also a solution for each exact antenna - helicopter installation.

Instead of pursuing such a futile exercise, a more promising approach is first to design a reflector which has dominant effects to the antenna driving element and then to study the residual antenna-helicopter interactions by experiments. This approach reduces the effects of the helicopter and ensures the antenna - reflector system can be useful on different helicopters. The effects of the antenna-helicopter interactions can be most cost effectively studied with the help of subscale experiments. If these effects on the radar signals are negligible then only qualitative details of these effects would be necessary. The recommendations from the subscale experiments can apply the full scale VHF antenna on a helicopter without depending on the solution of complex boundary value problems.

In the subscale experiment, the effects of the antenna-helicopter interactions were estimated by first measuring the power radiation pattern of the antenna with a given reflector. A metal plate with relative sizes and geometries representative of a subscale helicopter was then attached to the back of the antenna reflector (Fig. 35) and the power radiation pattern was measured again. Comparisons of the two sets of measurements gave «quantitatively» the order of magnitude of these effects and qualitatively their details. Measurements for the cylindrical reflectors are given in Figure 36a to f. Measurements for the rectangular reflectors are given in Figure 37 and 38a to g.

As expected, the metal plate at the back of an antenna with a cylindrical reflector has significant effects on the radiation pattern. With the antenna parallel to the metal plate which has the shape of a helicopter, the E-plane patterns differ significantly from those without the plate (see Fig. 31 and 32).

The effects of antenna-aircraft interactions on the radiation patterns are much less significant on a rectangular reflector, as can be observed in Figure 37. The measurements were, however, taken with a TRLD located diagonally in a box with a square aperture (see Fig. 35). With the dipole element horizontal and parallel to the simulated helicopter model (i.e. the metal plate), the E-plane radiation patterns are practically unaffected by the metal plate except between 500 and 700 MHz. Ironically, the metal plate has small effects even below 300 MHz down to 150 MHz. The significant effects of the metal plate on the radiation pattern at 500 to 700 MHz are probably due to resonant dimensions of the helicopter model at these frequencies. The H-plane

pattern has been obtained with botn the dipole and the helicopter model oriented vertically. The measurements in Figure 38 show that the radiation pattern is practically unaffected by the helicopter metal at all frequencies.

The results of the above measurements suggest that the rectangular antenna reflector will be extremely useful in reducing the antenna-aircraft interactions under real operation conditions.

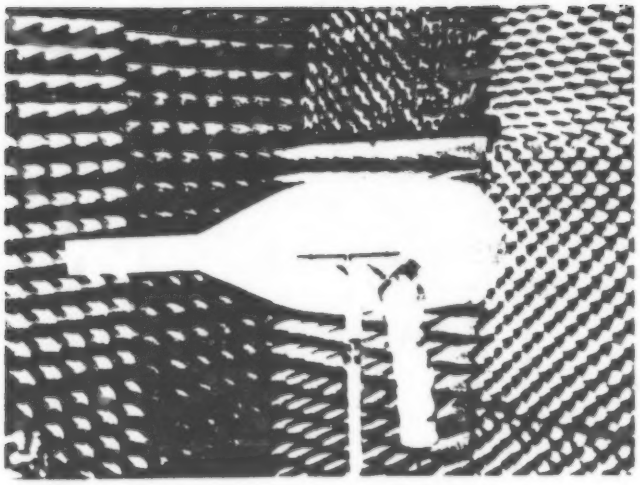

FIGURE 35(a) - Antenna with square reflector

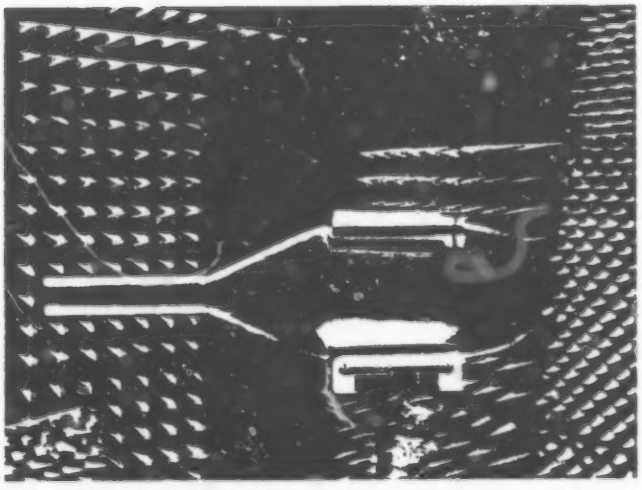

FIGURE 35(b) - Antenna with cylindrical reflector

FIGURE 35 - Experimental arrangement to study antenna effects of aircraft interaction on antenna radiation power pattern measurement.

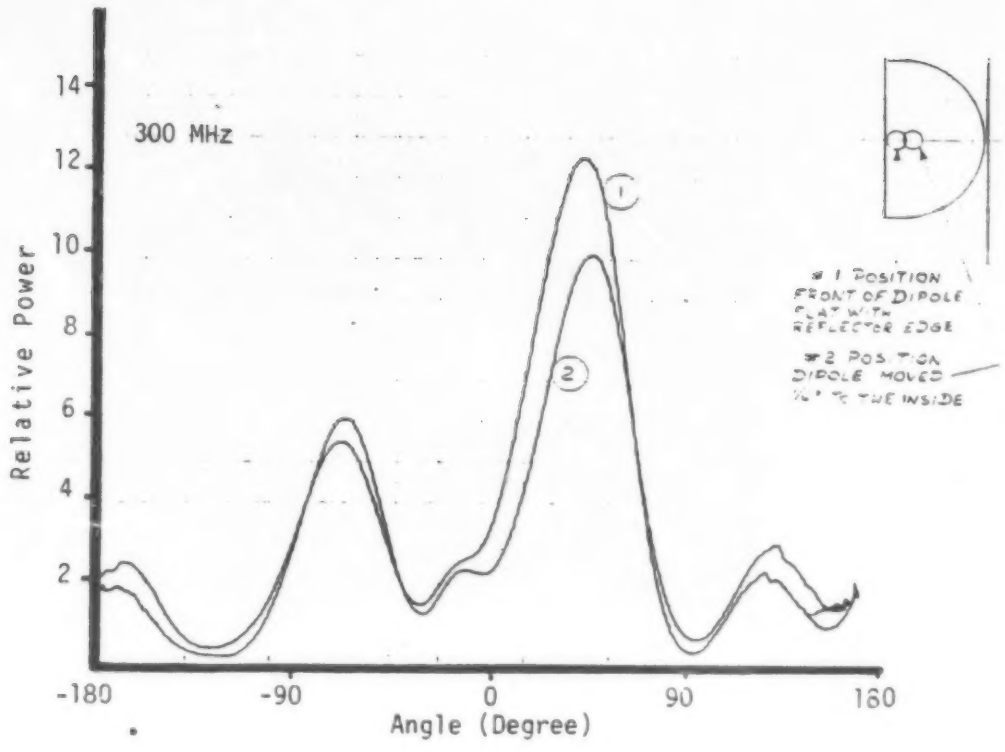

FIGURE 36(a)

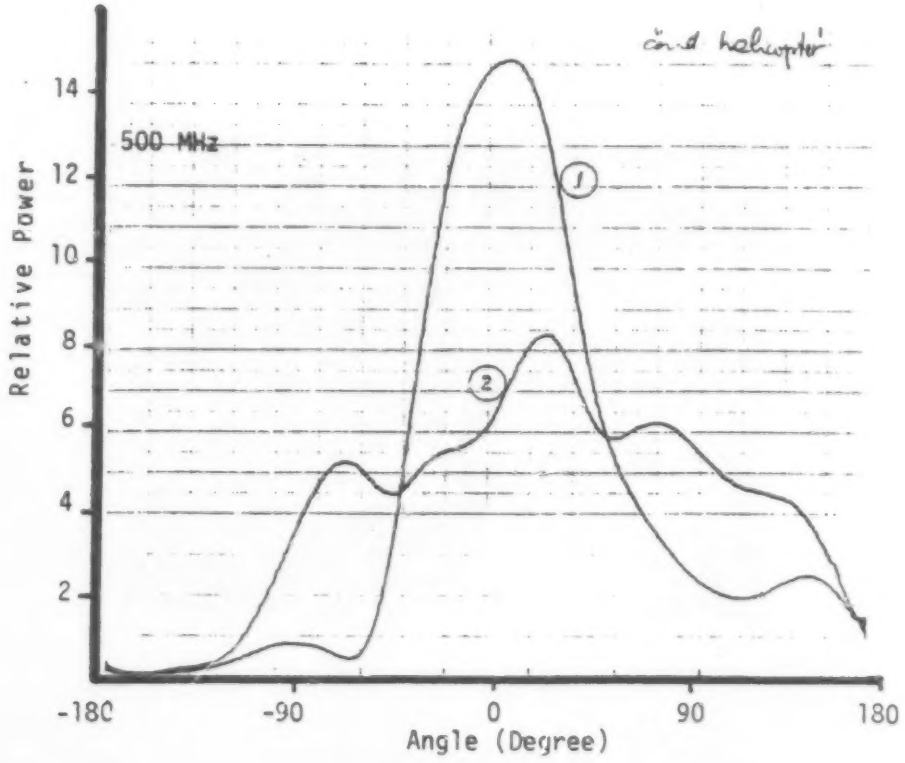

FIGURE 36(b)

FIGURE 36 - E-Plane radiation pattern for TRLD in a cylindrical cavity with subscale helicopter

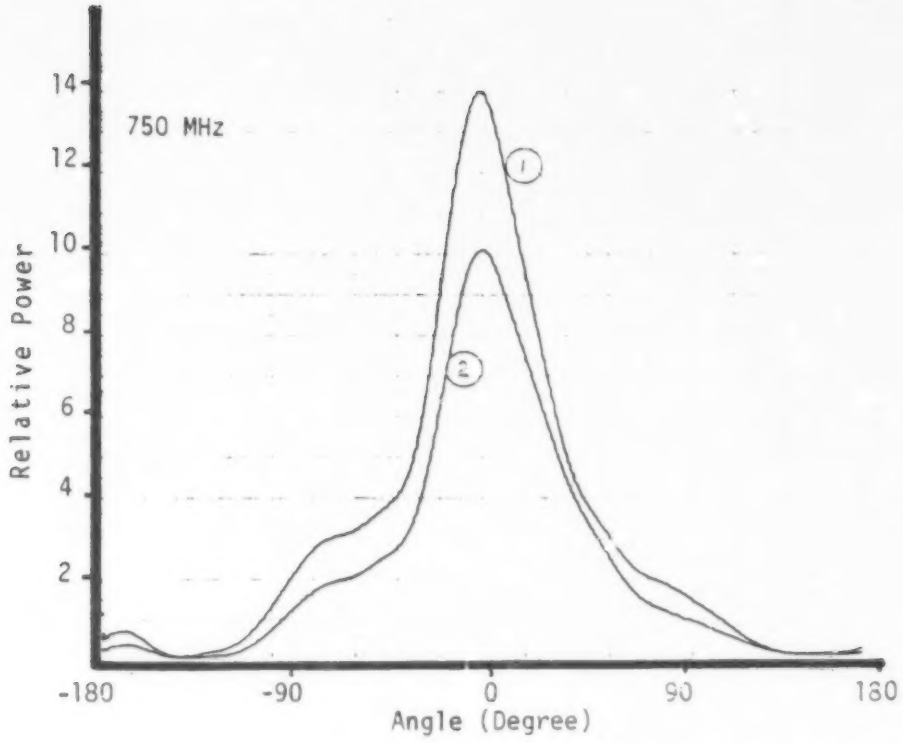

FIGURE 36(c)

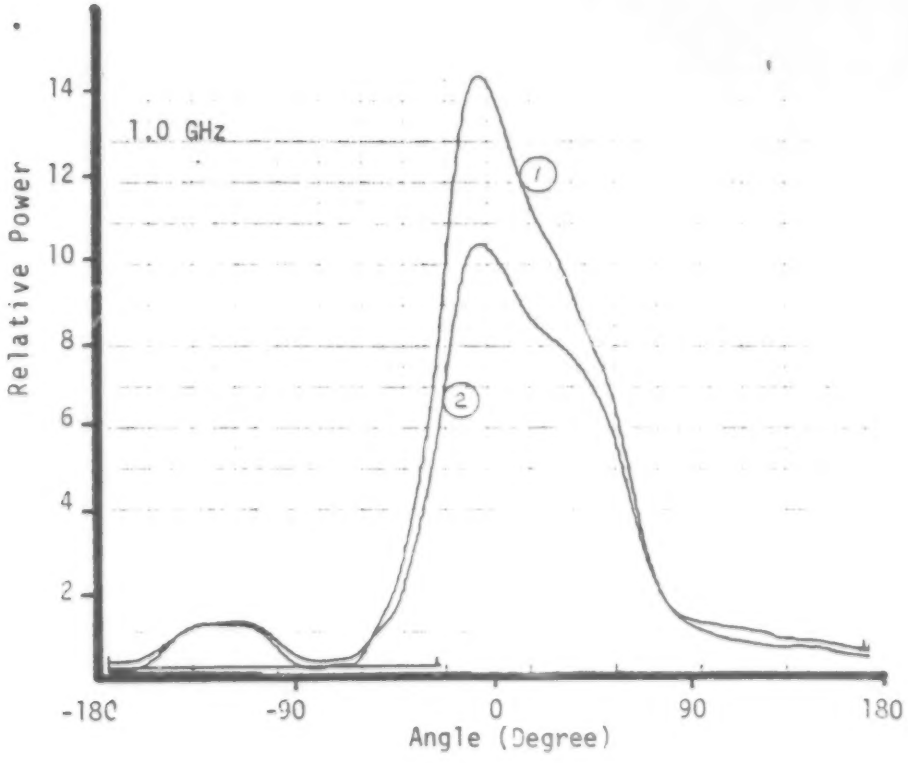

FIGURE 36(d)

FIGURE 36 - E-Plane radiation pattern for TRLD in a cylindrical cavity with subscale helicopter

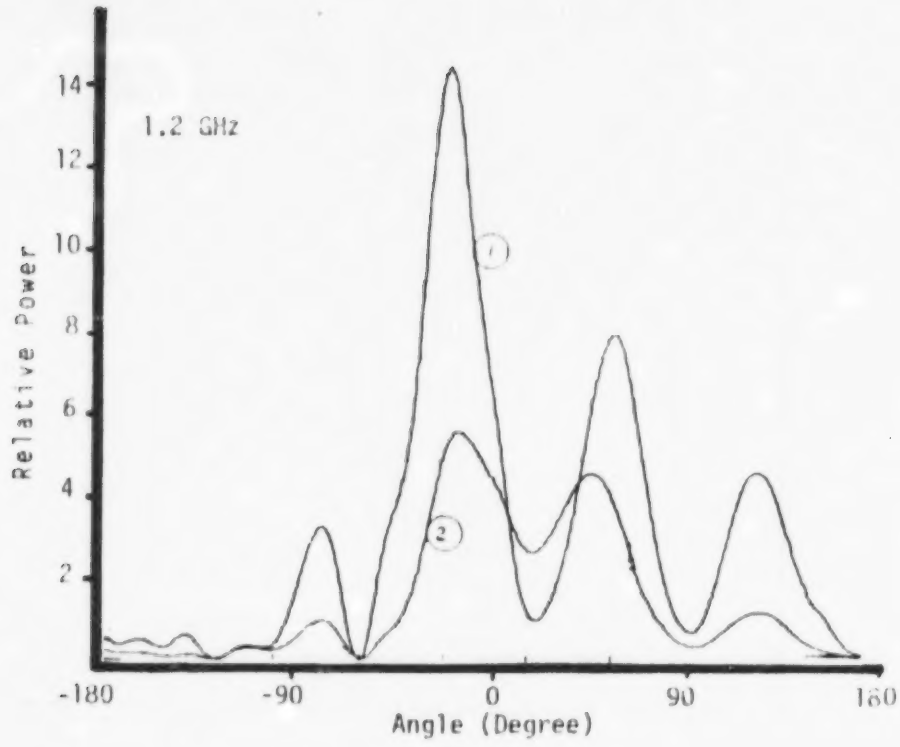

FIGURE 36(e)

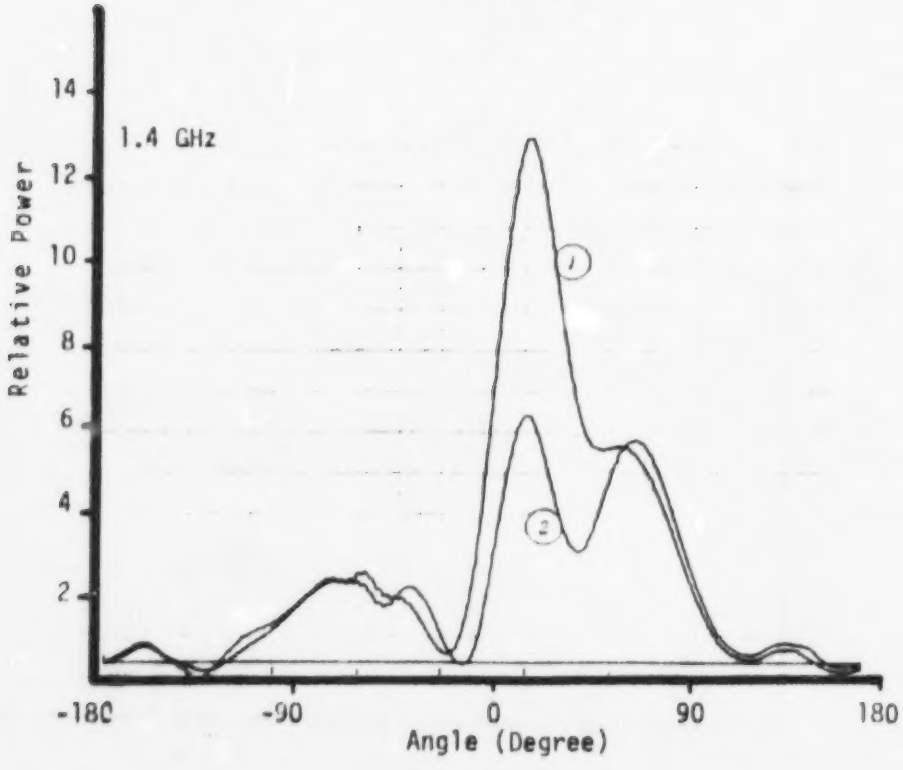

FIGURE 36(f)

FIGURE 36 - E-Plane radiation pattern for TRLD in a cylindrical cavity with subscale helicopter

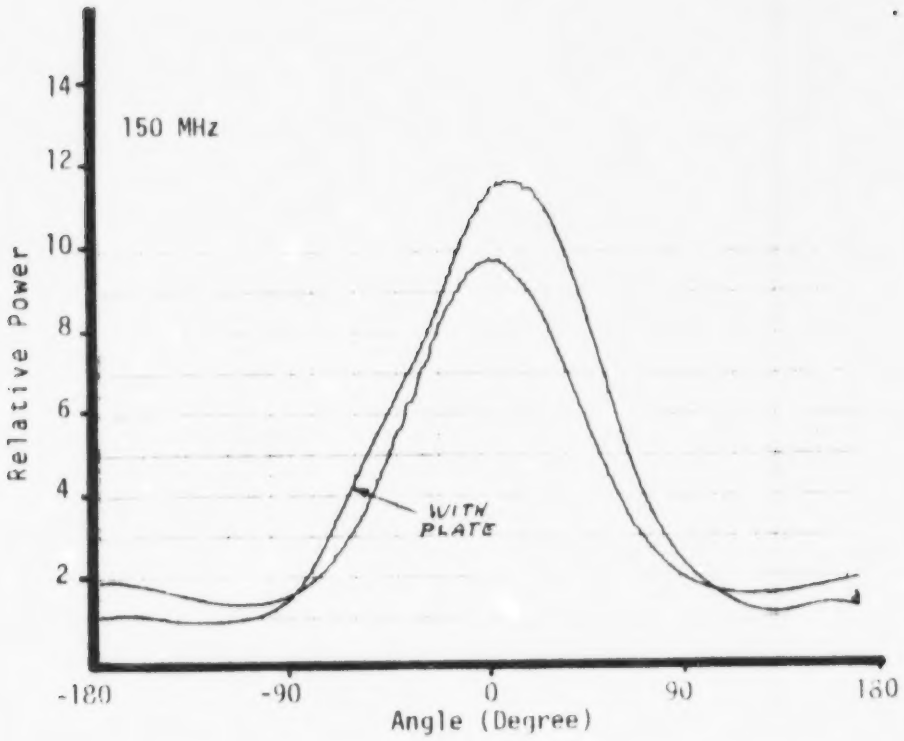

FIGURE 37(a)

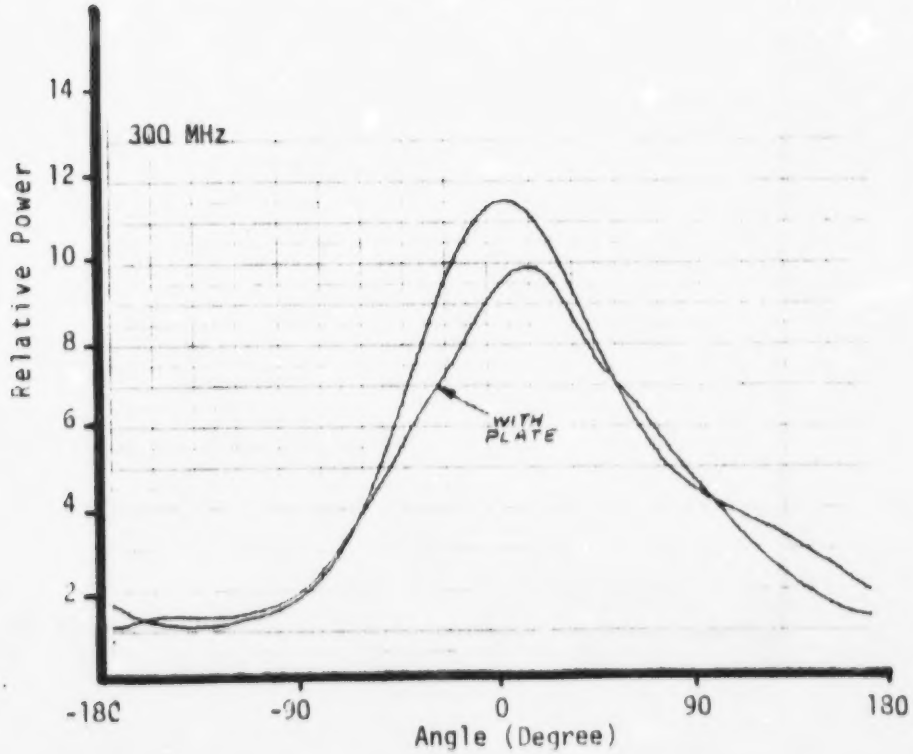

FIGURE 37(b)

FIGURE 37 - E-Plane radiation patterns for TRLD in a square cavity with and without metal back plate.

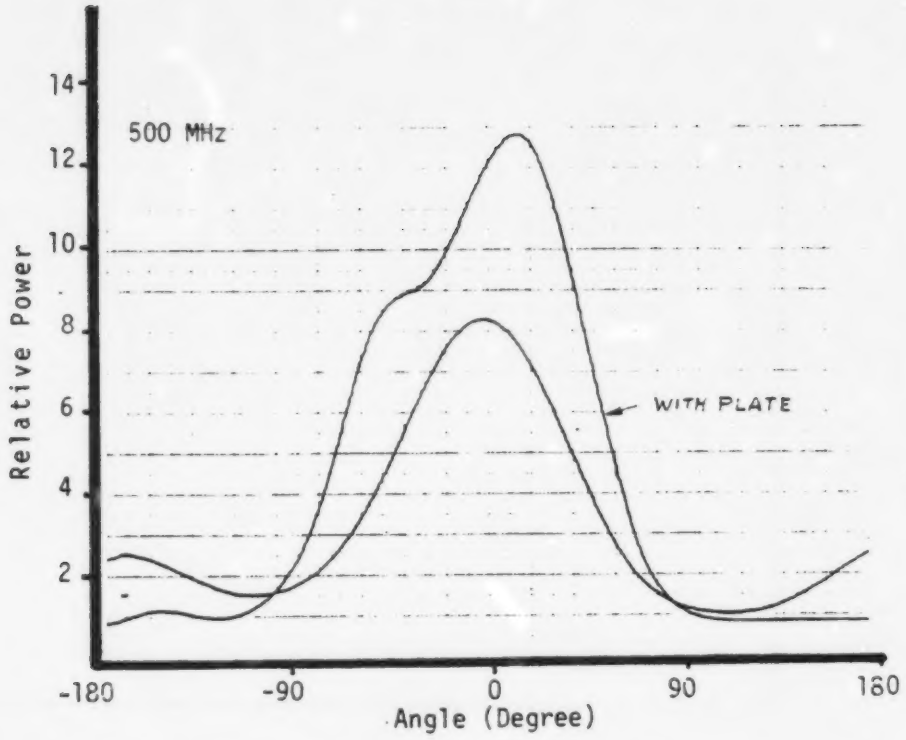

FIGURE 37(c)

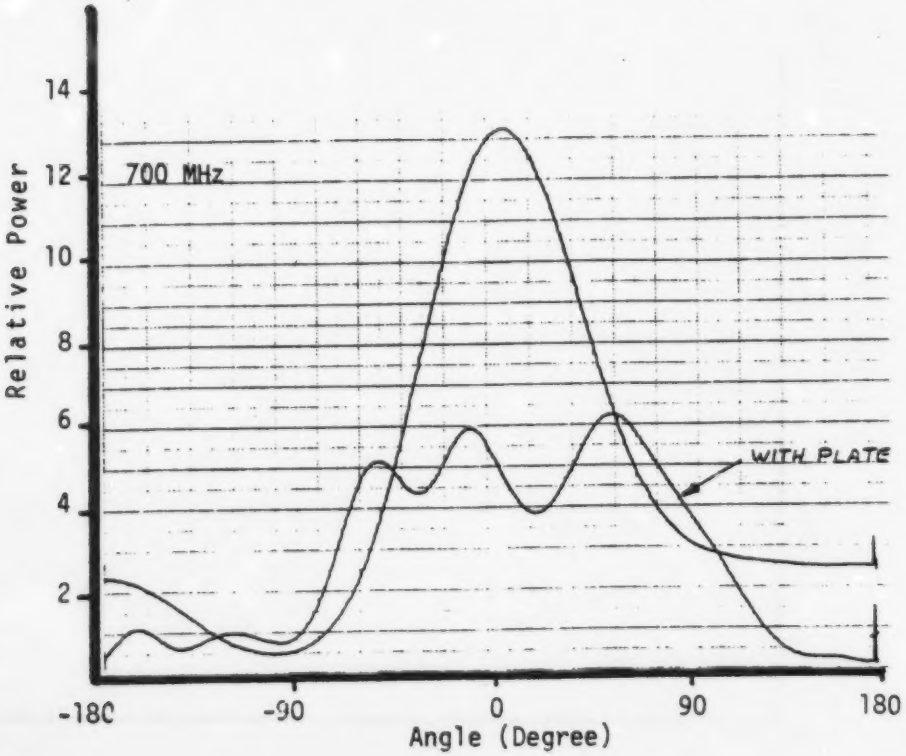

FIGURE 37(d)

FIGURE 37 - E-Plane radiation patterns for TRLD in a square cavity with and without metal back plate.

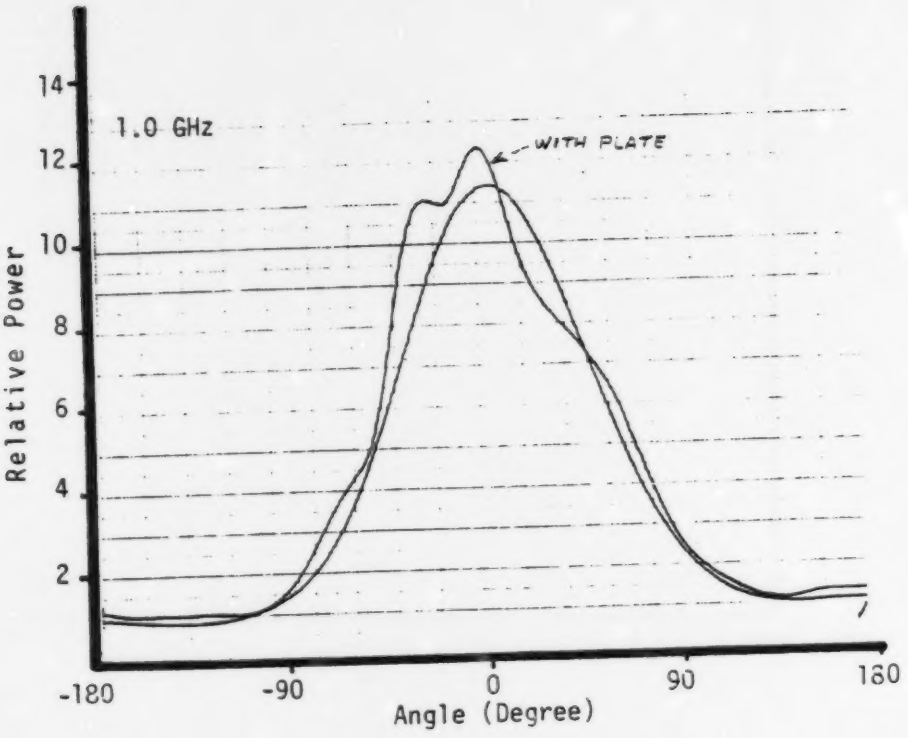

FIGURE 37(e)

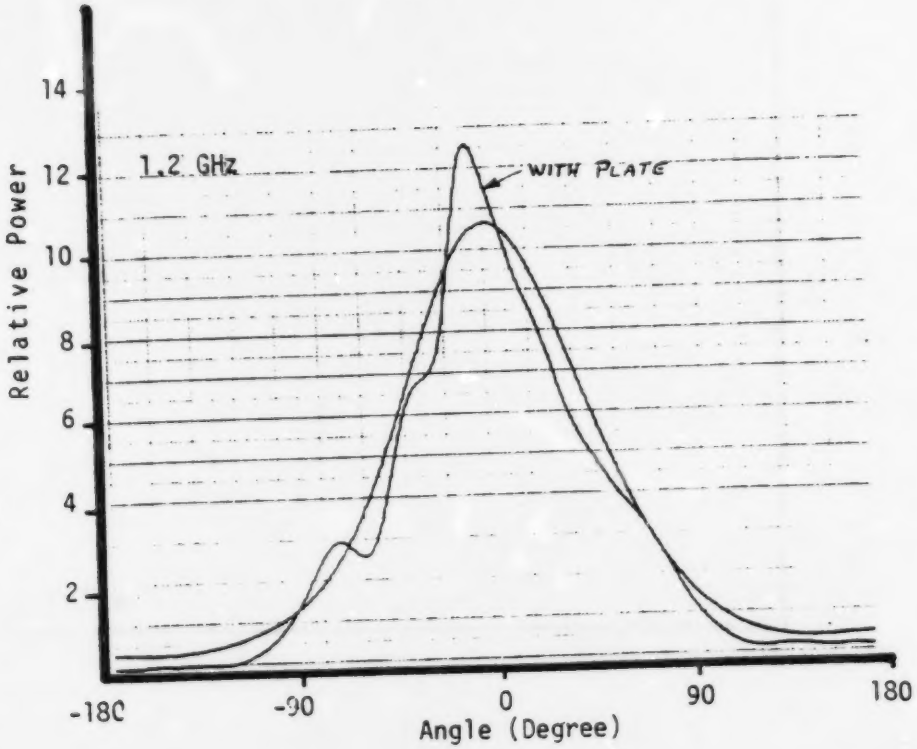

FIGURE37(f)

FIGURE 37 - E-Plane radiation patterns for TRLD in a square cavity with and without metal back plate.

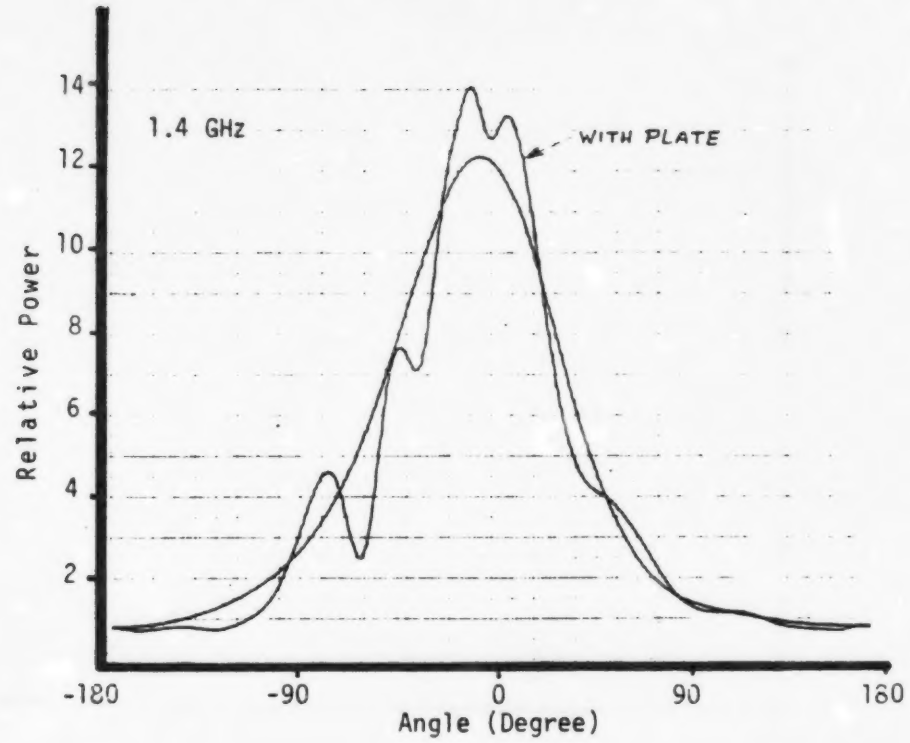

FIGURE 37(g)

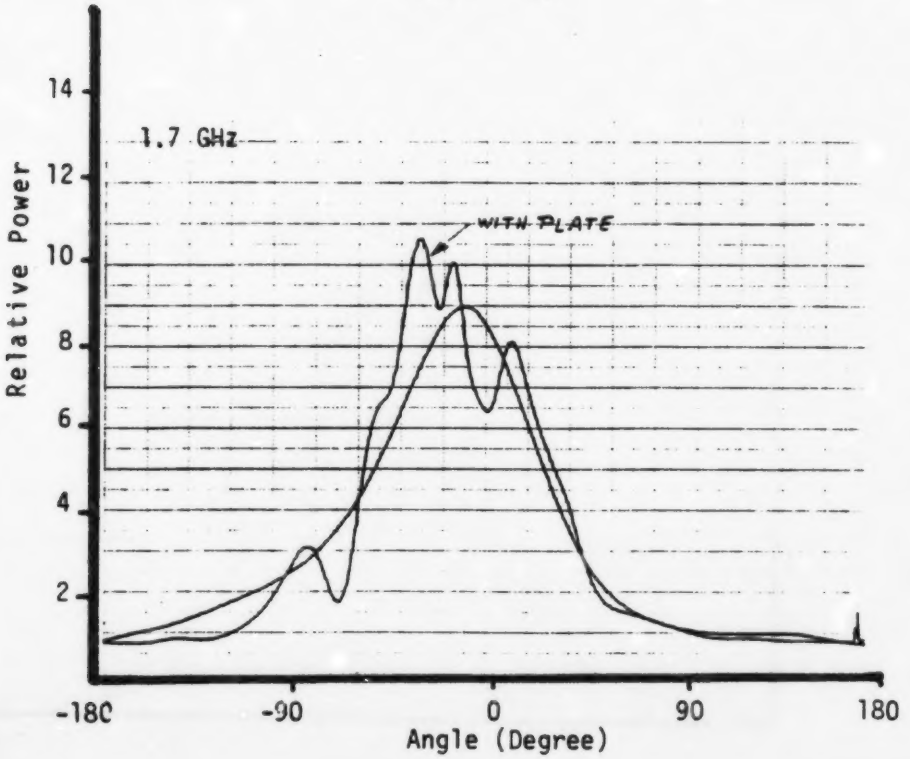

FIGURE 37(h)

FIGURE 37 - E-Plane radiation patterns for TRLD in a square cavity with and without metal back plate.

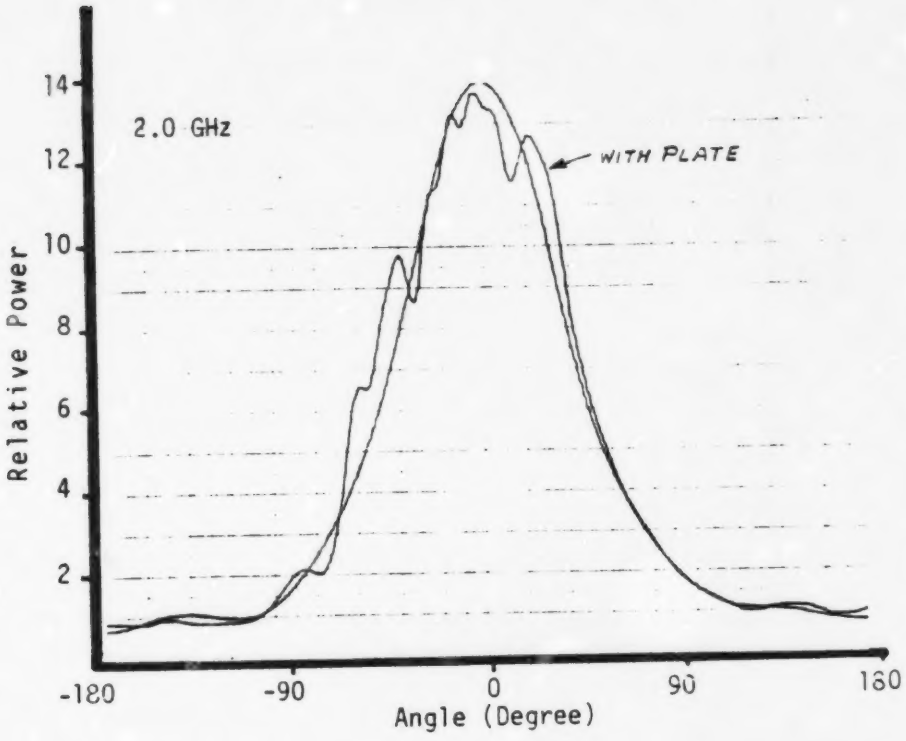

FIGURE 37(i)

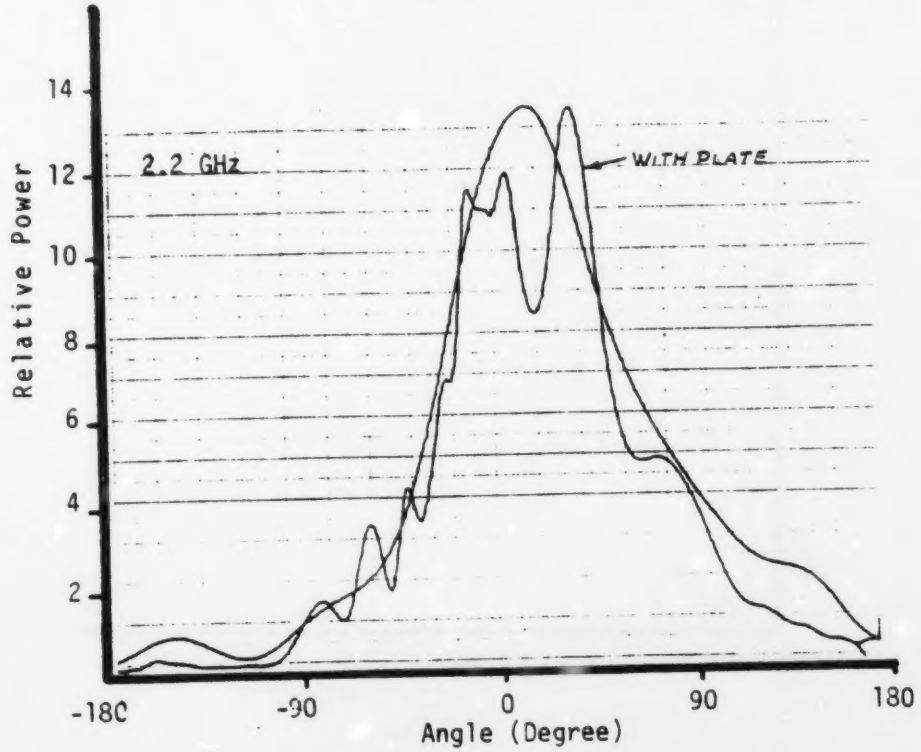

FIGURE 37(j)

FIGURE 37 - E-Plane radiation patterns for TRLD in a square cavity with and without metal back plate.

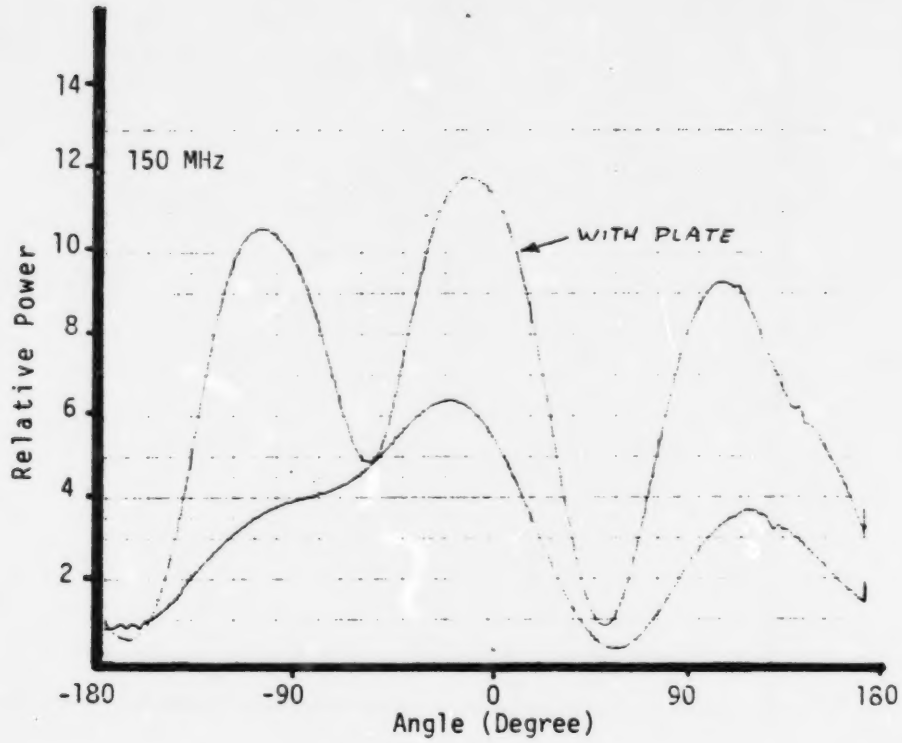

FIGURE 38(a)

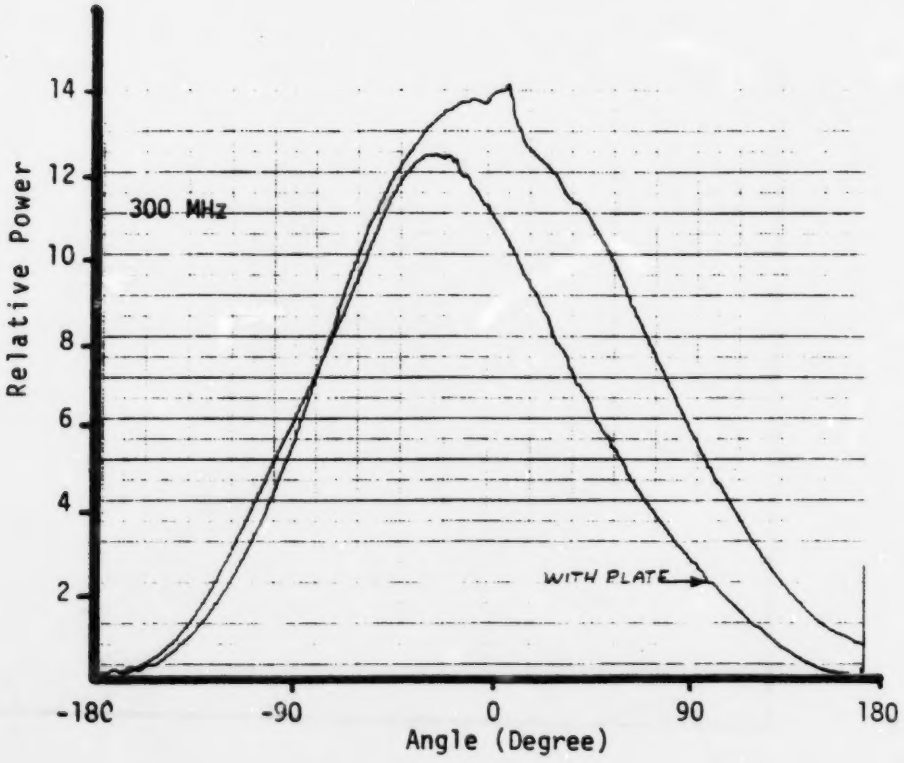

FIGURE 38(b)

FIGURE 38 - H-Plane radiation patterns for TRLD in a square cavity, with and without metal back plate.

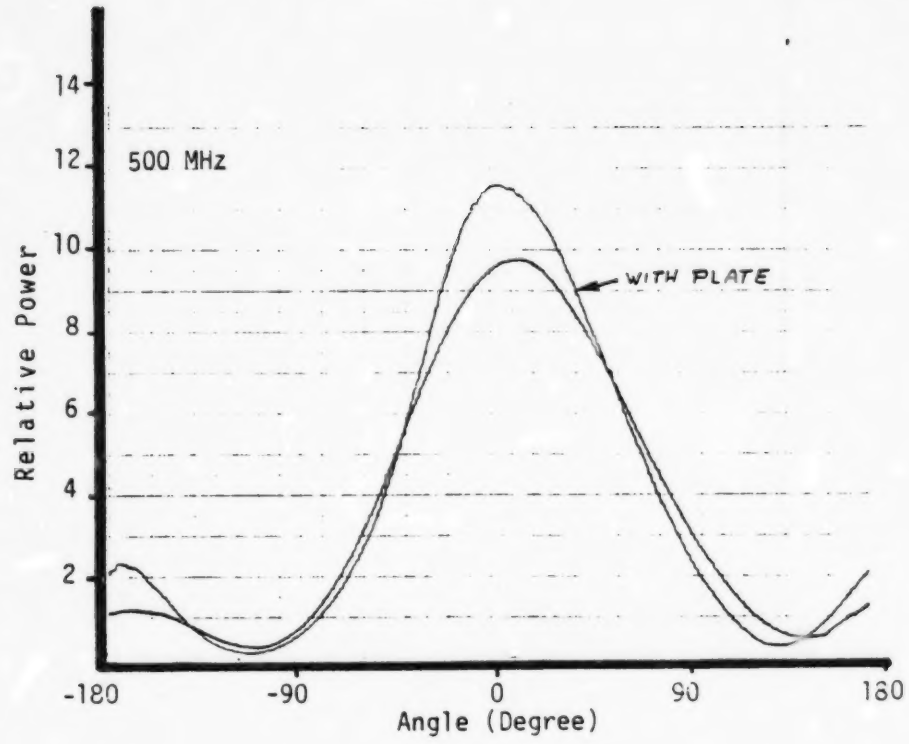

FIGURE 38(c)

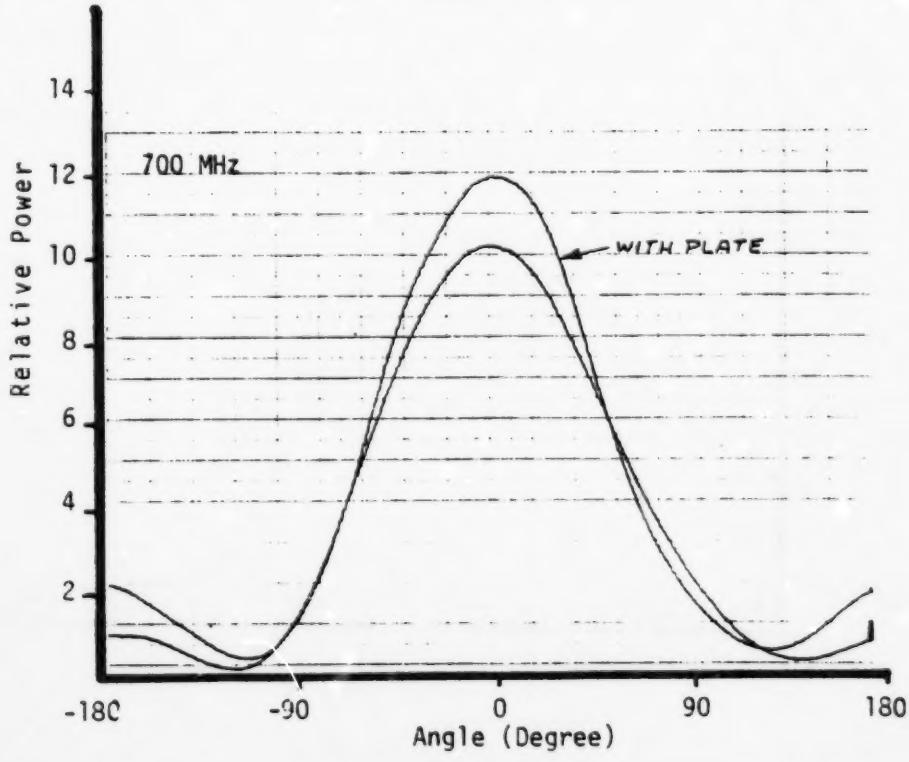

FIGURE 38(d)

FIGURE 38 - H-Plane radiation patterns for TRLD in a square cavity, with and without metal back plate.

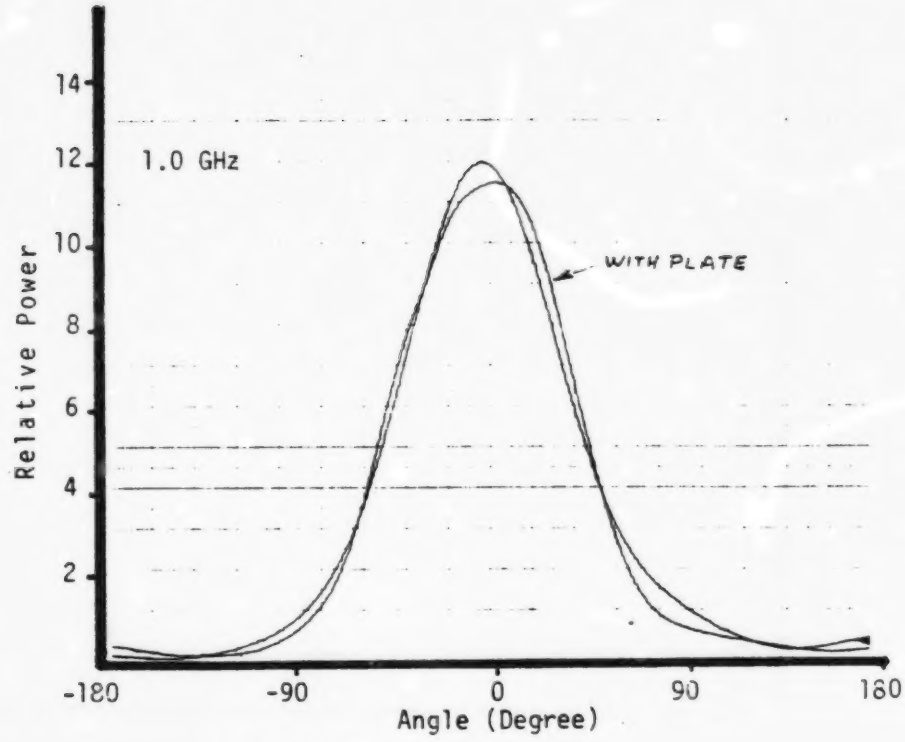

FIGURE 38(e)

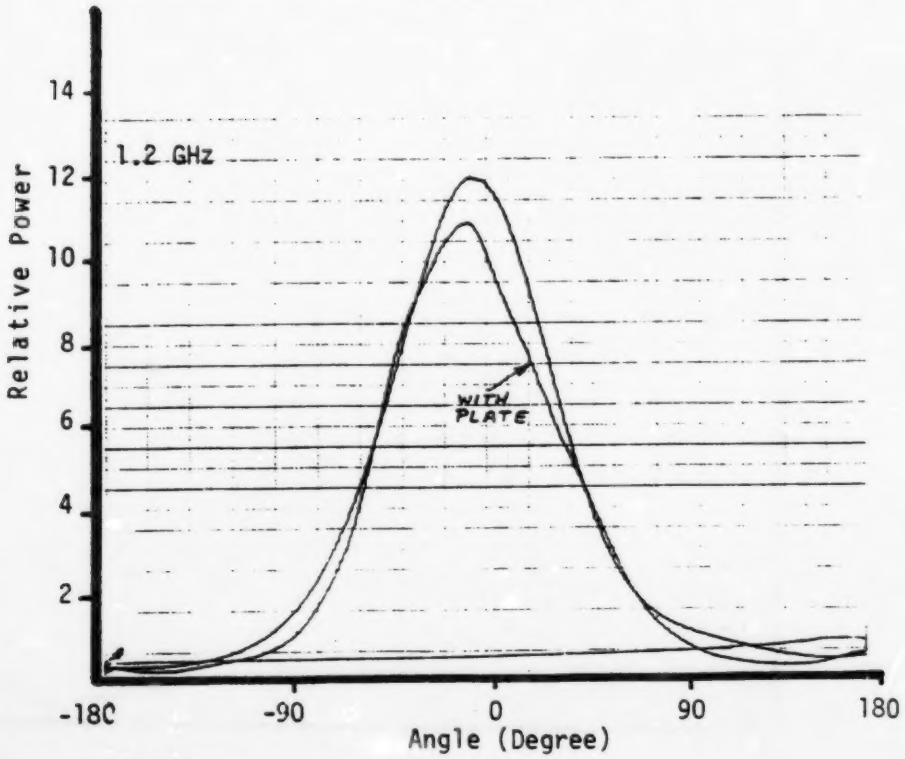

FIGURE 38(f)

FIGURE 38 - H-Plane radiation patterns for TRLD in a square cavity, with and without metal back plate.

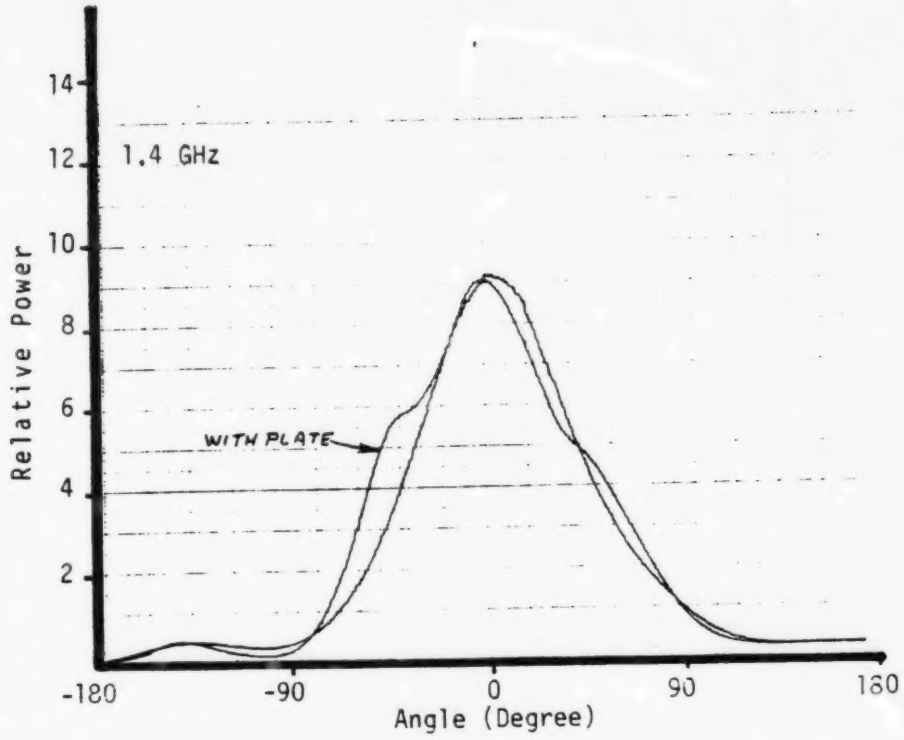

FIGURE 38(g)

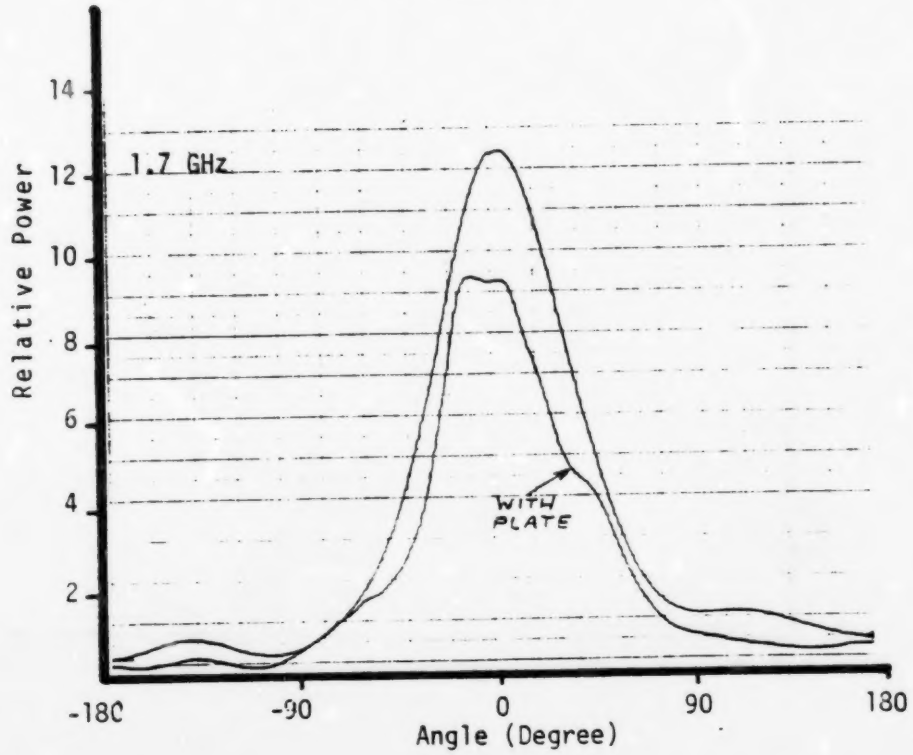

FIGURE 38 (h)

FIGURE 38 - H-Plane radiation patterns for TRLD in a square cavity, with and without metal back plate.

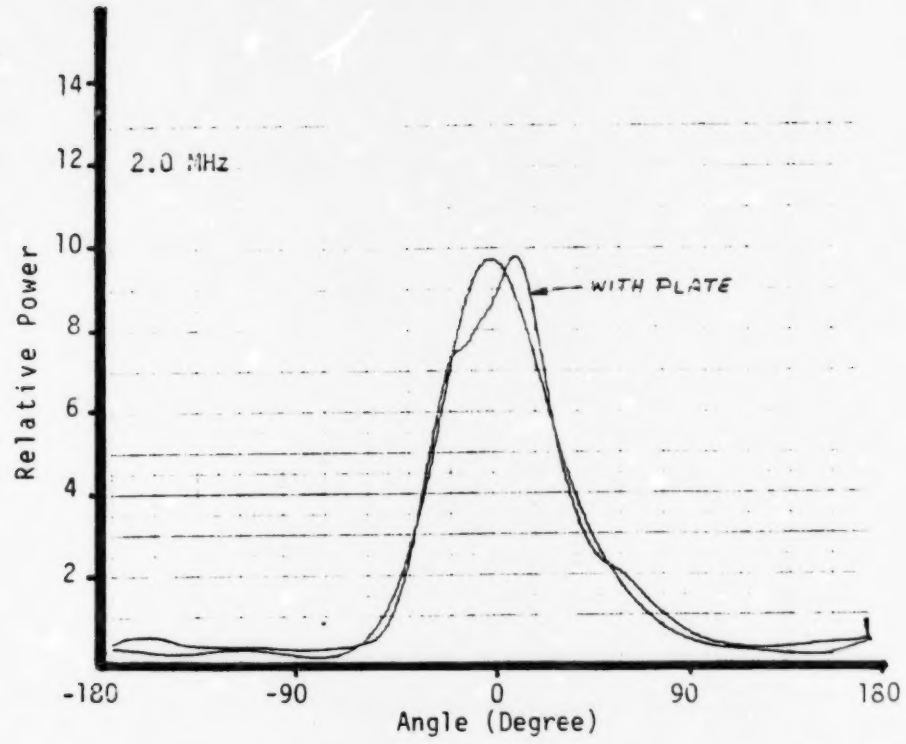

FIGURE 38(i)

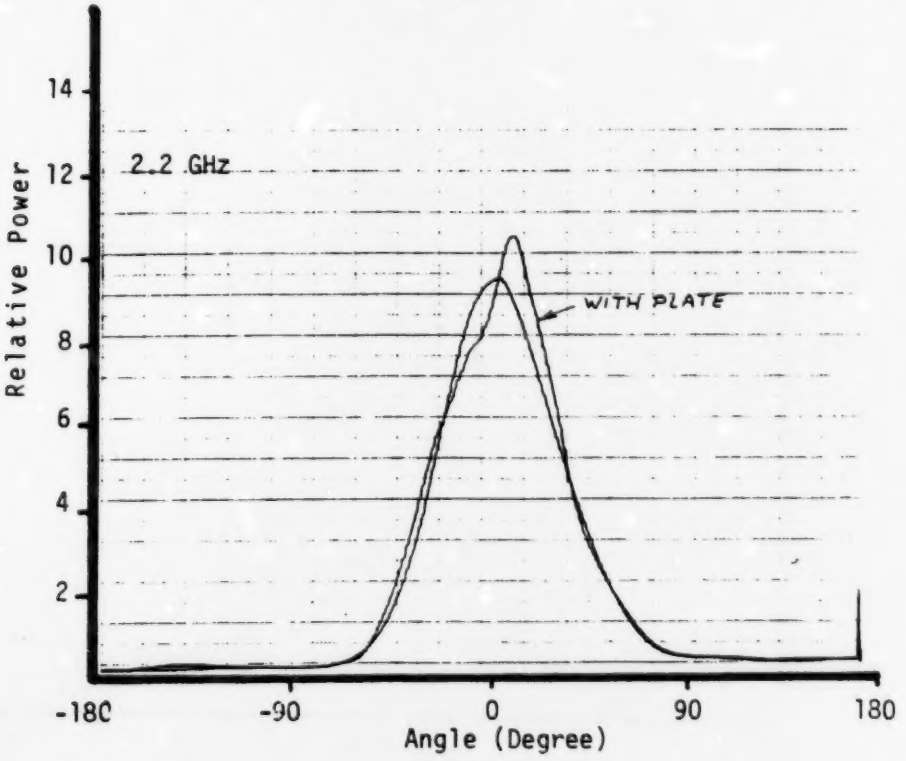

FIGURE 38(j)

FIGURE 38 - H-Plane radiation patterns for TRLD in a square cavity, with and without metal back plate.

6.0 SUMMARY AND RECOMMENDATIONS

The performances of various candidate antennas for a sea-ice thickness sensor have been studied. Using subscale antennas with a scaling factor of 10, it was possible to measure the frequency responses, transient characteristics, transmission properties and radiation patterns indoors in a test range of manageable dimensions. The antennas studied included the superturnstile (Bow Tie), the triangular dipole, the spiral, the modified spiral and the tapered resistively loaded dipole (TRLD).

The effects of antenna-aircraft interactions which have been considered a major problem was found to be almost greatly suppressed when a TRLD was installed in a suitable reflector. The reflector also gave improved directivity. Both the cylindrical and the rectangular reflector geometries were studied in anticipating different possible mounting arrangements on a helicopter.

The study suggests that:

(a) The tapered resistively loaded dipole has the best overall performance, i.e., a good transient response in a small size. It is recommended for the sea-ice thickness sensor applications.

(b) Within the constraints of physical laws, i.e. size and airworthiness limitations, either the cylindrical or the rectangular can be used as an antenna reflector to provide a workable directivity and a shield from the antenna-aircraft interactions.

(c) Although the driving antenna dipole element such as the TRLD has a good transient response and frequency characteristics, the

reflector geometry with its relatively small size is expected to have significant effects on the ultimate antenna characteristics. Since the interaction between the dipole and the reflector is a near field effect, it is strongly dependent on the exact geometries of the various components. It is, therefore, important to decide on the exact geometry in the actual VHF (full size) antenna and reflector including the location of the antenna-reflector on the helicopter. The overall performance of the helicopter borne antenna is better studied on actual full size VHF antenna itself.

(d) Since the antenna reflector is fairly large, a particular configuration may not be acceptable for fix-mounting on a helicopter. Discussions with a helicopter pilot and aerodynamic experts are essential. Compromise configurations may be necessary.

(e) The study using subscale antennas has provided valuable information on the candidate antennas, their characteristics and their most suitable configurations. The next step is to develop the full scale antenna using the relevant results from the subscale experiment.

7.0 REFERENCES

[1] S.Y.K. Tam, J.M. Keelty, G. Riedel and I.P.W. Sinclair «Development of a Remote Sea-Ice Thickness Sensor: Simulation Experiments in the Experimental Prototype. Vol. 1, MPB Technologies Inc., Report No. MPBT-134-1; Transport Canada Report TP 2634, 1980.

[2] J.M. Keelty and S.Y.K. Tam «Sea-Ice Thickness Radar Measurements in the Beaufort Sea», MPB Technologies Inc., Report No. MPBT-157R-1, Transport Canada Report TP2677, 1980.

[3] H. Jasik, Ed. Antenna Engineering Handbook, New York 1961.

[4] G.H. Brown and O.M. Woodward, Jr., «Experimentally Determined Radiation Characteristics of Conical and Triangular Antennas», RCA Rev., Vol. 13, p.425, December 1952.

[5] V.H. Ramsey, Frequency Independent Antennas, Academic Press, 1966.

[6] J.D. Dyson, «The equiangular spiral», IRE Trans. vol.AP-7, No. 2, April 1959.

[7] T.T. Wu and R.W.P. King, «The Cylindrical Antenna with Non-Reflecting Resistive Loading», IEEE, AP, May 1965.

[8] J.F. Lally and D.T. Rouch, «Experimental Investigation of the Broadband Properties of a Continuously Loaded Resistive Monopole», IEEE Trans. AP, Nov. 1970.

[9] L.C. Shen, «An Experimental Study of the Antenna with Non-Reflecting Resistive Loading», IEEE Trans. AP, March 1966.

[10] E.E. Altshuler, «The Travelling Wave Linear Antenna», IEEE, AP, July 1961.

[11] L.C. Shen and T.T. Wu, «Cylindrical Antenna with Tapered Resistive Loading», Radio Science, Vol. 2, Feb. 1967.

[12] C.D. Taylor, «Cylindrical Transmitting Antenna: Tapered Resistivity and Multiple Impedance Loading», IEEE, AP, March 1968.

[13] W.H. Kummer et al,«IEEE Standard Test Procedures for Antennas» IEEE and Wiley, Interscience, 1979.

[14] J.D. Krans, Antennas, McGraw Hill, 1950

[15] S. Silver, Ed., Microwave Antenna Theory and Design, MIT Press, 1963.

MPB TECHNOLOGIES INC.
1725 North Service Road | Trans-Canada Highway
Dorval, Québec H9P 1J1
(514) 683-1490 Telex 05-823509

MPB

PART 2

ANTENNA DESIGN, CONSTRUCTION, FIELD MEASUREMENTS, TRIALS AND LICENSING

PART 2

TABLE OF CONTENTS

		PAGE NO.
1.0	INTRODUCTION	1
	1.1 Survey of Antenna Development Results	1
	1.2 Requirement and Limitations of VHF Test Range	3
	1.3 Approaches to VHF Antenna Measurements	5
2.0	LOCAL FIELD MEASUREMENTS	6
	2.1 Field Measurements at MPB Technologies Inc.	6
	2.1.1 Experimental Arrangement	6
	2.1.2 Types of Antennas Tested	12
	• Resistively Loaded Dipole	12
	• Multiple Dipole (MD) Antenna	14
	• Helical Dipole	16
	2.1.3 Types of Reflectors Tested	19
	• Cylindrical Reflector	19
	• Rectangular Reflector	19
	• Square Reflector	19
	• Airborne Reflector	19
	2.1.4 Results of Measurements	22
	2.2 Field Measurements at Outdoor Test Range	40
3.0	LOCAL HELICOPTER TRIALS	42
4.0	AIRWORTHINESS TESTS AND LICENSING	43
	4.1 Certification Tests at DOT Heliport, Ottawa	43
	4.2 Re-certification Tests at DOT Heliport, St.Johns, Nfld.	43
5.0	SUMMARY AND RECOMMENDATIONS	44

LIST OF FIGURES

		PAGE NO.
FIGURE 1.1	A comparison of two reflector geometries (a) cylindrical and (b) rectangular, showing possible locations for installation on a helicopter.	2
FIGURE 2.1 (a) & (b)	Full-scale tapered resistively loaded dipoles (TRLD) mounted in cylindrical reflectors	8
(c) & (d)	Full-scale tapered resistively loaded dipoles (TRLD) mounted in cylindrical reflectors	9
FIGURE 2.2	Full-scale tapered resistively loaded dipoles (TRLD) mounted in (a) rectangular and (b) square reflectors	10
FIGURE 2.3	Experimental arrangement to test radar with antenna. etc.	11
FIGURE 2.4	Drawing of resistively loaded dipole showing construction of final airborne version	13
FIGURE 2.5	Multiple dipole antenna	15
FIGURE 2.6	Photos showing comparison of a CW signal transmitted through multidipole antennas, 12 m apart.	17
FIGURE 2.7	Helically wound short antenna	18
FIGURE 2.8 (a) & (b)	Sea-ice antenna assembly installed under Bell 206 helicopter	20
FIGURE 2.8 (c) & (d)	Sea-ice antenna assembly installed under Bell 206 helicopter	21
FIGURE 2.9	Mock-up of antenna reflector used to determine final mounting position on helicopter	23
FIGURE 2.10	Transmission characteristics of TRLD in rectangular reflector for impulse of 100 MHz signal.	25

....

LIST OF FIGURES, cont'd....

		PAGE NO.
FIGURE 2.11	Transmission characteristics of TRLD in rectangular reflector for impulse of 100 MHz signal.	26
FIGURE 2.12	Transmission characteristics of TRLD in rectangular reflector for 4 ns, d-c pulse.	28
FIGURE 2.13	Oscillogram showing 4 ns d-c pulse at input of transmit antenna X-axis = 10 ns/div Y-axis = 5 V/div	28
FIGURE 2.14 (a) & (b)	Radiation pattern measurements for TRLD in a rectangular reflector, etc...	30
•FIGURE 2.14 (c) & (d)	Radiation pattern measurements for TRLD in a rectangular reflector, etc...	31
FIGURE 2.15	VSWR characteristic of TRLD in a rectangular reflector. etc...	33
FIGURE 2.16	Plot of VSWR as a function of frequency for a TRLD in a rectangular reflector.	34
FIGURE 2.17	VSWR characteristic of TRLD in a rectangular reflector with resistive matching	36
FIGURE 2.18	Measurements of 4 ns, d.c., pulse transmitted and received by TRLD's in side by side, square reflectors.	37
FIGURE 2.19	Oscillogram showing repeat of Fig.2.18-B with the return signal expanded in time and amplitude	38
FIGURE 2.20	Oscillogram showing the cross-talk and return signal reflected from a conductive wall 6 m away.	39

1.0 INTRODUCTION

1.1 Survey of Antenna Development Results

Previous experiments [1] using subscale antennas have yielded valuable information on the expected performances of several candidate antennas. The antenna configurations investigated included the super-turnstile (Bow Tie) antenna, the triangular dipole, the spiral, the modified spiral and the tapered resistively loaded dipole (TRLD). The TRLD was found to give the best overall performance characteristics and was recommended for the full scale VHF antenna.

In order to reduce the antenna-aircraft interaction and to improve the directivity of the antenna, two antenna reflector geometries were chosen and tested. The cylindrical reflector was chosen in the event that the antenna had to be installed next to the helicopter skids (see Fig.1.1a). A cylindrical geometry was expected to reduce the aerodynamic disturbance on the downward draft from the helicopter propeller blades. A rectangular reflector geometry was studied assuming that it could be installed between the skids under the helicopter body (see Fig.1.1b). Results of the subscale experiments suggest that the TRLD in a rectangular reflector would be best for the sea-ice thickness sensor applications.

Despite the promising results from the subscale experiments, there were many unresolved problems before the exact antenna geometry can be decided. Since the antennas were developed for Canadian Coast Guard helicopters, the detailed designs had to meet stringent safety requirements by Transport Canada. Two important considerations related to convenience and safety are:

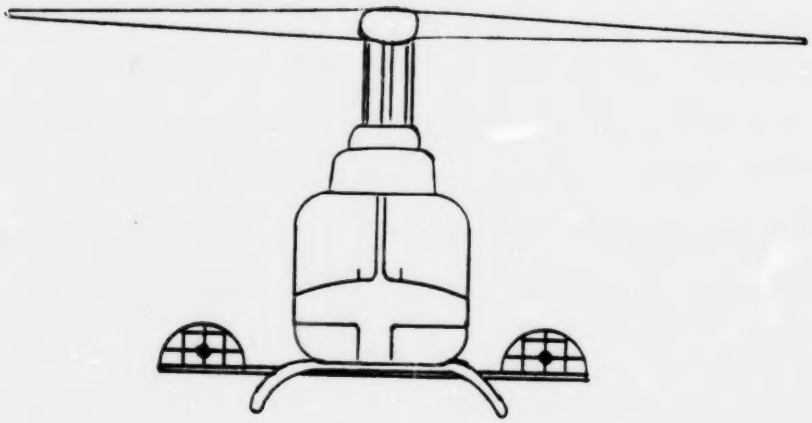

FIGURE 1.1(a)

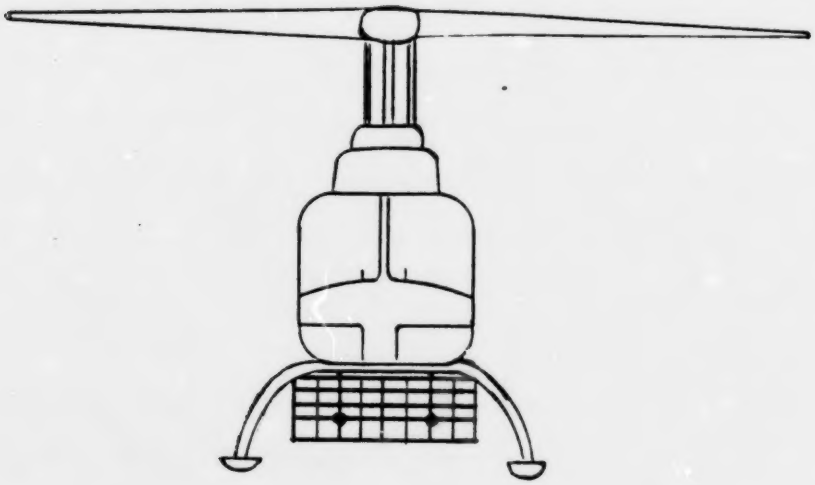

FIGURE 1.1(b)

FIGURE 1.1 - A comparison of two reflector geometries (a) cylindrical and (b) rectangular, showing possible locations for installation on a helicopter.

(a) Size and Configurations of the Antenna

Since the antenna would have dimensions comparable to the helicopter dimensions, it was not certain what antenna configurations would be tolerable. Besides, the choice of configurations and antenna location on the helicopter were very limited.

(b) Airworthiness and Safety

Even when a suitable antenna configuration with reasonable dimensions could be found, there was doubt concerning aspects of the structural integrity especially because the antenna had to have light weight and relatively low aerodynamic resistance. If a reasonable configuration could be found, it could be so bulky, inconvenient, and difficult to manipulate during flights, that helicopter pilots would be reluctant to use it.

1.2 Requirements and Limitations of VHF Test Range

Some basic requirements for a good test range for antenna radiation and transmission measurements have been discussed in Part I of this study [1]. A more detailed discussion can be found in [2]. Essentially, the far field radiation pattern of the test antenna has to be measured with a probing antenna at distance $R > 2D^2/\lambda$, where D is the aperture of the test antenna and λ the relevant wavelength of the rf signal. The transmit receive antennas should be located at sufficient heights and the probing antenna should have a sufficient directivity so as to avoid confusing results due to ground reflections. These limitations can be overcome when subscale antennas are used or when the signal wavelengths are short, e.g. when microwave signals are used.

Unfortunately, VHF signals at frequencies required for the sea-ice thickness sensor, the signal wavelengths range from a meter (300 MHz) to ten meters (30 MHz). Unless the antennas are located several tens of meters above ground, reflections from the ground can have significant effects on the measurements.

At the beginning of this antenna study, an attempt was made to locate a suitable test range for VHF antenna measurements. Unfortunately, most antenna manufacturers that were approached either had no experience in transient antennas, or not interested in renting out a test facility. Besides, the relatively limited resources available in the development program prevented major undertaking or installation of an antenna test facility.

Besides the problems of antenna test ranges, interferences by VHF signals from amateur radios, FM radio stations and VHF TV stations severely hampered the antenna transmission measurements.

After some serious considerations, it was decided that the most cost effective approach would be to test some specific aspects of the VHF antennas such as transmission efficiency and VSWR in a test range at the MPB Technologies Inc. facilities. These tests essentially would verify some of the results from the subscale experiments. The ultimate tests of the usefulness of the antennas and other aspects such as the antenna-helicopter interaction would best be studied with the antenna installed on the helicopter.

Despite the previously mentioned problems, important and quantitative results could be obtained using pulse VHF signals.

Since the real signals and spurious reflections from the ground or other nearby objects, are separated in time, it was possible to study not only the transient properties of various antenna arrangements, but also their transmission properties.

1.3 Approaches to VHF Antenna Measurements

The approaches taken to conduct the VHF antenna measurements are conditioned by the resources available, the schedule, convenience of measurements and limitations of a VHF test range. After the subscale experiments which identified the suitable antenna for the sea-ice thickness sensor, the VHF antenna measurements were carried out in three stages. First, preliminary measurements were obtained in a test range near MPB Technologies Inc. These measurements provided better understanding on the transient response of the full scale VHF antennas using actual VHF components. They also provided qualitative results on the VSWR and qualitative data on the transmission characteristics. The next stage of the measurements were to conduct measurements in a test facility remote from the city. In an environment relatively free from VHF air waves due to the radio and TV stations and the amateur radio stations, it was possible to increase the sensitivity of the radar receiver so as to obtain radar echoes from targets. In the third stage, the antenna was mounted on a helicopter and the antenna responses to radar return from lake water or ice were studied. The final tests on the antenna were to conduct sea-ice thickness measurements in a relatively real environment.

2.0 LOCAL FIELD MEASUREMENTS

2.1 Field Measurements at MPB Technologies Inc.

2.1.1 Experimental Arrangement

In an attempt to design an antenna to meet the physical constraints required for airborne application without severaly compromising the electrical performance, several configurations of dipoles and reflectors were investigated.

It was obvious at the onset of the program that conventional designs of antennas, for this frequency range, would be unacceptably large for helicopter installation. A conventional, half-wave, dipole for 30 MHz is five metres long requiring a reflector of even larger dimensions.

In order to reduce the dimensions to a reasonable size, it was necessary to achieve an acceptable trade-off between bandwidth, radiation efficiency and directivity. To make quantitative measurements of these parameters, full-scale outdoor tests were necessary.

Initial field tests of the full-scale antennas (Fig.2.1 a,b,c&d) were conducted outside the MPB Technologies Laboratories, on a roof-top location. Because of its proximity to the laboratories, this site provided a protected indoor operating environment for the electronic test equipment during inclement weather conditions.

The antennas were mounted on wooden supports, approximately two metres above the roof level to minimize ground effects (Fig. 2.2 a & b). The antennas could be positioned at appropriate

distances for direct transmission measurements or rotated to observe reflected signals from a convenient conductive wall of the building (Fig. 2.3 a & b).

The measurements using this arrangement included the following:

(i) VSWR;

(ii) Mutual coupling between two antennas;

(iii) Antenna bandwidth;

(iv) Transient response;

(v) Transmission and reception by two identical antennas;

(vi) Reflections from a wall;

(vii) Effects of reflector geometry and location of TRLD inside reflector;

(viii) Impedance matching.

In general, these results were consistent with the measurements using the subscale antennas. The full size VHF antenna was found to have a wide bandwidth and a good transient response suitable for the sea-ice thickness sensor. However, since the antenna measurements were obtained in a test arrangement where the near field of the antenna would be significant, a confirmation was necessary using an outdoor test range described in Section 2.2

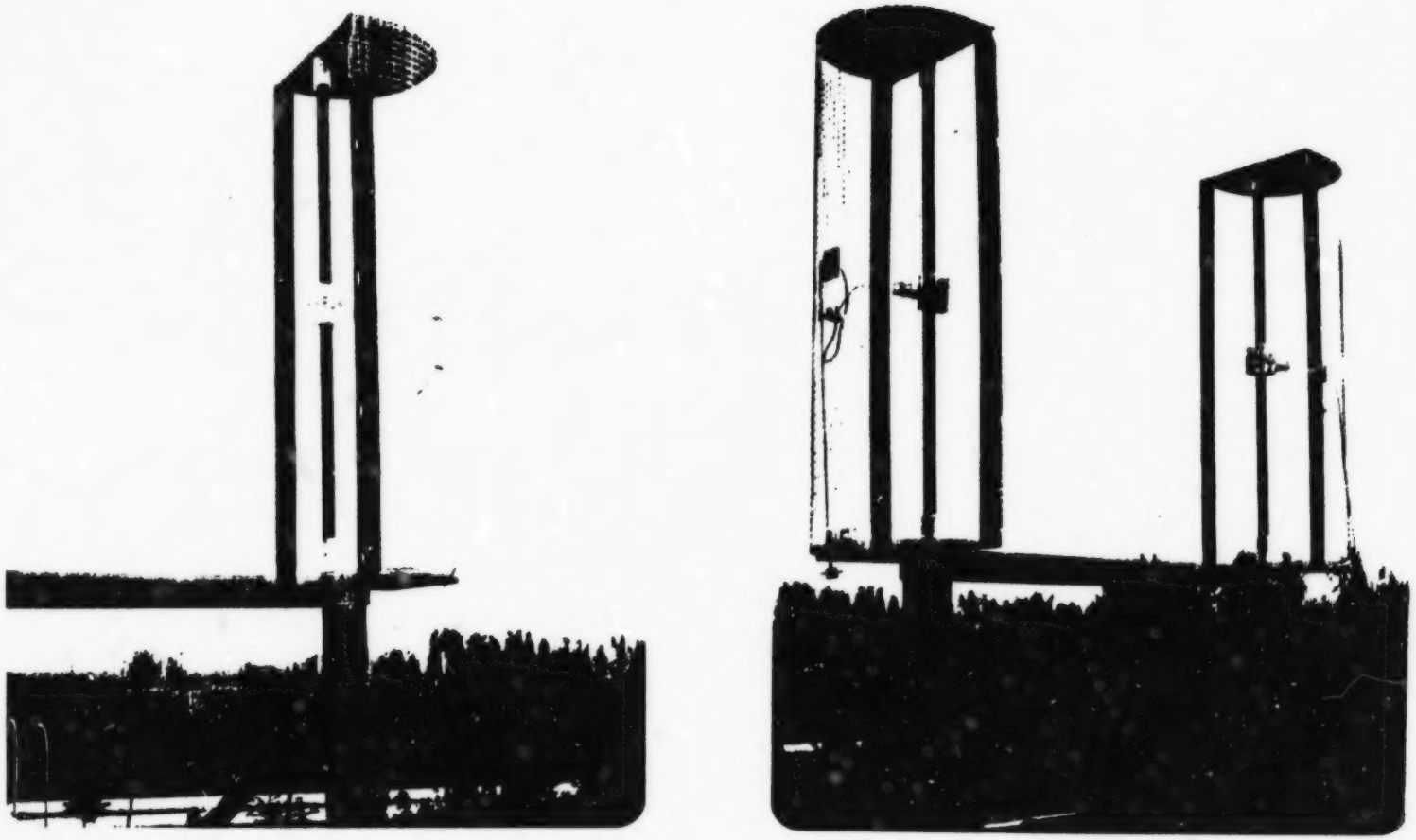

(a) (b)

FIGURE 2.1 - Full-scale tapered resistively loaded dipoles (TRLD) mounted in cylindrical reflectors

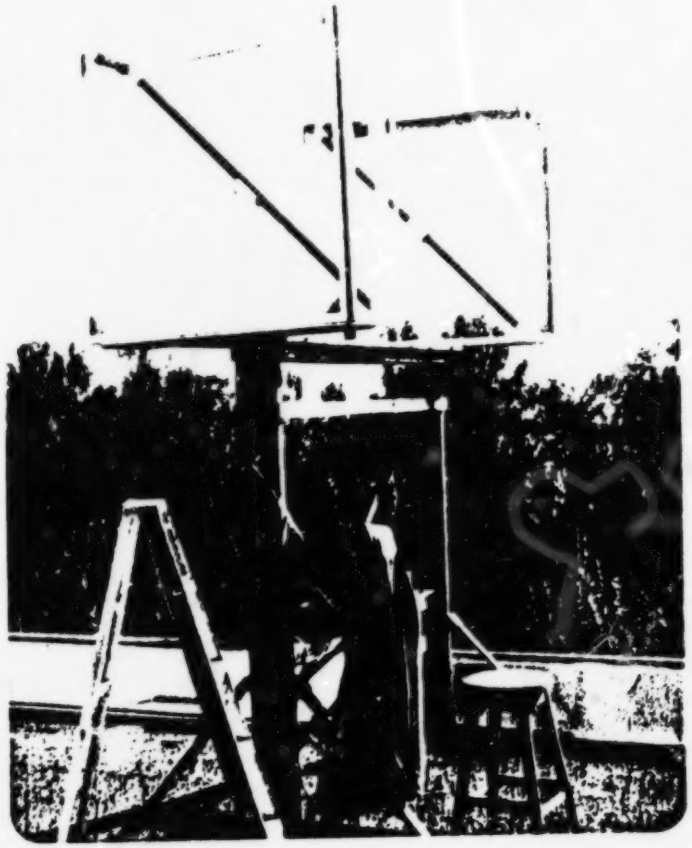

(c)

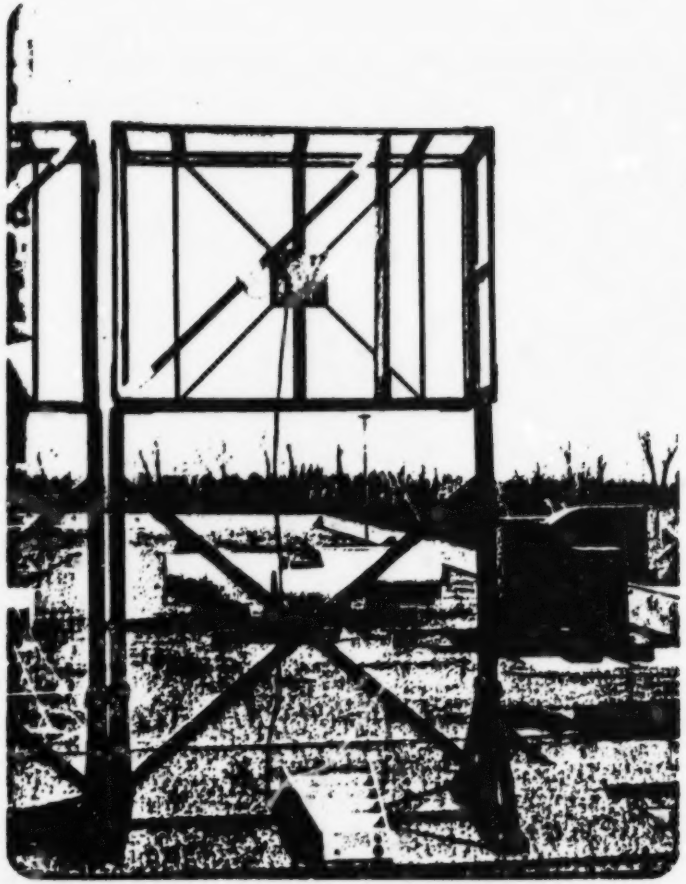

(d)

FIGURE 2.1 - Full-scale tapered resistively loaded dipoles (TRLD) mounted in cylindrical reflectors

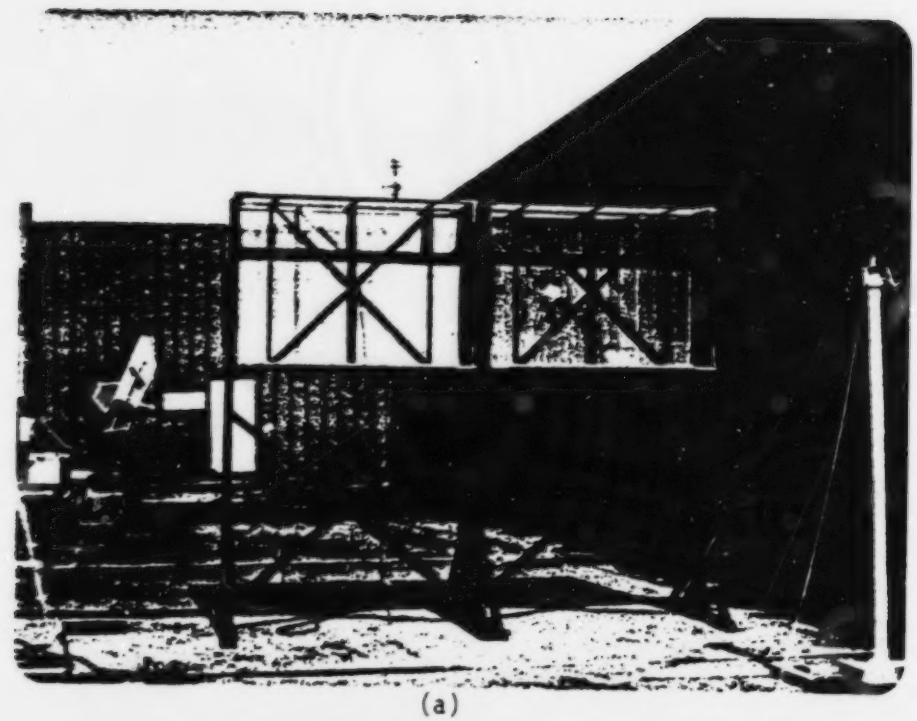

(a)

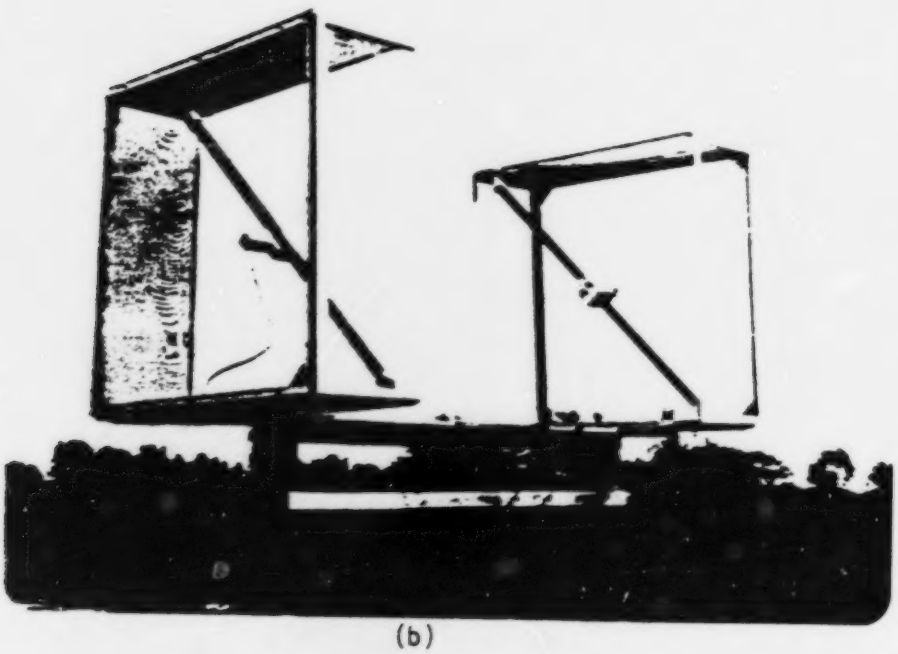

(b)

FIGURE 2.2 - Full-scale tapered resistively loaded dipoles (TRLD) mounted in (a) rectangular and (b) square reflectors.

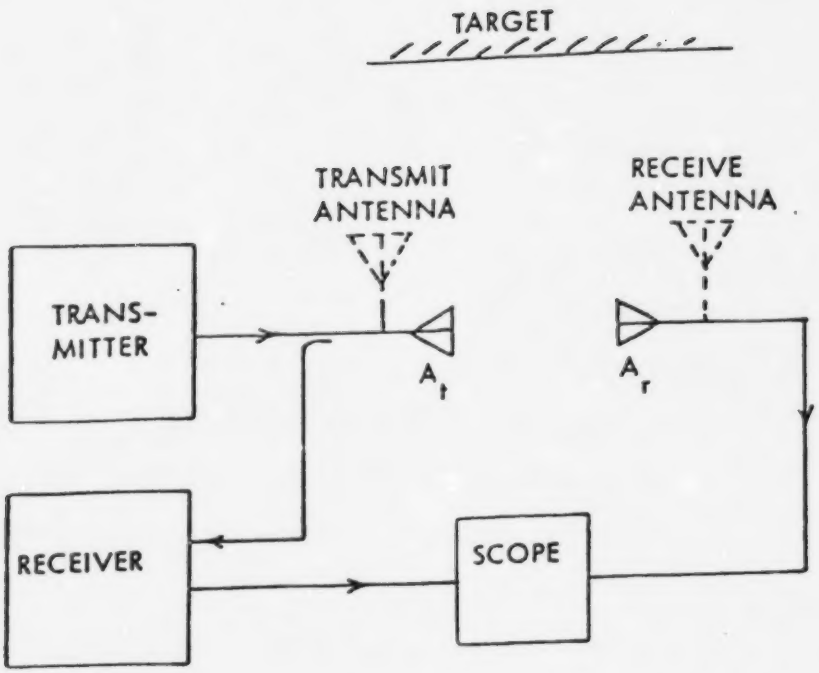

(a) Arrangement with monostatic radar

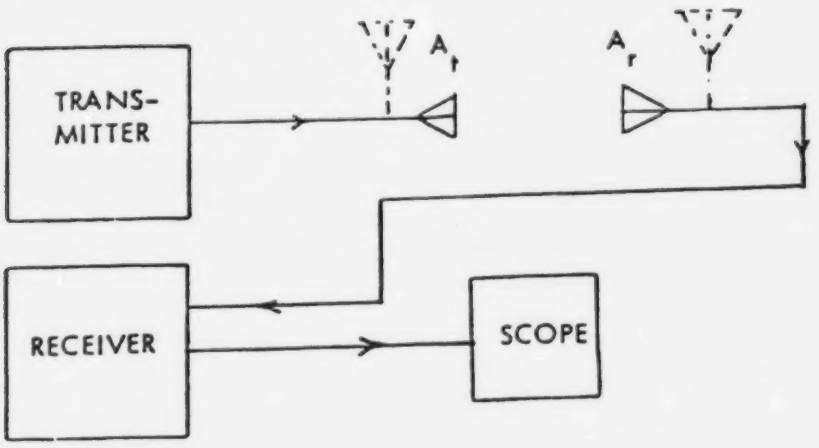

(b) Arrangement with bistatic radar

FIGURE 2.3 - Experimental arrangement to test radar with antenna. Arrangement (a) allowed studies of antenna mismatch and observation of signals transmitted and reflected by antenna A_t respectively. Arrangement (b) enabled study of distortion due to radar receiver by comparing received signal with those obtained in arrangement (a).

2.1.2 Types of Antennas Tested

2.1.2.1 Resistively Loaded Dipole

In the initial lab test the tapered resistively loaded dipole (TRLD) was shown to have a wide bandwidth and a good transient response. Because of this, most of the roof tests involved the full size TRLD mounted in various reflector configurations.

The resistively loaded full-scale dipoles (Fig. 2.4) were constructed using basically the same techniques as in the sub-scale models. A dielectric tube, 6 cm in diameter by 150 cm long was coated with a resistive paint. The coating was applied in successive layers, producing short segments, increasing in resistivity from the centre to the outer ends of the dipole arms. The resistivity of each segment was controlled to simulate an expotentially loaded dipole with the desired characteristics. The feed point at the centre was connected by means of a matching balun transformer and resistor network to minimize the VSWR.

The final version was wrapped with a protective, low temperature, dielectric foam and thin fiberglass tape. A hardwood support rod was inserted through the tube and the whole assembly was sealed with an epoxy coating. Considerable care was taken in the choice and application of these materials so that electrical specifications would not be adversely affected.

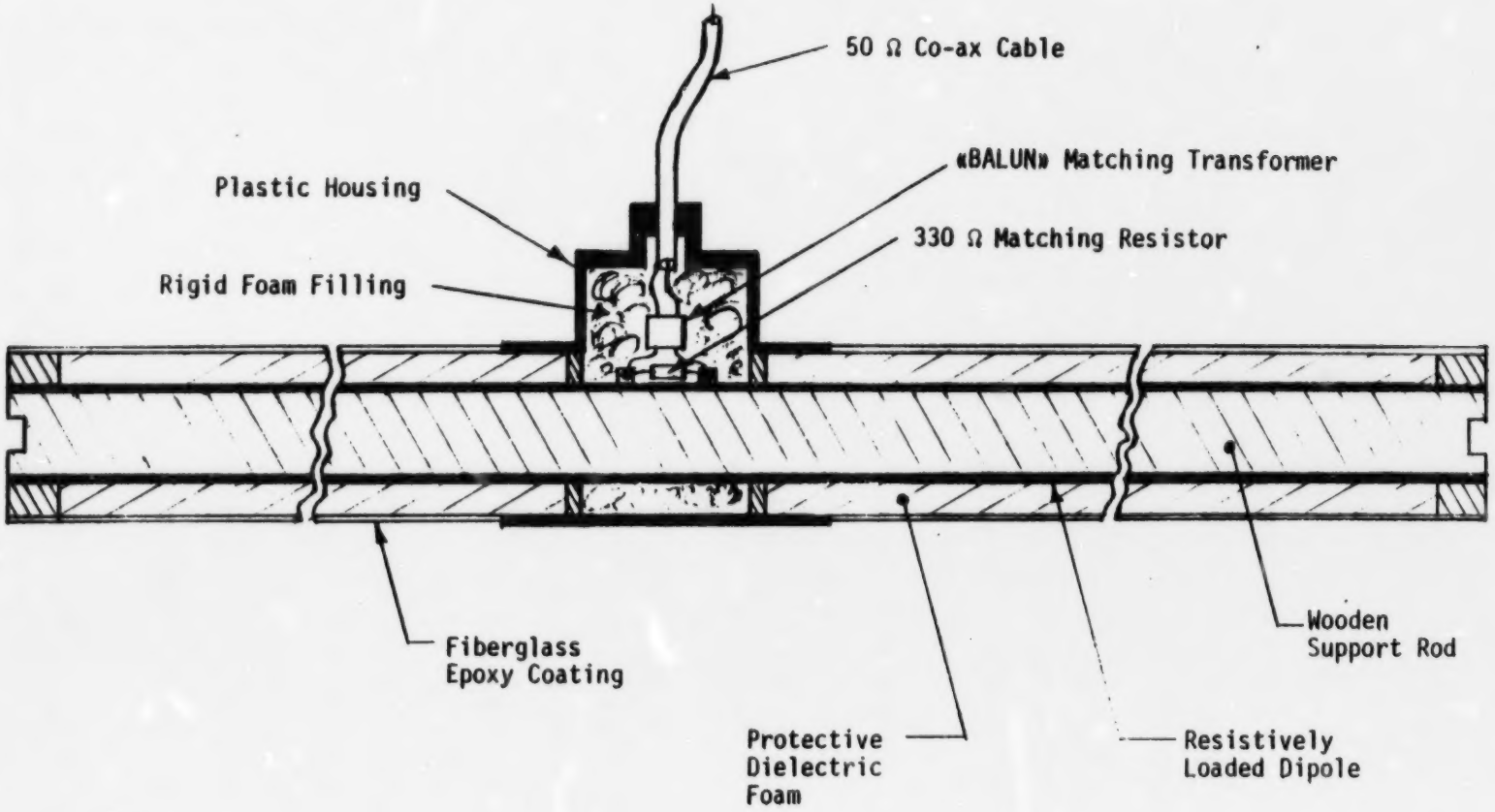

FIGURE 2.4 - Drawing of resistively loaded dipole showing construction of final airborne version.

2.1.2.2 Multiple Dipole (MD) Antenna

Although the TRLD in an appropriate reflector has suitable characteristics for a narrow pulse, broadband signal for sea-ice thickness measurements, its transmission efficiency is reduced by the resistive loading. Attempts were made, in testing other antennas, to find a configuration which would provide better efficiency.

One configuration tested was the multiple dipole which consists of individual dipole elements optimized for transmitting video pulses whose frequency components are confined within narrow bands around isolated frequencies. Specifically, a multiple dipole antenna was constructed for transmitting 30, 60, 90, 120 and 150 MHz signals simultaneously (Fig. 2.5).

Despite the inconvenient length, the multiple dipole antenna has the advantage that it can be tuned to radiate the discrete frequency components efficiently.

Because of its already large linear dimension, the addition of a reflector is not practical and the antenna-aircraft interaction would, therefore, be significant. However, this interaction could be overcome if the MD antenna is used in the synthetic pulse radar[2]. In the synthetic pulse mode the transmitted signal consists of the fundamental and the next four harmonics of 30 MHz. Each harmonic is transmitted for 200 ns and repeated at a rate of 20 KHz.

---

2 J.M. Keelty, S.Y.K. Tam - «Sea-Ice Thickness Radar Measurement in the Beaufort Sea» Transport Canada Report TP2677, (1980)

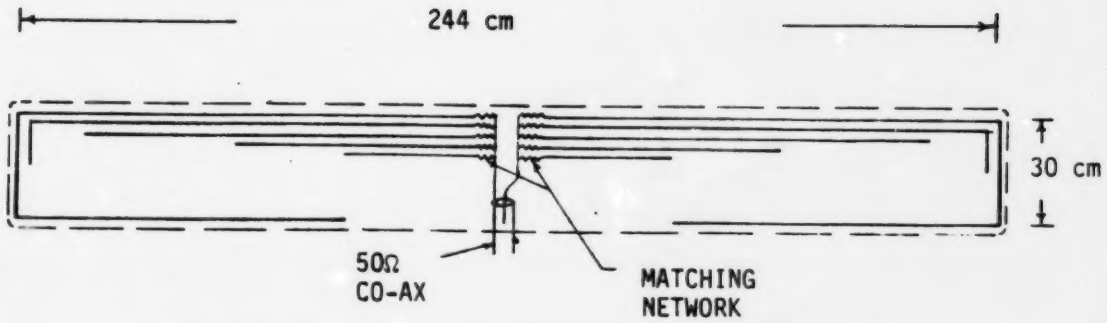

FIGURE 2.5 - Multiple dipole antenna

The phase and amplitude of the individual frequency components are adjustable. Based on the principle of superposition and the fact that each frequency component is transmitted over a long time (over 200 ns) compared with the signal transit over the helicopter dimensions, the antenna-helicopter interaction should only vary the phase and amplitude of each individual harmonic and can be cancelled out by proper phase and amplitude adjustment.

The result of the MD antenna is given in Fig. 2.6(a) in which a CW signal is transmitted and received through identical MD antennas spaced 12 metres apart. By comparing with the signal fed into the transmit MD antenna (Fig. 2.6(b), the output from the receive MD antenna (Fig. 2.6(a) is found to give excellent characteristics with minimal ringing and distortion.

2.1.2.3 Helical Dipole

Another configuration of a short-dipole was investigated. This consisted of a full-wavelength dipole of 10 metres, wound in a helical form around a 4 cm diameter dielectric tube, 162 cm long (Fig. 2.7). This is a technique used by ham operators in locations where space is a limitation.

These helical dipoles, with suitable matching networks, were constructed and tested outside.

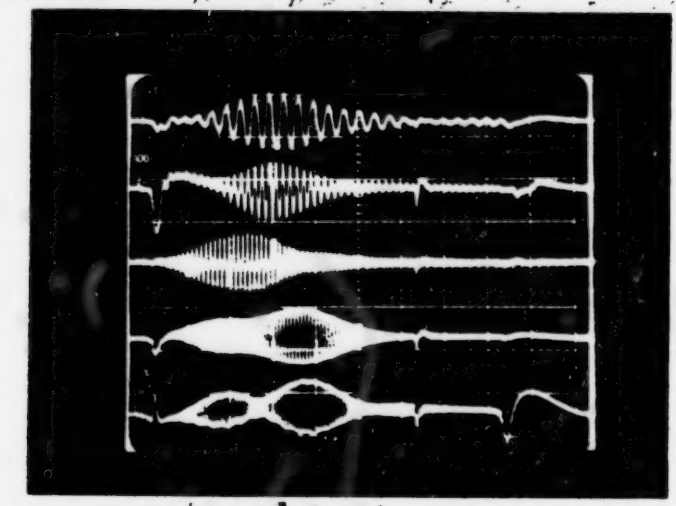

(a)

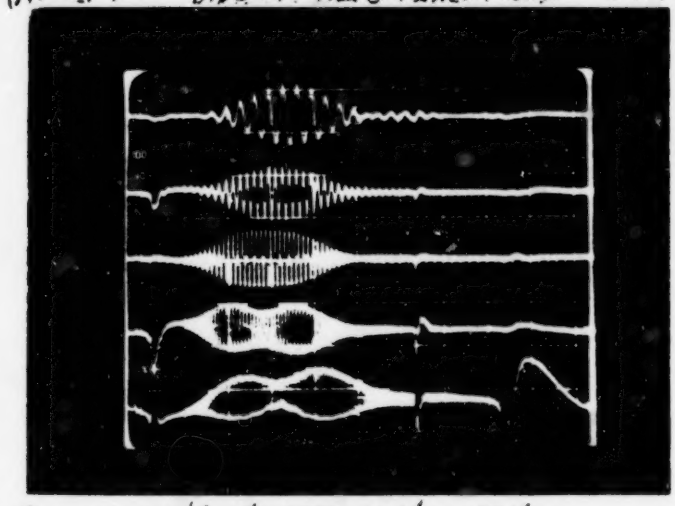

(b)

FIGURE 2.6 - Photos showing comparison of a CW signal transmitted through multidipole antennas, 12 m apart
(a) Signal measured at receive antenna output
(b) Signal measured at transmit antenna input

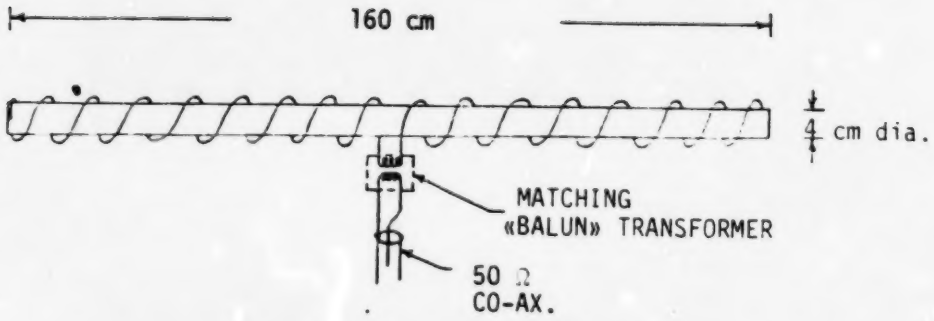

FIGURE 2.7 - Helically wound short antenna

2.1.3 Types of Reflectors Tested

2.1.3.1 Cylindrical Reflector

Full scale cylindrical reflectors were fabricated from plywood and wire mesh (Fig. 2.1) for outdoor test measurements. Allowance was made for positioning the dipole within the reflector, to study the effect on the radiation pattern and mutual coupling between the transmitter and receiver when mounted side by side.

2.1.3.2 Rectangular Reflector

Separate rectangular panels of wood frame and metal screening were constructed. These panels could be assembled to produce full-scale rectangular reflectors of various dimensions (Fig.2.2(a)). The dipoles were mounted on separate, styrofoam, supports for adjustable positioning within the reflector boxes.

2.1.3.3 Square Reflector

A set of square reflectors were assembled using commercial, aluminum screens ordered to size and screwed together with corner supports (Fig. 2.2(b)).
The dipoles were mounted diagonally, at various positions within the box, and secured in place by end screws.

2.1.3.4 Airborne Reflector

After extended tests of the reflector a final version was designed for helicopter application (Fig. 28 (a,b,c,d).
A single structure, consisting of two TRLD's with two separate rectangular reflectors side by side, was chosen as the best compromise between electrical performance and physical constraints

(a)

(b)

FIGURE 2.8 - Sea-ice antenna assembly installed under Bell 206 helicopter.

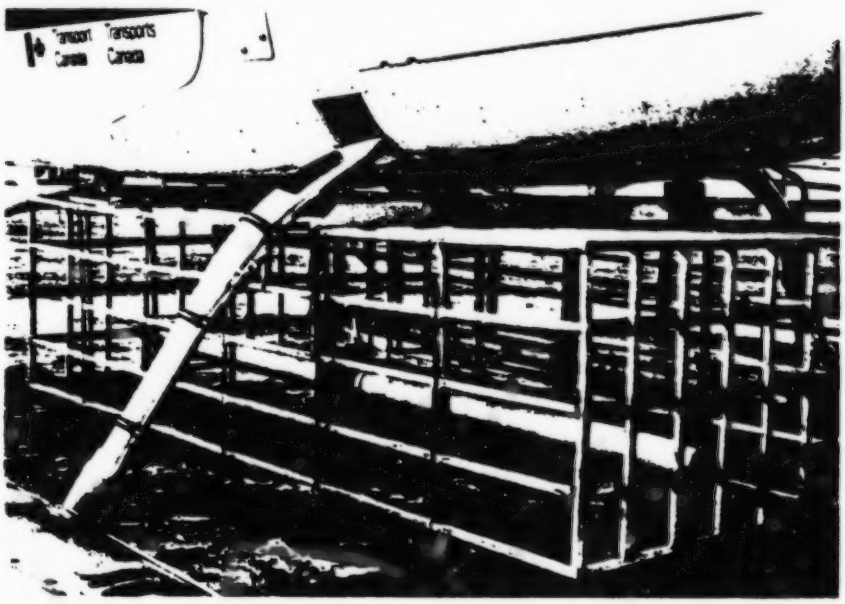

(c)

(d)

FIGURE 2.8 - Sea-ice antenna assembly installed under Bell 206 helicopter.

imposed by aerodynamic considerations. Separate transmit-receive antennas were used since it was difficult at that time to obtain a transmit receive switch suitable for the measurements.

A styrofoam mock-up of the proposed reflector was constructed and fitted under the actual helicopter (Fig. 2.9) to determine the exact position and attachment points.

The reflector was constructed of square thin-wall, aluminum tubing welded together in an open structure to minimize drag and turbulence. The assembly was mounted to the helicopter using the three existing attachment points normally used to connect the U-frame support for the belly-hook. Two standard, spring-release pins are the only pieces of hardware needed to quickly install or remove the entire antenna assembly.

The complete unit weighed 35 kg and was positioned with the centre of gravity directly below the main rotor shaft to maintain aircraft stability.

In the event of an emergency landing, on rough terrain, the structure was designed to collapse on impact without causing damage to the helicopter. When installed the normal ground clearance was 20 to 25 cm.

2.1.4 Results of Measurements

A large number of measurements using various antenna driving elements (TRLD, multiple dipole, and helical dipole) and reflectors (rectangular, square, and cylindrical) have been obtained. These measurements were taken with either a CW or pulse signal source; whichever was more appropriate for the particular measurements

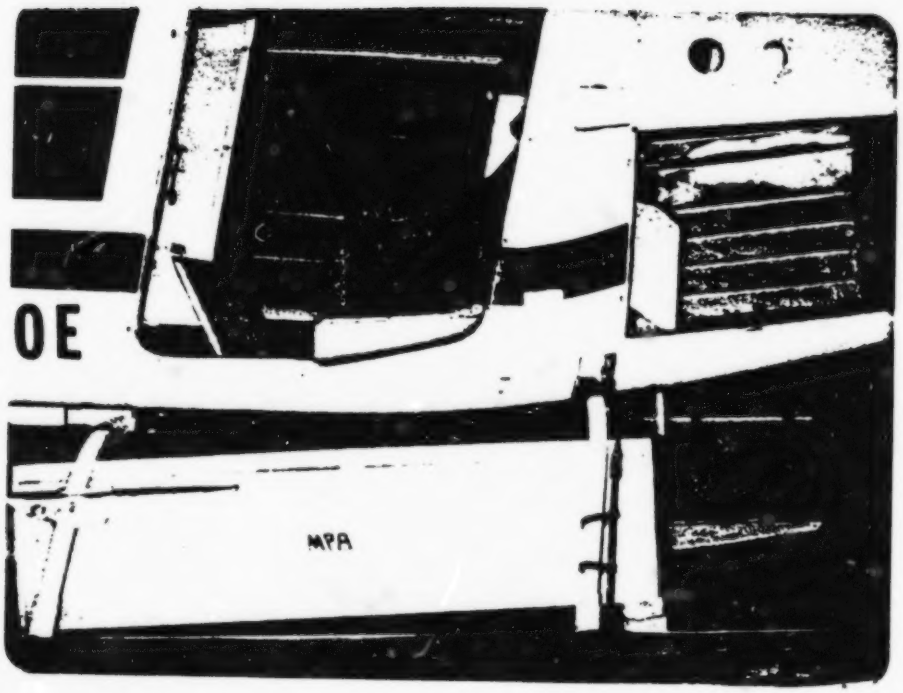

FIGURE 2.9 - Mock-up of antenna reflector used to determine final mounting position on helicopter.

being conducted. The following are representative of the results obtained.

2.1.4.1 Tapered Resistively Loaded Dipole (TRLD) in a Rectangular Reflector

a) Response to impulse of 100 MHz signal

The response of a rectangular, 100 MHz signal (carrier), amplitude modulated by a repetitive rectangular pulse of 50 ns and PRF (pulse repetition frequency) of 20 KHz is as shown in Fig. 2.10 & 2.11. The oscillogram in Fig. 2.10 gives the reference signal being fed to the transmit antenna (bottom trace). The other traces show the signal output from the receive antenna, 13 metres away, for varying positions of the TRLD in the reflector cavity. As expected, the transmission efficiency varies with X, the distance of the TRLD from the back plane of the reflector. The efficiency is maximum when X = 60 cm (24") and minimum when X = 30 cm (12"). The reflector was 75 cm (≈30") deep.

Although the different antenna arrangements gave varying efficiency, the antenna response was adequate since none of the oscillogram traces showed any significant ringing or lengthening of the amplitude modulated pulse. The received signals had the same pulse width as those transmitted. There were additional spurious signals caused by multipath reflections from metal objects in the vicinity of the test facility.

Measurements shown in Fig. 2.11 were made with the transmit and receive antennas located side by side facing a conductive wall 7.3 m away. The reflectors were separated by 40 cm.

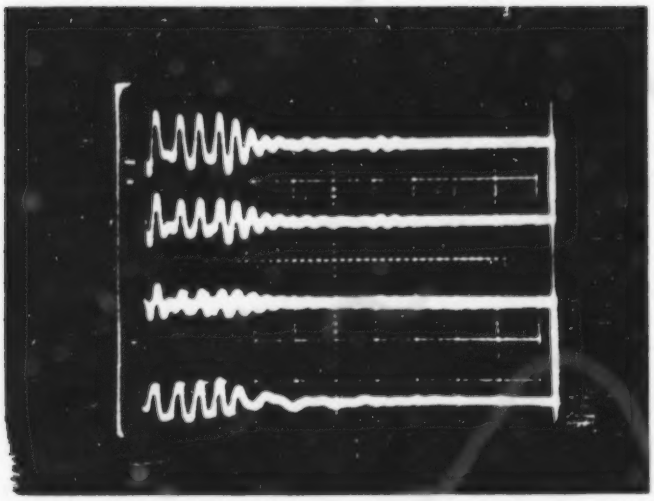

FIGURE 2.10 - Transmission characteristics of TRLD in rectangular reflector for impulse of 100 MHz signal.

TRACES A,B,C show output of receive antenna 13 metres away from transmit antenna for various positions of the TRLD in the reflector.
X-axis = 20 ns/div, Y-axis = 5 mV/div.

TRACE D - shows signal to input of transmit antenna.
X-axis = 20 ns/div, Y-axis = 5 V/div.

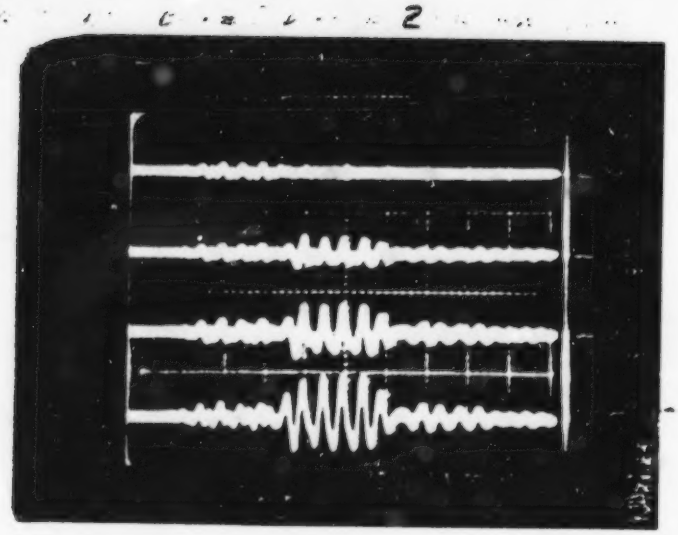

FIGURE 2.11 - Transmission characteristics of TRLD in rectangular reflector for impulse of 100 MHz signal.
X-axis = 20 ns/div, Y-axis = 5mV/div.

TRACE A - shows cross-talk only with transmit/receive antennas facing over edge of roof.

TRACE B, C, D - shows signal reflected from conductive wall 7.3 m away for various positions of the TRLD in the reflector.

The four oscillogram traces correspond to various TRLD positions inside the reflector. Each of these traces shows «cross-talk» (mutual coupling) in the initial 60 ms followed by the transmitted pulse and then spurious signals due to nearby objects. The top trace corresponds to the case where the antennas were side by side facing out, over the edge of the roof, into free space. This gives an accurate measure of the «cross-talk» signal.

b) Response to a 4 ns wide d-c pulse

As explained previously, the relatively long wavelength of the signals being studied caused difficulty from «spurious» signal paths. Since multipath and spurious reflections, due to nearby objects, cannot be eliminated easily, it would be difficult to conduct meaningful transmission measurements using CW (continuous wave) signals.

This problem was eliminated by studying transmission characteristics using short, video pulses. Because of the short duration of these pulses it was possible to separate the spurious signal in time, and actually identify the objects causing the reflections by measuring their relative positions between the transmitter and the target wall. Figure 2.12 shows the receive antenna (A_r) output giving the reflection from a conducting wall 7.3 m away when a 4 ns d-c pulse (Fig. 2.13) is fed to a similar transmit antenna (A_t). A_t and A_r were located side by side with their reflectors 10 cm apart from each other. The oscillogram, in Fig. 2.12 shows the receive antenna output for three different

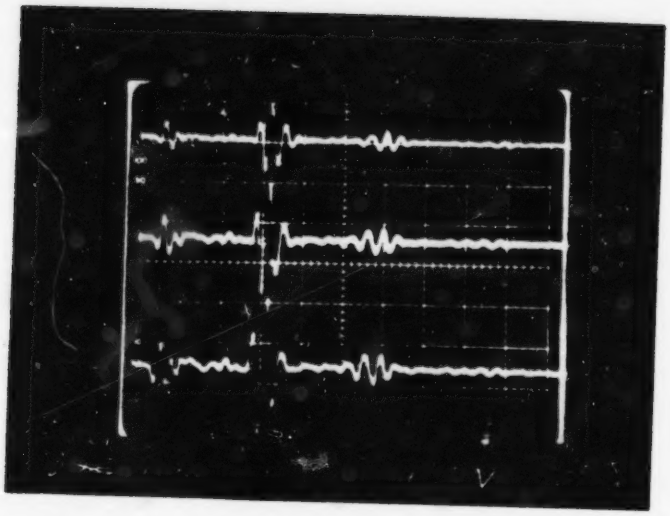

FIGURE 2.12 - Transmission characteristics of TRLD in rectangular reflector for 4 ns, d-c pulse. Traces A,B & C show receive antenna output for signal reflected from conducting wall 7.3 m away, X-axis=20 ns/div
Y-axis=50 mV/div

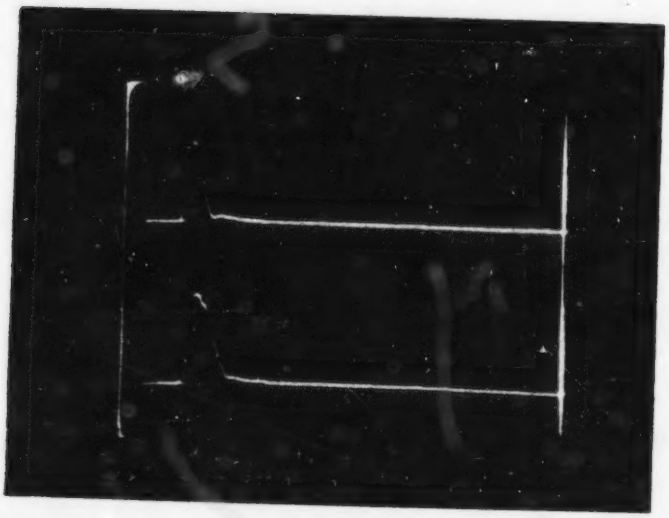

FIGURE 2.13 - Oscillogram showing 4 ns d-c pulse at input of transmit antenna
X-axis = 10 ns/div Y-axis = 5 V/div

TRLD locations in the reflector. For each oscillogram trace, the signal in the first 20 ns is the result of «cross-talk» picked up directly by the receive antenna, at the beginning of transmission. In fact, this «cross-talk» pulse provides a convenient marker that precisely indicates the instant the propagating, R-F pulse leaves the transmit antenna.

The signal between 25 and 35 ns is the reflected signal from the conductive wall, 7.3 m away. Signals that occur after 35 ns are the result of multiple reflections, between the antenna and the wall.

As expected, the transmit/receive antennas would change a d.c. pulse into an a.c. signal. But the received signal shows no sign of broadening as a result of resonance. The observed reflected signal between 25 and 35 ns in Fig. 2.12 shows that the TRLD in a rectangular reflector is suitable for transmitting and receiving the impulse shown in Fig. 2.14.

c) Radiation Pattern

The power radiation pattern of the TRLD in a rectangular reflector was measured with the transmitting antenna (A_t), located at the edge of the roof of MPB Technologies Inc. about 13 metres high, above the ground. The transmitted signal was picked up by an identical antenna (A_r) in the field 30 metres away, mounted on a 13 metre high tower, equipped with a remotely controlled rotary positioner. The two-way radiation pattern of the receive antenna was obtained by transmitting a 4 ns pulse from A_t and receiving the signal at various aspect angles of

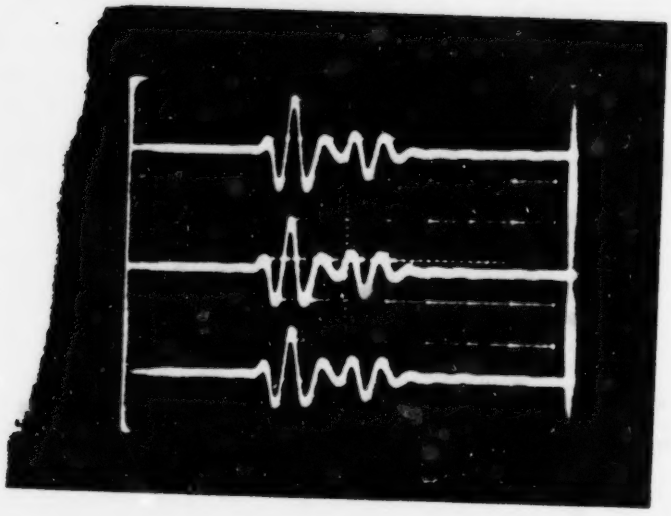

(a)

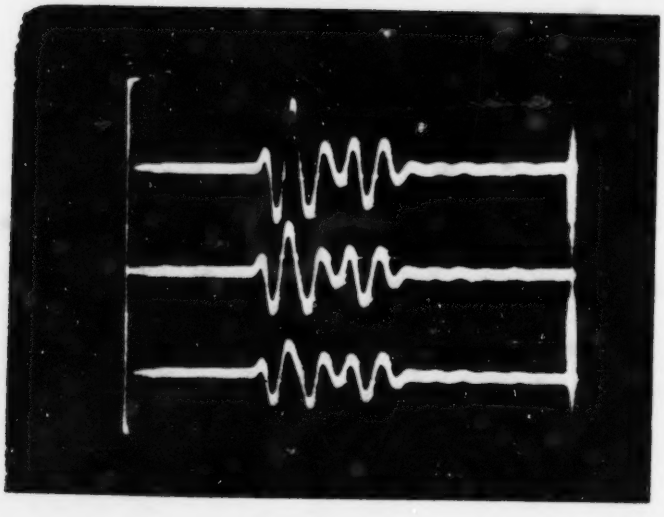

(b)

FIGURE 2.14 (a & b) - Radiation pattern measurements for TRLD in a rectangular reflector, using a 4 ns d.c. pulse from the transmitting antenna and receiving the signal at various aspect angles of the receiving antenna.
X-axis = 10 ns/div, Y-axis = 20 mV/div (a)
= 10 mV/div (b)

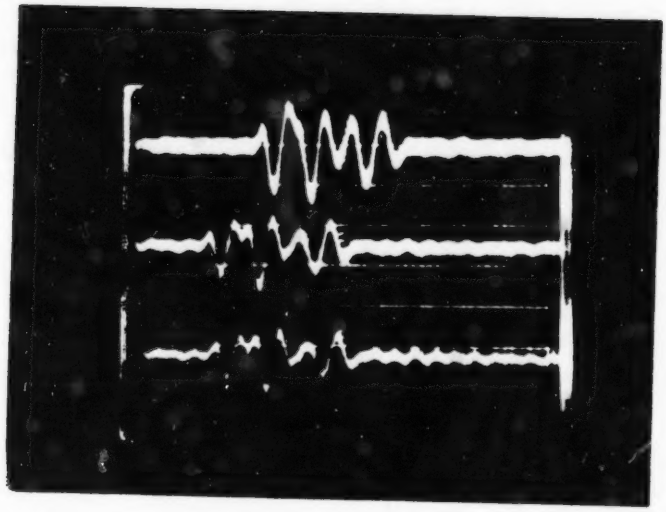

70°

80°

90°

(c)

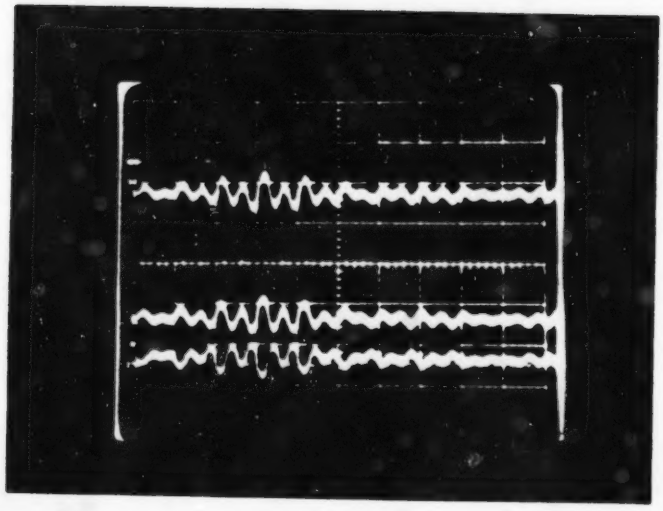

100°

110°

120°

130°

Noise

(d)

FIGURE 2.14(c&d) - Radiation pattern measurements for TRLD in a rectangular reflector, using a 4 ns, d.c. pulse, from the transmitting antenna and receiving the signal at various aspect angles of the receiving antenna
X-axis = 10 ns/div Y-axis = 5 mV/div

A_r (Fig. 2.14(a,b,c,d,)). The measurements were made using short video pulses rather than CW signals. This way it was possible to separate the spurious reflections from nearby objects in time. In fact, each of the oscillograms (Fig. 2.14(a,b,c,d) shows the direct line of sight signal received from the transmitting antenna and an additional signal due to multipath reflection, in this case, from the ground.

If CW signals had been used, the multipath effects would have confused the radiation pattern results. The previous measurements (Fig. 2.14) demonstrate the difficulty in VHF antenna radiation measurements using CW signals.

d) VSWR Measurements

The VSWR characteristics of the TRLD in a rectangular reflector were obtained using CW signals. To minimize the effects of nearby objects, the antenna was located near the edge of the roof, so that it would be transmitting into free space.

The reflected signal, V_a, from the antenna was measured at varying transmitting frequency (Fig. 2.15(a)). For comparison the signal V_s reflected by a short circuit at the antenna input terminal was also obtained (Fig. 2.15(b)).

A plot of the VSWR versus frequency is given by Fig. 2.16.

It is usually possible to provide a matching network at the antenna input to achieve proper impedance matching between the signal source and the antenna. This is generally rather straight forward for narrow band signals and is normally done

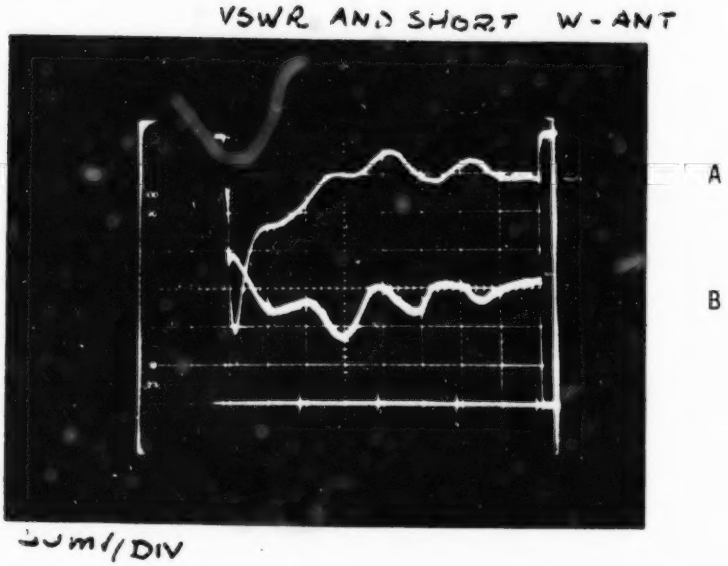

FIGURE 2.15 - VSWR characteristic of TRLD in a rectangular reflector.

X-axis = 25 MHz/div (0 to 200 MHz)
Y-axis = -50 mV/div

A - shows signal reflected by antenna
B - shows signal reflected by short circuit at antenna input terminal

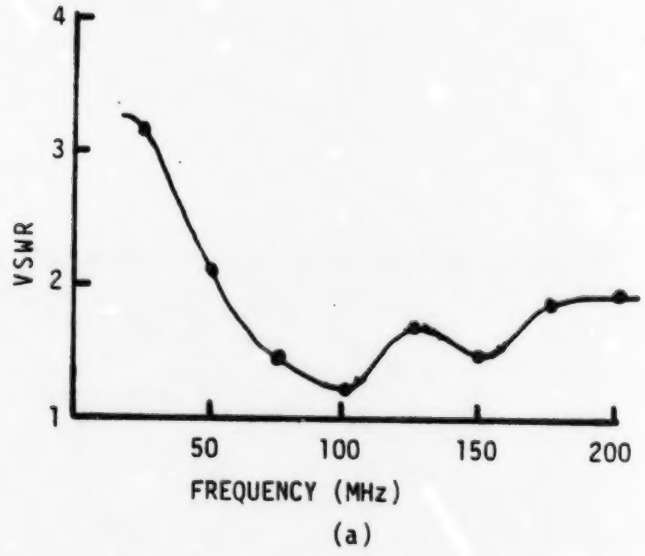

(a)

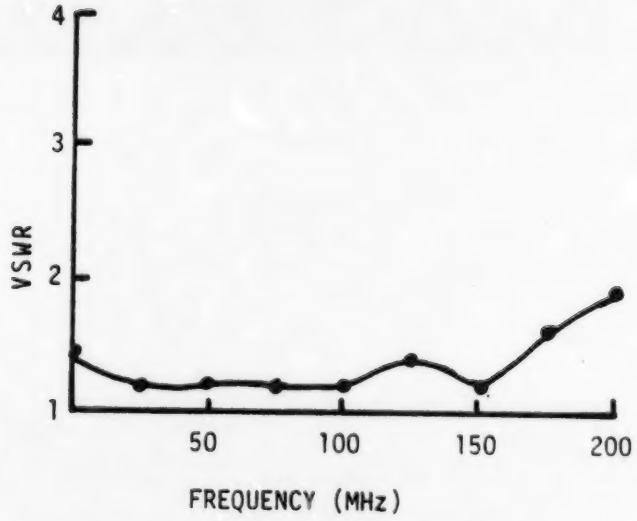

(b)

FIGURE 2.16 - Plot of VSWR as a function of frequency for a TRLD in a rectangular reflector.

(a) Shows TRLD without any matching resistor

(b) Shows TRLD with a 330 Ω matching resistor

by introducing reactive components in the network. However, this is practically impossible for a broadband signal since the reactive components are intrinsically frequency dependent. In the antenna under test, it was possible to reduce the VSWR from the antenna by adding a resistive load at the antenna input terminal. This was done by experiment and the resulting VSWR is shown in Fig. 2.17(a).

2.1.4.2 Tapered Resistively Loaded Dipole (TRLD) in a Square Reflector

Measurements of the transmission properties of a 4 ns pulse were obtained with the transmit/receive antennas side by side facing a conductive wall 20 m away (Fig. 2.18). The reflected signal from the wall was about 120 ns after transmission. The cross-talk occurred within about the first 40 ns. In the oscillogram (Fig. 2.18) the top trace shows the signal input to the transmit antenna, and the bottom two traces are for two different TRLD locations inside the reflector. In Fig. 2.19 the signal reflected from the conductive wall is expanded in time. It shows a reasonably good waveform indicating the good transient response of the antenna. The signals observed after the occurence of the wall reflection is spurious signals from nearby objects.

2.1.4.3 Tapered Resistively Loaded Dipole (TRLD) in a Cylindrical Antenna

Measurements of a TRLD in a cylindrical reflector were also obtained as before. The transmission characteristics for a 4 ns

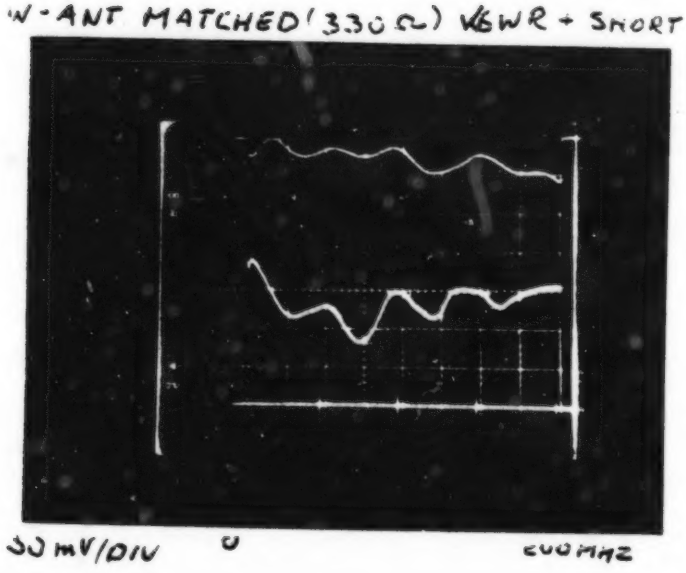

FIGURE 2.17 - VSWR characteristic of TRLD in a rectangular reflector with resistive matching
X-axis = 25 MHz/div (0-200 MHz)
Y-axis = -50 mV/div

A - shows signal reflected by antenna with 330 Ω, matching at input terminals

B - shows signal reflected by short circuit at antenna input terminal

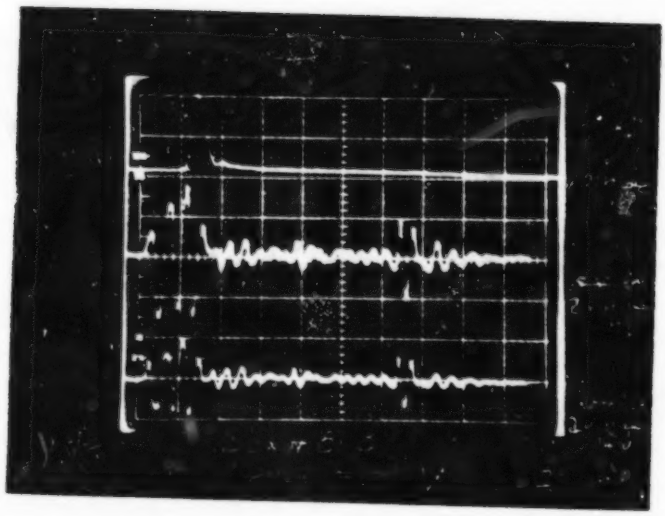

FIGURE 2.18 - Measurements of 4 ns, d.c., pulse transmitted and received by TRLD's in side by side, square reflectors.

A - shows 4 nsec pulse at transmitter input
X-axis = 10 nsec/div Y-axis = 5 V/div

B &C - show 4 ns pulse signal reflected from conductive wall, 20 m away for two locations of the TRLD in the reflector
X-axis = 20 ns/div Y-axis = 10 mV/div

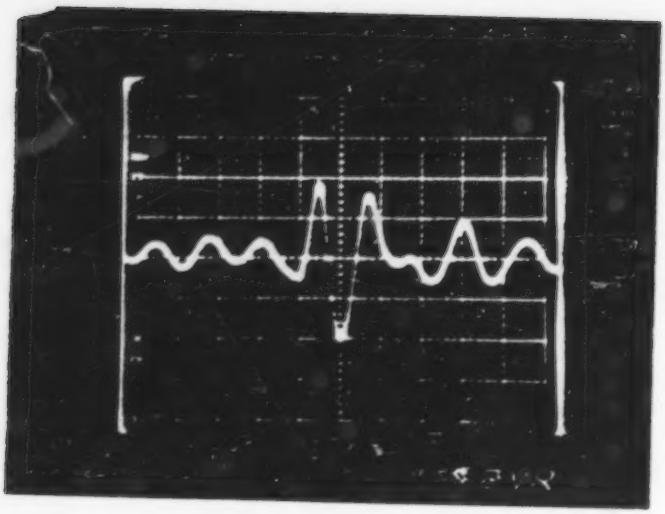

FIGURE 2.19 - Oscillogram showing a repeat of Fig.2.18-B with the return signal expanded in time and amplitude

X-axis = 5 ns/div Y-axis = 5 mV/div

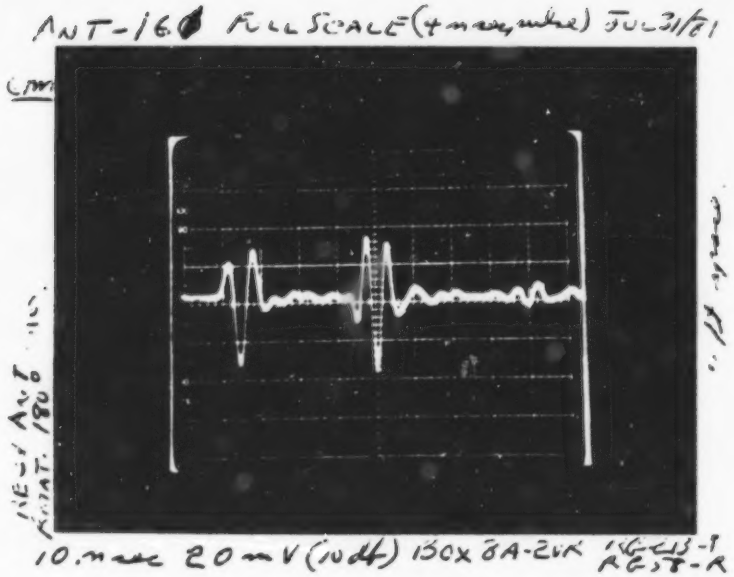

FIGURE 2.20 - Oscillogram showing the cross-talk and return signal reflected from a conductive wall 6 m away. Two TRLD's in cylindrical reflectors side by side were used to transmit and receive a 4 ns pulse.

X-axis = 10 ns/div Y-axis = 20 mV/div

pulse are shown in the oscillogram in Fig. 2.20. Again the oscillogram shows the receive antenna output for a reflected signal from a wall 6 m away. The signal input to the transmit antenna remains the same shape as before (Fig. 2.18).

The good pulse shape as shown in Fig. 2.20 suggests that this antenna configuration is suitable for the required transient response.

2.2 Field Measurements at Outdoor Test Range

Measurements at an outdoor test range was conducted at a Drive-In Theatre about 40 km west of the City of Montreal. The choice of this was conditioned by the following requirements.

(a) Limitations Due to EMI (Electromagnetic Interference)

Since the radar sensor and its antennas operate at the VHF, it was necessary to restrict the radar's transmitting power so as to keep its interference to the FM radio and the TV transmission to the minimum. On the other hand, the transmitted power should be sufficiently high in order that a suitable radar echo from a target can be obtained with a suitable signal to interference ratio. Interferences due to the FM radio, TV stations and the citizen's band, were found to be severe near the city. These problems were greatly reduced when the outdoor theatre was used.

(b) Choice of Target

The outdoor theatre with a large screen for movie projection provided an excellent target for testing the VHF radar sensor. Since the theatre was far away from the city and there were no

buildings in the neighbourhood, it enabled measurements to be taken at a lower transmitting power and at a varying target distance from 10 m to 150 m.

(c) Choice of Antenna Height

As explained in [1], a sufficient antenna height is important to reduce the near field effects and reflections from the ground. For preliminary and qualitative measurements, the antenna was mounted about 5 m from the ground. When more quantitative results were required, the antenna was hoisted about 13 m above ground with the help of a special retractable antenna mast supplied by MPB Technologies Inc. With this arrangement, it was possible to obtain reflections from the movie screen with minimal ground reflections when the antenna-target distance was suitably chosen.

Results of the measurements at the outdoor range did not add any new information but they confirmed the results obtained before in the test facility at MPB Technologies Inc.

3.0 LOCAL HELICOPTER TRIALS

The antenna measurements obtained on the ground using the facilities of MPB Technologies Inc. and the outdoor test range described provided valuable information on the antenna characteristics in general. Specific information concerning the antenna aircraft interactions, the EMI of the radar to the helicopter operation and communication system, the EMI to the radar by the helicopter, the radar sensitivity and various other aspects of the radar operation remained to be studied or confirmed. This could only be done by conducting field measurements using a helicopter. Local fields close to a local airport were chosen to reduce costs and to obtain as much operational information as possible before a large scale field trial in an arctic environment, was conducted.

The local field trials were conducted in January 1983 on the Ottawa River with the antenna fix-mounted underneath a Bell 206 helicopter provided by the Canadian Coast Guard. During the trials the river ice thickness was reported to be about 30 cm or less because of an unusually mild winter. The objectives of this local field trials were to study the antenna electrical characteristics, antenna-aircraft interaction, the structural integrity of the antenna, and the airworthiness of the antenna-helicopter combination.

Results of the helicopter trials confirmed the airworthiness of the antenna-helicopter arrangement and the convenience of the antenna mounting arrangement. Drawings of the antenna installation on the helicopter are given in Appendix A. The antenna electrical characteristics did not differ significantly from the ground measurements.

4.0 AIRWORTHINESS TESTS AND LICENSING

4.1 Certification Tests at D.O.T. Heliport, Ottawa

A series of prescribed flight tests were conducted out of Uplands Airport in Ottawa in order to obtain airworthiness certification for further field measurements.

The initial tests were carried out with only the antenna installed, to verify its structural integrity and any aerodynamic effects it might have on the operation of the aircraft.

During all prescribed test manoeuvers, no abnormal effects were detected, even at speeds up to 150 knots. The open structure and location of the antenna, underneath the helicopter presented little resistance to the down flow of air from the main rotor blades.

These tests were repeated with the electronics installed and connected.

The antenna passed the airworthiness tests quickly and was certified for installation on a Bell 206 helicopter, despite some initial delay in scheduling and arrangement for a helicopter from the Coast Guard.

4.2 Re-certification Tests at D.O.T. Heliport, St.Johns, Nfld.

Prior to transfer of the sea-ice equipment to the icebreaker for further field trials, a second certification was required. Similar flight testing was conducted at the D.O.T. Heliport in St.Johns, Nfld.

Although the wind conditions were more severe than in Ottawa, there was almost no detectable effect over the normal performance of the helicopter.

Information Centre
RECEIVED - REÇU LE
APR 1985
Transports Canada

5.0 SUMMARY AND RECOMMENDATIONS

A broadband VHF antenna suitable for a helicopter borne sea-ice thickness sensor has been designed, built and tested both for its electrical performance and airworthiness. The antenna consists of a tapered resistively loaded dipole in a reflector which is fabricated with metal tubing. After conducting electrical measurements on the ground, the antenna aircraft interaction and airworthiness of the antenna was tested on a Bell 206 helicopter supplied by the Canadian Coast Guard. The overall electrical performance was found to be suitable for a sea-ice thickness sensor using VHF signals. The antenna was found to have sound mechanical design with good structural integrity, small air resistance and had convenient arrangement for quick installation on a helicopter.

The following are recommendations based on the results and experience obtain in the local field trials:

(1) The antenna tested is suitable for the sea-ice thickness sensor and is ready for a more extensive field trial in an arctic environment.

(2) Due to the difficulty in scheduling, the Canadian Coast Guard cannot easily provide a helicopter at short notice and cannot accommodate quick changes in schedule due to unforeseen circumstances. It is advisable to have the antenna licensed for similar helicopters from a private helicopter company.

(3) The antenna in its present configuration has relatively large dimension. It is important that suitable transportation arrangements be investigated before any field trials, to ensure arrival at the site of the antenna system.

(4) In view of its significant dimensions, the reflector should be modified using a design that can reduce the antenna size during transportation (i.e. a collapsible structure).